

University of Montana

ScholarWorks at University of Montana

Graduate Student Theses, Dissertations, &
Professional Papers

Graduate School

1996

Investigation of carbene/allene pathways

David J. Squire

The University of Montana

Follow this and additional works at: <https://scholarworks.umt.edu/etd>

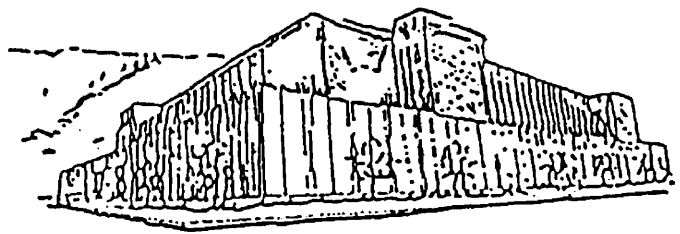
Let us know how access to this document benefits you.

Recommended Citation

Squire, David J., "Investigation of carbene/allene pathways" (1996). *Graduate Student Theses, Dissertations, & Professional Papers*. 8299.

<https://scholarworks.umt.edu/etd/8299>

This Thesis is brought to you for free and open access by the Graduate School at ScholarWorks at University of Montana. It has been accepted for inclusion in Graduate Student Theses, Dissertations, & Professional Papers by an authorized administrator of ScholarWorks at University of Montana. For more information, please contact scholarworks@mso.umt.edu.



Maureen and Mike
MANSFIELD LIBRARY



The University of **MONTANA**

Permission is granted by the author to reproduce this material in its entirety,
provided that this material is used for scholarly purposes and is properly cited in
published works and reports.

*** Please check "Yes" or "No" and provide signature ***

Yes, I grant permission

No, I do not grant permission

Author's Signature



Date

4/9/96

Any copying for commercial purposes or financial gain may be undertaken only with
the author's explicit consent.

INVESTIGATION OF CARBENE / ALLENE PATHWAYS

By

David J. Squire

B.S., University of Montana, 1991

Presented in Partial Fulfillment of the Requirement


for the Degree of

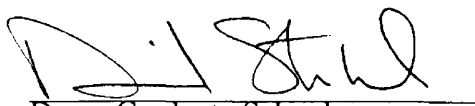
Master of Science

UNIVERSITY OF MONTANA

1996

Approved by:


Chairman, Board of Examiners


Dean, Graduate School

April 10, 1996
Date

UMI Number: EP39100

All rights reserved

INFORMATION TO ALL USERS

The quality of this reproduction is dependent upon the quality of the copy submitted.

In the unlikely event that the author did not send a complete manuscript and there are missing pages, these will be noted. Also, if material had to be removed, a note will indicate the deletion.



UMI EP39100

Published by ProQuest LLC (2013). Copyright in the Dissertation held by the Author.

Microform Edition © ProQuest LLC.

All rights reserved. This work is protected against unauthorized copying under Title 17, United States Code



ProQuest LLC.
789 East Eisenhower Parkway
P.O. Box 1346
Ann Arbor, MI 48106 - 1346

Investigation of Carbene / Allene Reaction Pathways

Director: Edward E. Waali



A kinetic study of the singlet state cycloheptatrienyldene (**1**)-cycloheptatetraene (**9**) system was undertaken. The sodium salt of tropone tosylhydrazone was heated in the presence of *n*-butyl alcohol and 1,3-diphenylisobenzofuran. Two isomers of the DIBF product (**14**) were discovered, separated by chromatographic methods, and their structures elucidated by 2-D COSY ^1H NMR and computer modeling programs. The presence of bitropyl (**24**) was discovered in the course of this work. The formation of several DIBF products, the use of a heterogeneous mixture, and the possible presence of a third intermediate made a kinetic conclusion impossible.

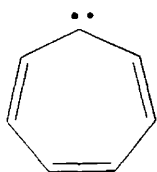
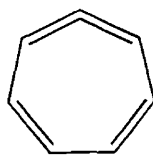
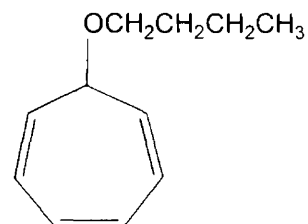
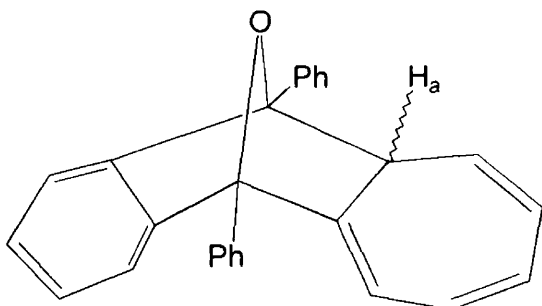
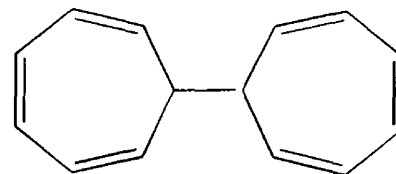
**1****9****20****14****24**

Table of Contents

Abstract	ii
Table of Contents	iii
List of Figures	v
List of Schemes	vi
List of Tables	vii
Acknowledgments	viii
1. INTRODUCTION	1
1.1. Carbene Chemistry	2
1.1.1. Generation of Carbenes	2
1.1.1.1. α -Elimination	2
1.1.1.2. Decomposition of Compounds Containing Certain Π -Systems	3
1.1.2. Two Electronic States of Carbenes	4
1.1.3. Reactions of Carbenes	5
1.1.3.1. The Addition Reaction of Carbenes	5
1.1.3.2. Carbene Addition Reactions via Carbenoid Intermediates	7
1.2. Allene Chemistry	10
1.2.1. Hybridization of Simple Allenes	10
1.2.2. Generation of Allenes	11
1.2.3. Stability of Cyclic Allene Systems	12
1.2.4. Allene Reactions	12
1.3. Prelude to the Current Study	13
1.3.1. Stabilization of a Singlet State Carbene	13
1.3.2. Evidence Supporting the Nucleophilicity of Carbene 1	14
1.3.3. Allene Intermediate Proposed	16
1.3.4. Different Precursors, Same Products	17
1.3.5. Possible Carbene/Allene Equilibrium	19
1.3.5.1. Equilibrium Studies	20
1.3.6. Definite Allene Presence	22
1.3.6.1. Optical Activity Study	22
1.3.6.2. Isotope Study	24
1.3.7. Carbene Makes a Come-Back	26
1.3.8. Summary of the Evidence	27
1.4. Objectives	28
1.4.1. Synthesis of Expected Products	28

1.4.2. Kinetics Reactions	29
1.4.3. Intermediate Reaction Mechanisms	29
1.4.4. The Role of Kinetics	32
1.5. Preliminary Results of Zepp	34
2. RESULTS AND DISCUSSION	37
2.1. Synthesis of the Sodium Salt of Tropone Tosylhydrazone (2)	37
2.2. Synthesis of the <i>n</i> -Butyl Tropyl Ether (20)	38
2.3. Bitropyl Formation	42
2.4. Elucidation of the Structures of the DIBF Product (14)	46
2.4.1. Isomers Discovered	46
2.4.2. The Third DIBF Product	57
2.5. Reaction Time vs. DIBF Product Generation	59
2.6. Competition Reactions	60
2.6.1. Preparation for the Kinetic Study	60
2.6.2. Competition Kinetics	62
3. SUMMARY AND CONCLUSION	65
4. EXPERIMENTAL	66
4.1. Synthesis of Tropone (21)	67
4.2. Synthesis of 7,7-Dichlorocycloheptatriene (22)	67
4.3. Synthesis of Tropone Tosylhydrazone (23)	68
4.4. Synthesis of Sodium Salt of Tropone Tosylhydrazone (2)	69
4.5. Synthesis of 1-Butoxy-2,4,6-Cycloheptatriene (20)	69
4.6. Synthesis of DIBF Product (14)	71
4.7. Synthesis of Bitropyl (24)	72
4.8. Competition Reaction (synthesis of 20 and 14)	72
Appendix I	74
Appendix II	75
Bibliography	93

List of Figures

Figure 1-1: Singlet State Carbene	5
Figure 1-2: Triplet State Carbene	5
Figure 1-3: Allene Stereochemistry	10
Figure 1-4: Allene Orbitals	11
Figure 1-5: Select Cyclic Allene Systems	12
Figure 1-6: Cycloheptatrienyliene	14
Figure 1-7: Carbene 1 and Two Isomers of 9	20
Figure 1-8: Energy Diagram Indicating a Carbene Transition State	21
Figure 1-9: Butyl Ether Product 20 and DIBF Product 14	29
Figure 1-10: Kinetics Equations in Equation of a Line Format	32
Figure 1-11: Plot of a Single Intermediate Mechanism (Scheme 9)	33
Figure 1-12: Plot of a Two Intermediate Mechanism (Scheme 10)	34
Figure 1-13: Preliminary Results of Zepp	35
Figure 2-1: COSY of Butyl Ether Product 20	39
Figure 2-2: Butyl Ether Product 20	40
Figure 2-3: Spectra of Butyl Ether Product 20 from Two Precursors	41
Figure 2-4: Alternative Bitropyl Synthesis	42
Figure 2-5: Spectra of Butyl Ether Product 20 and Bitropyl (24)	43
Figure 2-6: COSY Spectrum of Bitropyl (24)	45
Figure 2-7: 1-D Spectrum of the Crude DIBF Reaction Mixture	47
Figure 2-8: Isomers of 14 Possible	48
Figure 2-9: COSY Spectrum of the Crude DIBF Reaction Mixture Before Chromatography	49
Figure 2-10: HPLC Chromatogram of Isomer Separation	50
Figure 2-11: Spectra of the DIBF Isomers	51
Figure 2-12: COSY Spectrum of DIBF Product's Isomers after Column Chromatography and TLC	53
Figure 2-13: COSY Spectrum of Minor Isomer	54
Figure 2-14: Calculated Stereochemistry of the Isomers	56
Figure 2-15: Spectra of the Competition Reaction Sample with Spiking	61
Figure 2-16: Spectra of Competition Reaction with Its Component Products	63

List of Schemes

Scheme 1: Reaction of Carbenes with Alkenes	15
Scheme 2: Two Possible Intermediates	17
Scheme 3: Summary of Possible Mechanistic Pathways	19
Scheme 4: Carbene/Allene Isomerization	22
Scheme 5: Optical Activity Study	23
Scheme 6: Isotope Study Results	25
Scheme 7: Carbene Intermediate Yielding Tropyl Ethers	26
Scheme 8: Allene Intermediate Yielding Vinyl Ethers	27
Scheme 9: Proposed Single Intermediate Mechanism	30
Scheme 10: Proposed Two Intermediate Mechanism	31
Scheme 11: Synthesis of Sodium Salt of Tropone Tosylhydrazone (2)	37
Scheme 12: Bitropyl Formation	44
Scheme 13: Possible Formation and Structure of Unknown DIBF Product	58

List of Tables

Table 1: Data of Zepp (observing one DIBF product)	35
Table 2: Chemical Shifts of Butyl Ether Product 20	42
Table 3: Chemical Shifts of the Major and Minor Isomers	52
Table 4: SYBYL Force Field Results	55
Table 5: HRMS Results of the DIBF Product's Isomers	57
Table 6: Stabilization of the DIBF Products Over Increasing Reaction Time	59

ACKNOWLEDGMENTS

I would like to thank the following people for their help, support, and mentorship during my tenure in graduate school here at UM:

Dr. Ed Waali for his patience, guidance, friendship, and entertaining stories (both chemistry-related and non-related),

Dr. Chuck Thompson for agreeing to be on my committee and for his valuable assistance with my thesis,

Dr. Todd Cochran for taking time out of his hectic schedule at the Pharmacy school to be on my committee,

Gayle Zachariassen for finding funds for me to continue my studies (not an easy task given the chemistry school's never-ending, bleak financial state), and for having some good stories to share,

Bonnie Gatewood also for some good advice, some good stories, and a lot of assistance, and

Mom for helping me through school for these many long years by emotional and financial assistance.

INTRODUCTION

Reactive intermediates are integral parts of chemical reactions which do not proceed by single-step concerted mechanisms. By studying the kinetics of reactions, chemists may gain knowledge of reactive intermediates and mechanistic pathways.

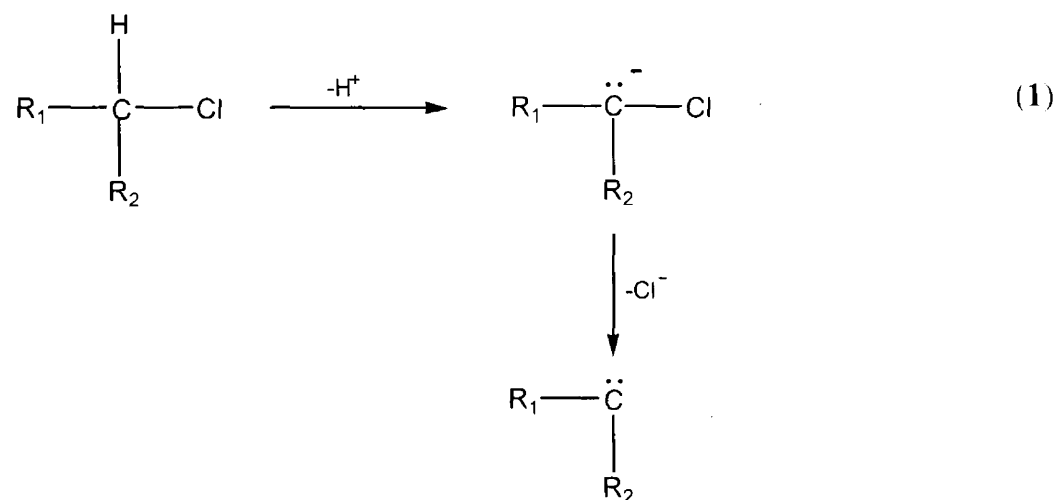
This work studied two potential reactive intermediates, a carbene and an allene. It is the focus of this work to obtain kinetic data which might indicate whether a particular reaction occurs by way of one or both of these reactive intermediates.

1.1. Carbene Chemistry

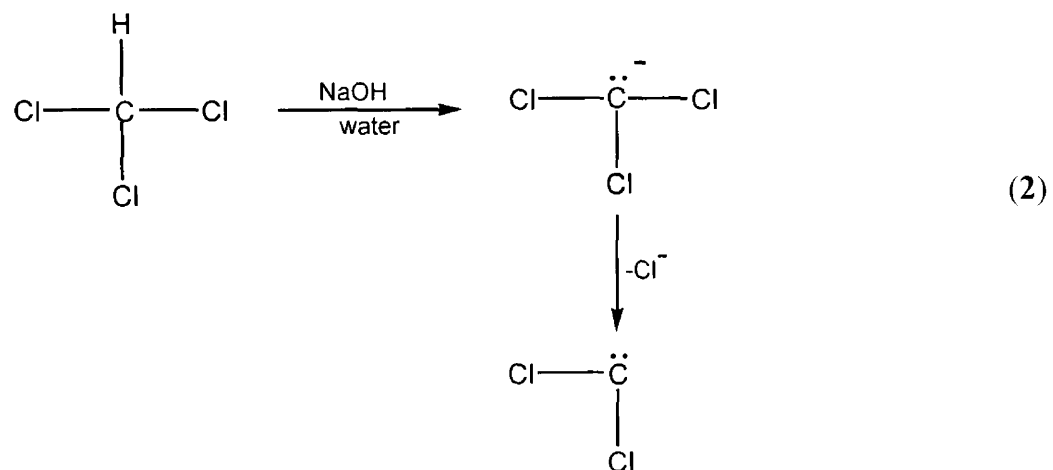
1.1.1. Generation of Carbenes

Carbenes are highly reactive intermediates which contain divalent carbon atoms and two non-bonding electrons.¹ Two ways of generating carbenes are via α -elimination (Equations 1.2; Section 1.1.1.1.) and decomposition of certain π -systems (Equations 3,4,5; Section 1.1.1.2.).

1.1.1.1. α -Elimination: net loss of HCl from the same carbon results in the production of the carbene.

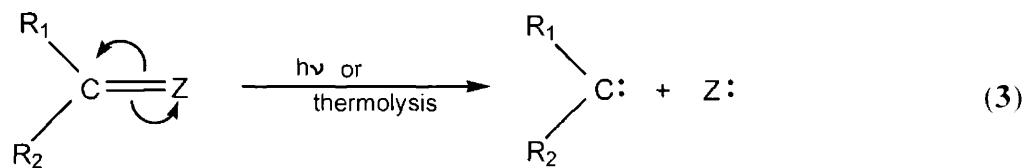


A classical example of α -elimination to generate carbenes is the treatment of chloroform with a hydroxide ion to yield dichlorocarbene (Equation 2).¹



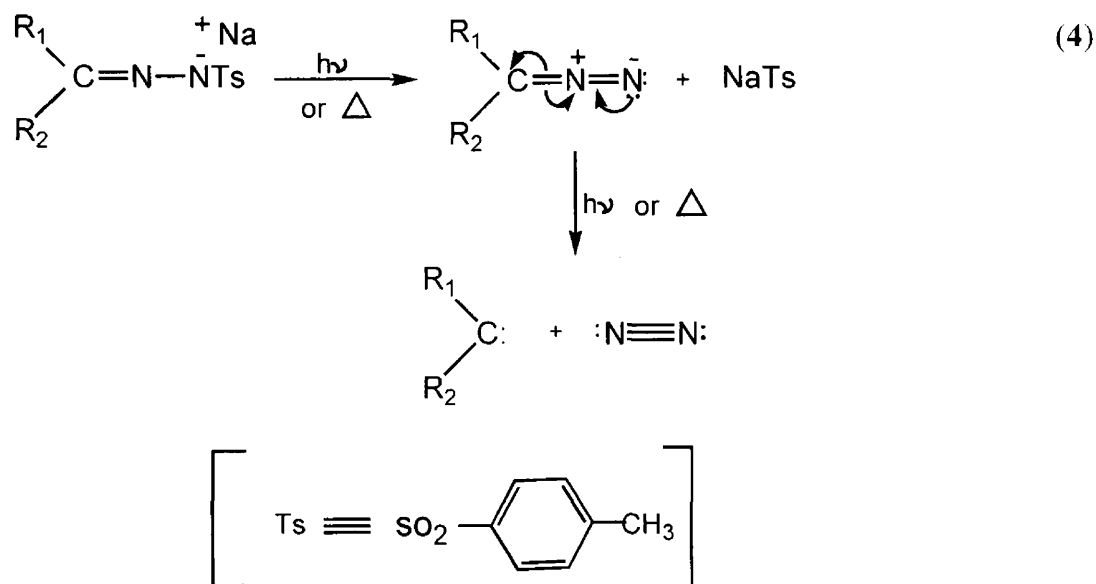
1.1.1.2. Decomposition of Compounds Containing Certain π -Systems.

General Reaction:

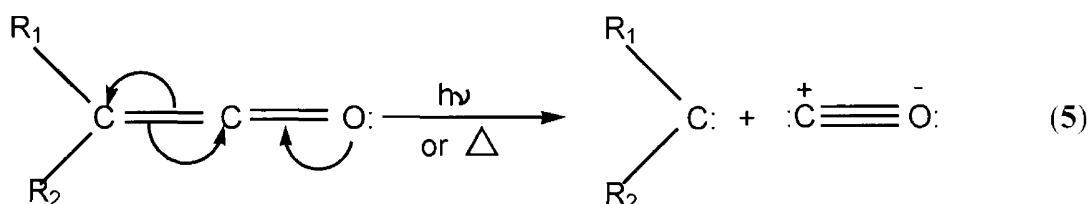


The two most important ways of generating the carbene via a decomposition pathway are exemplified in **Equations 4** and **5**.

a. decomposition of diazomethanes (Equation 4)



b. photolysis of ketenes



1.1.2. Two Electronic States of Carbenes

Two predominant electronic states are possible for carbenes, including the singlet state carbene (Figure 1-1) in which the electrons are paired with opposite spins in the same orbital ($\sim sp^2$), leaving an empty p orbital, and the triplet state carbene (Figure 1-2) where the unpaired electrons (having the same spin) occupy two different orbitals. Triplet carbenes, in **Figure 1-2**, exhibit approximately sp hybridization character.²

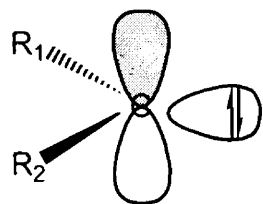


Figure 1-1
Singlet State Carbene

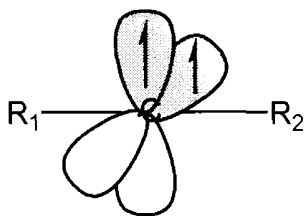


Figure 1-2
Triplet State Carbene

Normally, singlet state carbenes are less stable than their triplet counterparts. This is due to electron-electron repulsion that is relieved in the triplet. Hund's Rule dictates that the ground state of the lowest electronic configuration of an atom will be the one having the greatest multiplicity.³

1.1.3. Reactions of Carbenes

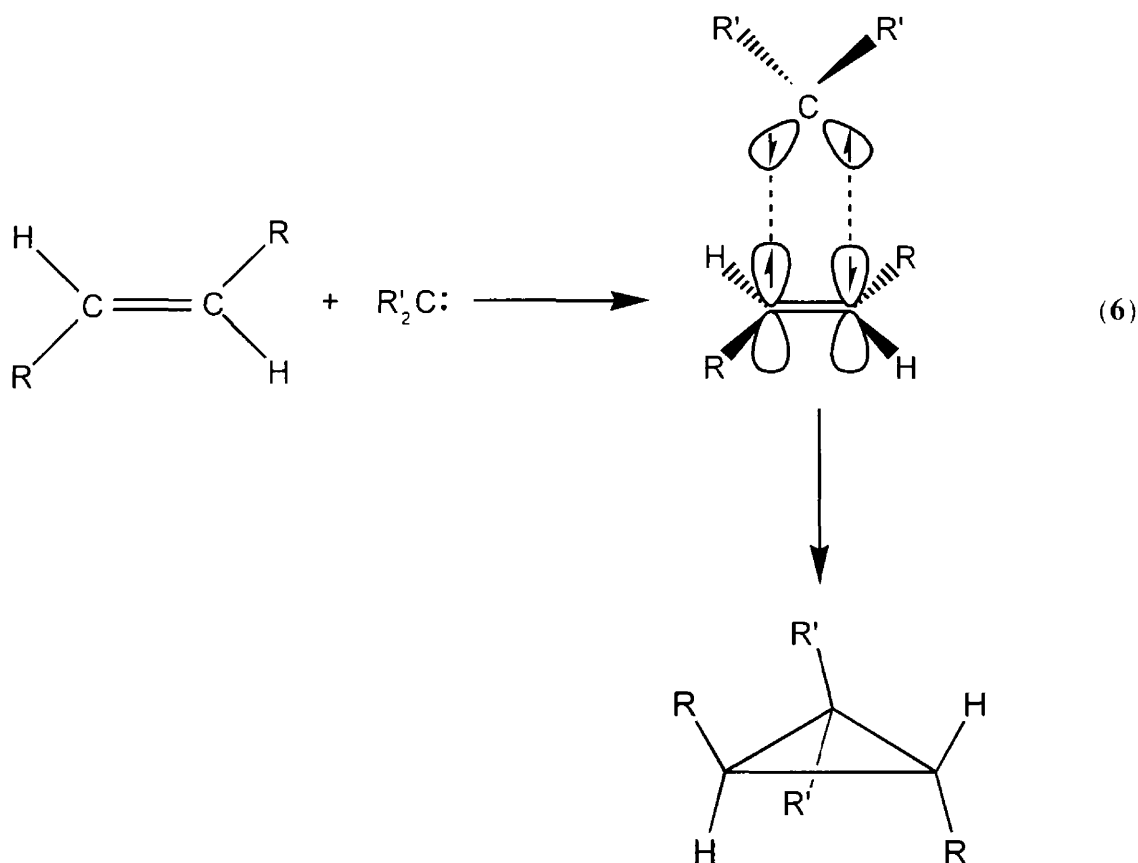
Two types of carbene reactions germane to the current study are the addition reaction (Section 1.1.3.1.) and the insertion reaction.⁴

1.1.3.1. The Addition Reaction of Carbenes

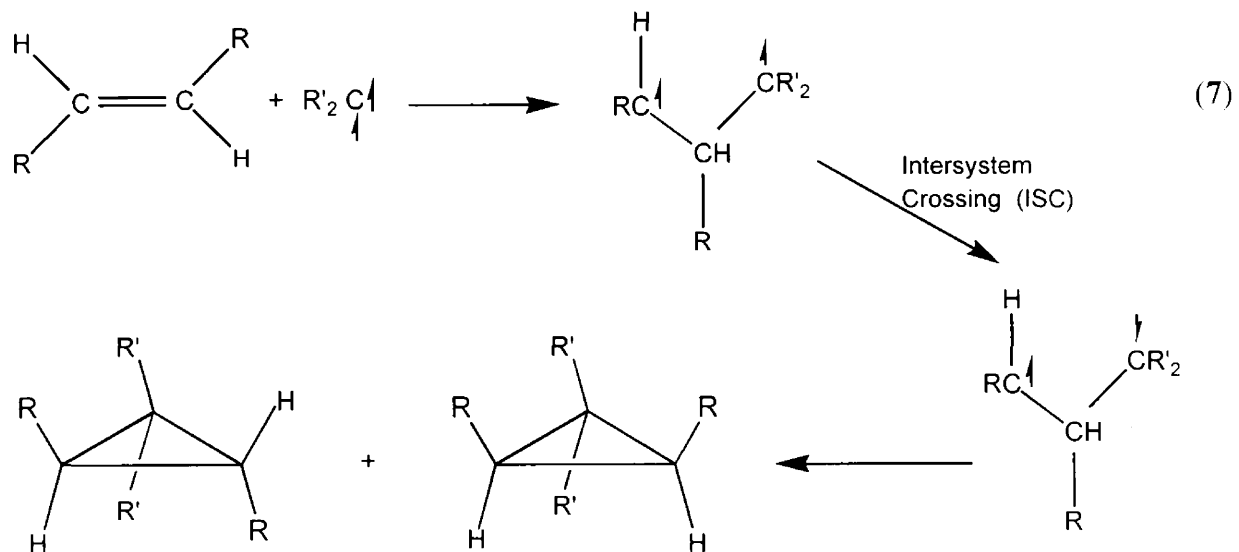
One of the best-studied reactions of carbene intermediates is their addition to alkenes generating cyclopropanes. The addition of singlet state carbene intermediates to alkenes occur stereospecifically (Equation 6). A singlet state carbene adding to a *cis* alkene will generate the *cis* cyclopropane. The triplet state carbene intermediates add nonstereospecifically to alkenes to generate cyclopropanes (Equation 7). This lack of

stereospecificity is determined just before intersystem crossing (ISC). Initially, the triplet state carbene adds to the double bond. Once the intermediate is formed, rotation about the single bonds of the carbons becomes possible. The orientation of the carbon atoms (in relation to one another before ISC) will determine the stereochemistry of the products. Once ISC occurs, the singlet state electrons will couple and form both *cis* and *trans* products. In the case of the singlet state carbene, no rotation about the bonds is possible because of the rigidity of the double bond. This is the reason for the singlet state's stereospecificity.

Singlet Mechanism (Equation 6)



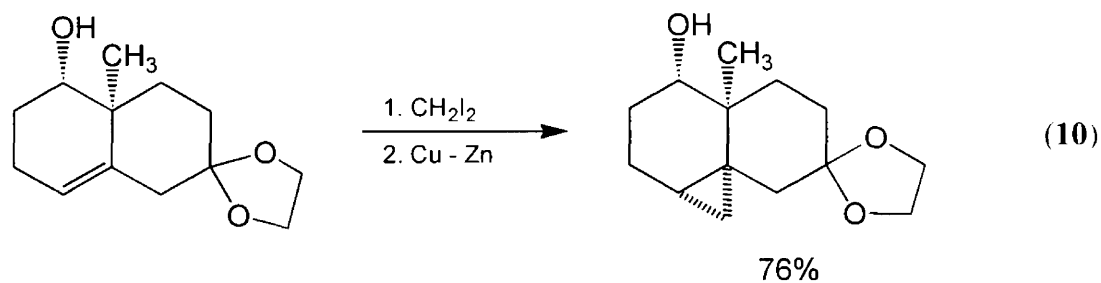
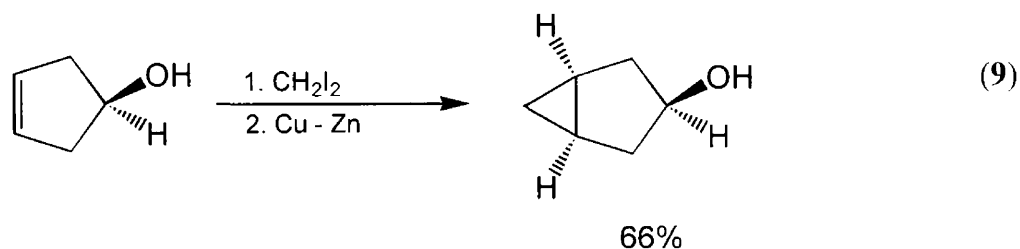
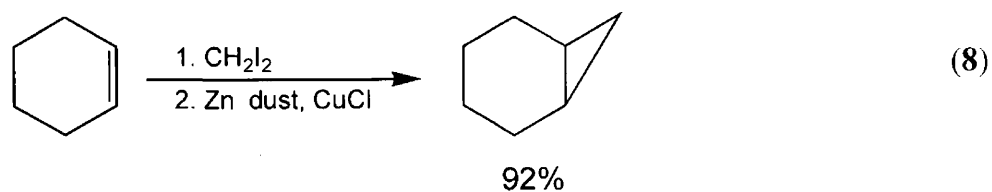
Triplet Mechanism (Equation 7)



1.1.3.2. Carbene Addition Reactions via Carbenoid Intermediates

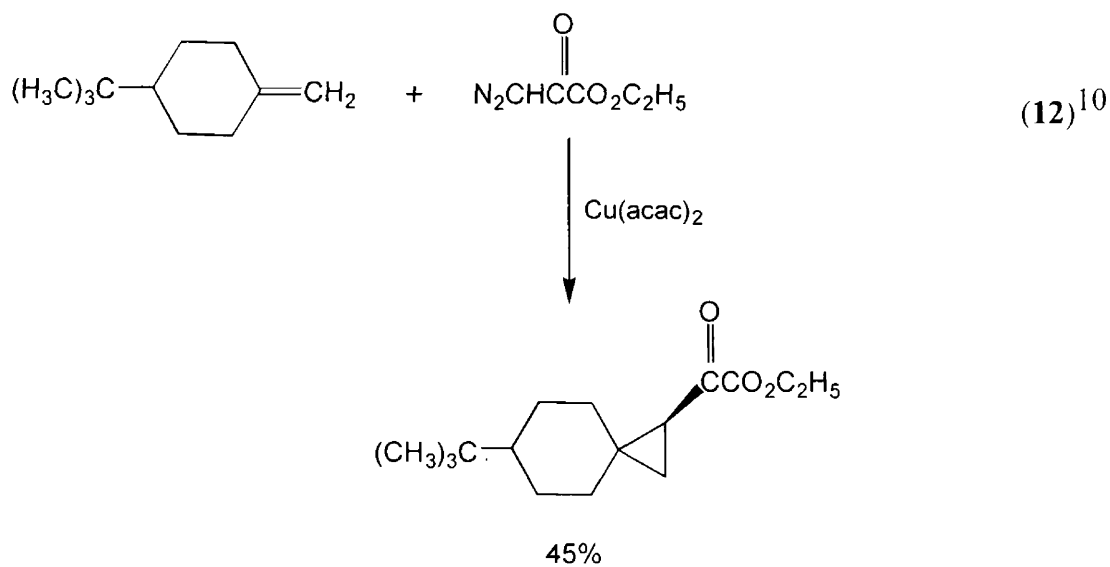
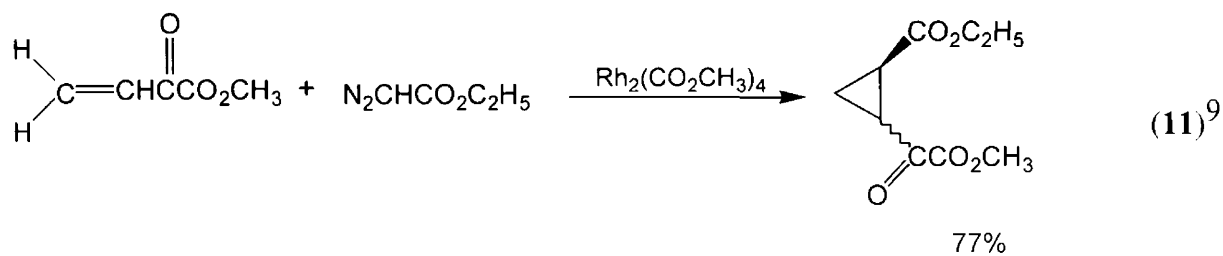
Addition reactions of carbenes to alkenes are important methods for the synthesis of many types of cyclopropanes. Singlet state carbenes are very reactive intermediates and sometimes require transition metals to make them less reactive (more selective) in practical syntheses. When carbenes are complexed to transition metals, the intermediates are called carbenoids. Select synthetic examples that utilize carbenoid intermediates are listed in **Equations 8-14**.

A. Cyclopropanes from Methylene Transfer

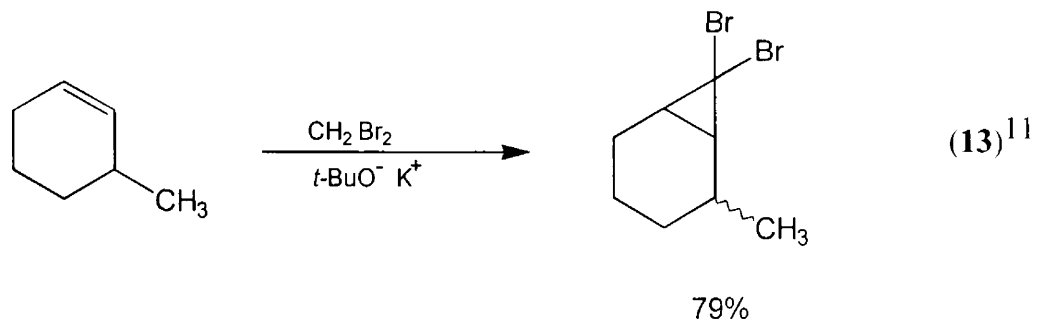


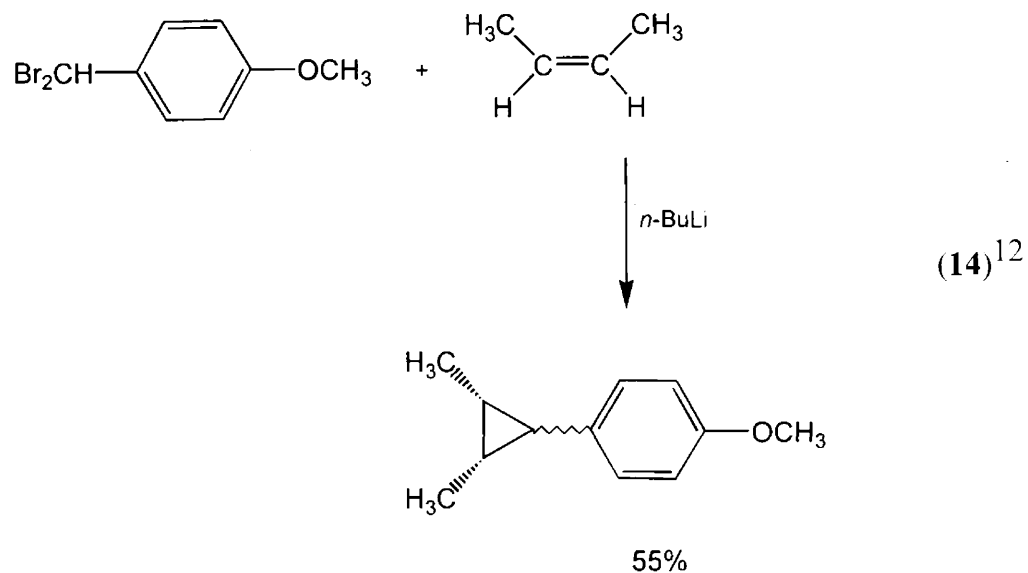
Equations 8⁵, 9⁶, and 10⁷ all proceed via the Simmons-Smith zinc-copper couple reaction.⁸ In **Equations 8-10**, an iodomethylzinc iodide intermediate forms. The stereochemistry in **Equation 9** and **10** results because the zinc present in the intermediate first couples with the hydroxyl group. The intermediate's methylene group then adds across the double bond *cis* to the hydroxyl group.

B. Catalytic Cyclopropanation by Diazo Compounds and Metal Salts (carbene formation via loss of dinitrogen).



C. Reactions of Carbenes Generated by α -Elimination





1.2. Allene Chemistry

1.2.1. Hybridization of Simple Allenes

Allenes, also known as cumulenes, are dienes which have two olefinic groups sharing a central carbon atom. The central carbon atom is sp hybridized, while the outer carbon atoms are sp^2 hybridized (Figure 1-3).

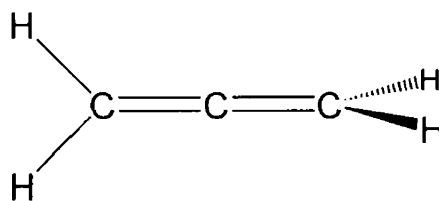


Figure 1-3. Allene Stereochemistry

Open chain allenes show the orbitals of the sp^2 carbons to be orthogonal to each other, as can be observed by viewing the positions of the hydrogen substituents in

Figure 1-3. This orthogonality is a result of the p orbitals of the sp hybridized carbon overlapping with each of the p orbitals of the sp^2 carbons (Figure 1-4).

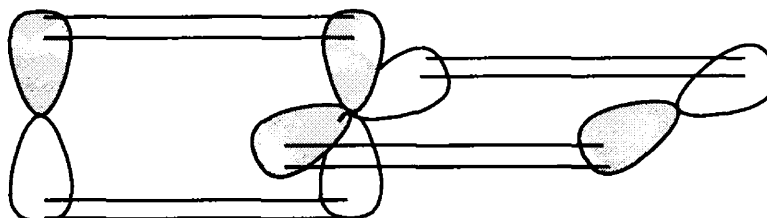
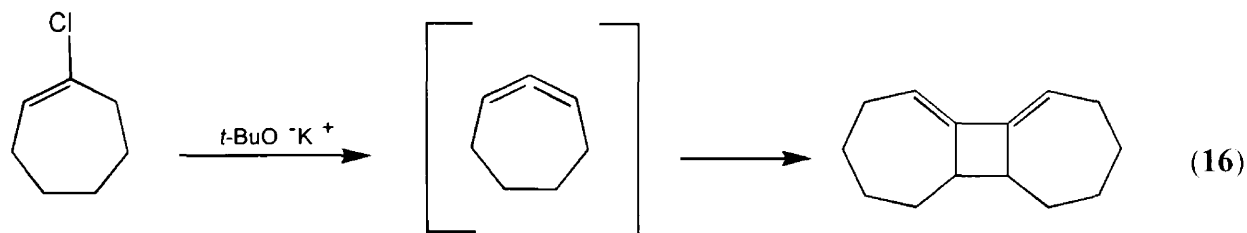
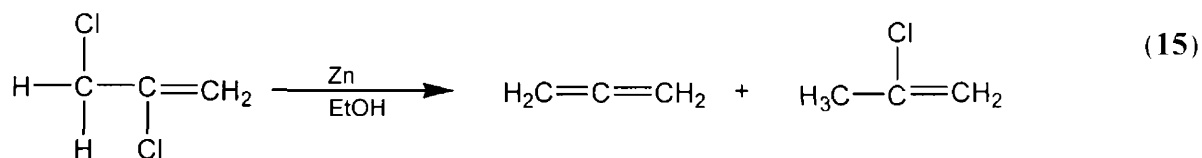


Figure 1-4. Allene Orbitals

1.2.2. Generation of Allenes

A common method of generating allenes is by dehalogenation of dihaloalkenes (Equation 15; allene elimination products and vinyl halide reduction products)¹³ and by dehydrohalogenation of haloalkenes (Equation 16).¹⁴ In **Equation 16**, 1-chlorocycloheptene reacts with the strong base to go to the allene intermediate. In the absence of other reagents, this intermediate then dimerizes to the cyclobutane product.



1.2.3. Stability of Cyclic Allene Systems

In a cyclic allene system, two major factors determine the stability or instability of that system: 1) size of the ring, and 2) presence of additional unsaturation and other functional groups. For example, 1,2-cyclononadiene (**25**) can be isolated at room temperature (Figure 1-5). The more unsaturated 1,2,4,6,8-cyclononapentaene (**26**) and the smaller-ringed 1,2-cyclohexadiene (**27**) are much less stable and not isolable under the same conditions. Inherently, cyclic allenes containing nine carbons or less are unlikely to be isolable under ordinary laboratory conditions.^{15,16}

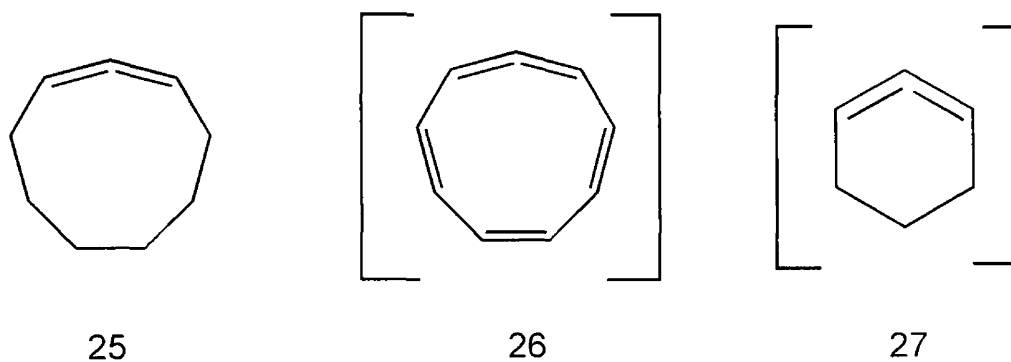
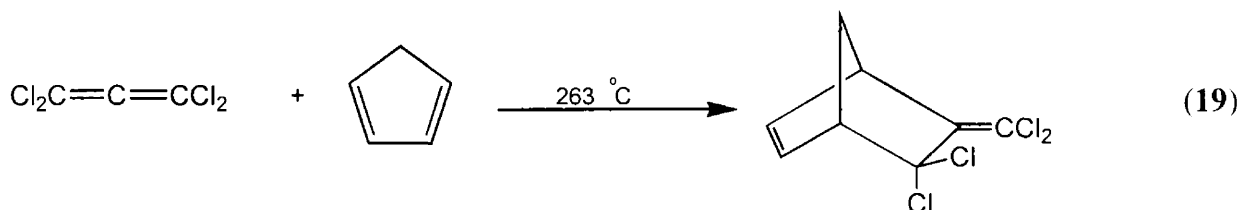
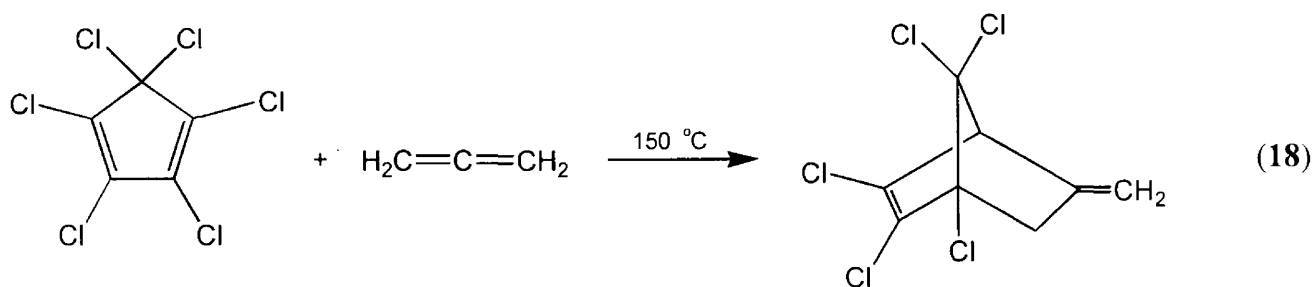
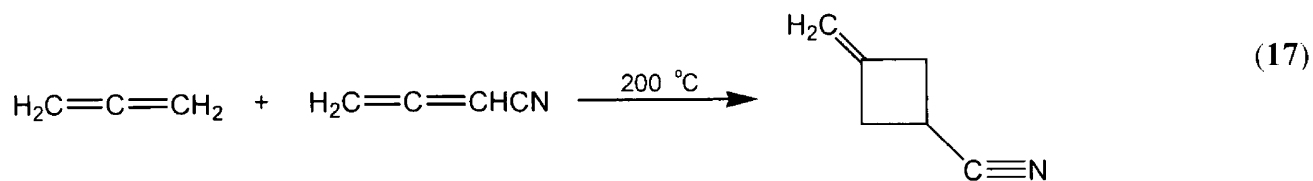


Figure 1-5. Select Cyclic Allene Systems

1.2.4. Allene Reactions

Allenes can dimerize to yield cyclobutanes. They can also undergo Diels-Alder cycloadditions with 1,3-dienes to yield cycloaddition products (Equations 17,18,19).¹⁷



1.3. Prelude to the Current Study

1.3.1. Stabilization of a Singlet State Carbene

A way of stabilizing a singlet state carbene, possibly making it the ground state, was hypothesized by Jones and Ennis.¹⁸ They proposed that by incorporating the empty *p* orbital of the singlet state carbene (as in Figure 1-1) into a carbocyclic, completely

conjugated, aromatic system at least two effects might be observed in the properties of the singlet state carbene (Figure 1-6). First, the electrophilic nature of the vacant orbital might be diminished. This would result in the π electron density from the aromatic system partially filling the vacant p orbital. Second, the nucleophilicity of the non-bonded pair of electrons might be enhanced. As a result, the singlet state would decrease in energy relative to its triplet state, and the singlet state might approach ground state energy.^{19,20}

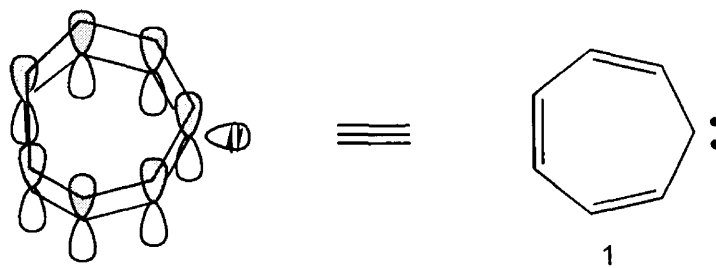


Figure 1-6. Cycloheptatrienyldiene

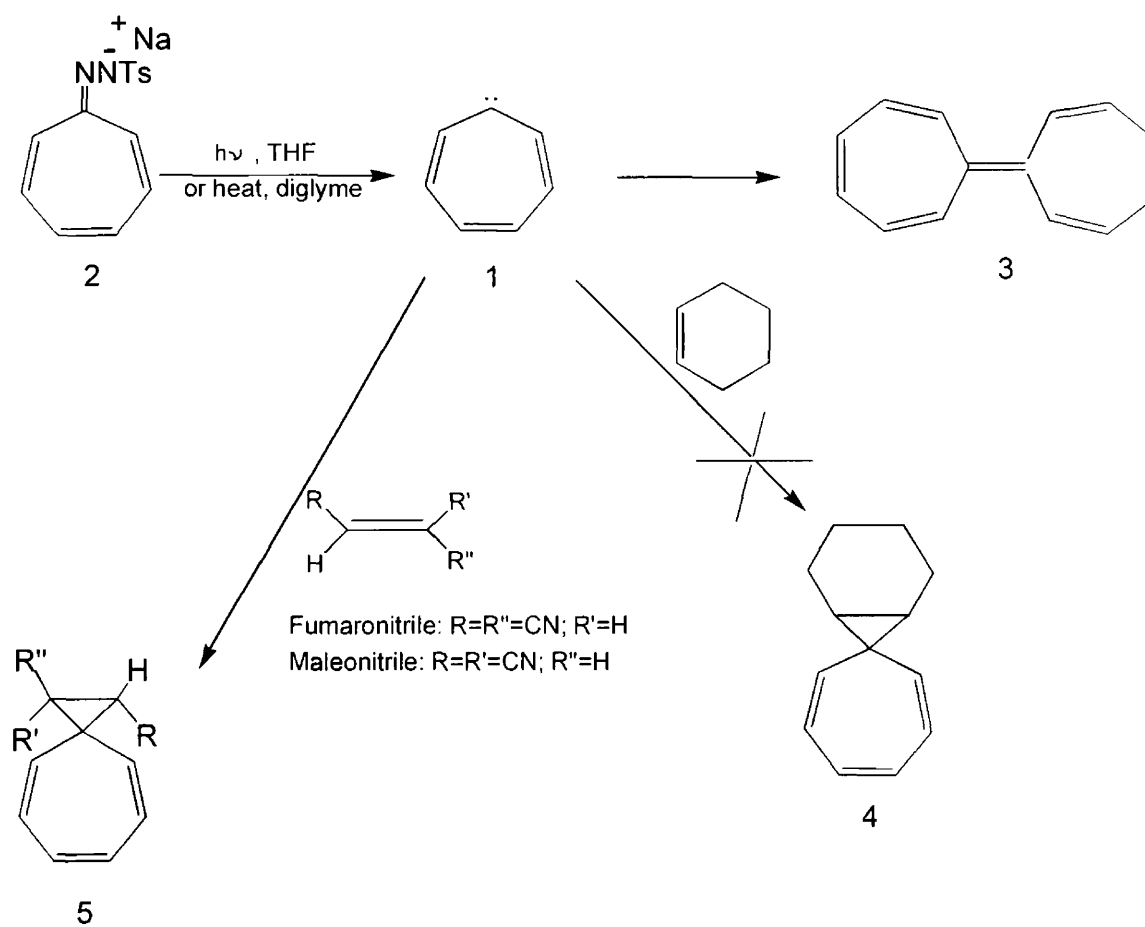
Jones and co-workers conducted experiments in which the sodium salt of tropone tosylhydrazone (**2**) was subjected to a thermolysis in diglyme, and a photolysis in tetrahydrofuran (THF) (Scheme 1). Both reactions yielded heptafulvalene (**3**) apparently via the cycloheptatrienyldiene intermediate (**1**). It was unusual that the formal dimer **3** was apparently generated by **1**, rather than carbene **1** reacting with the solvents present in the reaction. The significance of this will be more closely examined shortly.

1.3.2. Evidence Supporting the Nucleophilicity of Carbene **1**

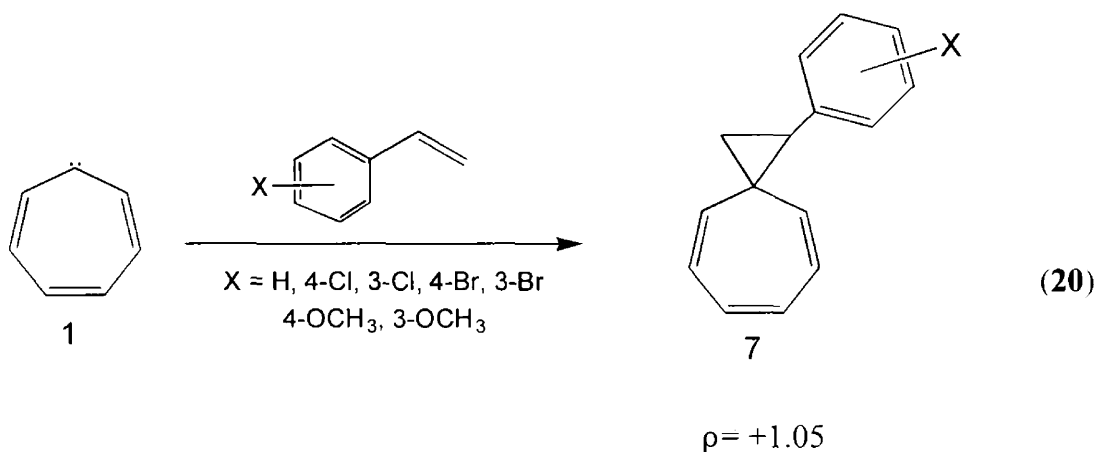
If cycloheptatrienyldiene (**1**) was electrophilic, like ordinary carbenes, it would

react with an electron-rich double bond. Normal, singlet state carbenes (such as Figure 1-1) have been observed to react with electron-rich olefins to yield cyclopropanes.²¹ However, these normal singlet state carbenes do not normally react with electron-deficient olefins. When **2** was decomposed in the presence of cyclohexene, the addition product (**4**) was not observed (Scheme 1). In order to obtain evidence indicating the nucleophilic nature of **1**, Jones then carried out a photolysis of **2** in the presence of the electron-deficient double bond in fumaronitrile and maleonitrile. This photolysis yielded cyclopropanes (**5**) stereospecifically. These experiments indicated that carbene intermediate **1** had nucleophilic character.

Scheme 1. Reaction of Carbenes with Alkenes



The nucleophilicity of this singlet state carbene was supported by Hammett studies performed by Christensen, Waali, and Jones in which **1** was generated in the presence of substituted styrenes ($X\text{-Ph-CH=CH}_2$) (Equation 20).²² Their results showed $\rho = +1.05$. (The positive ρ value indicates the nature of the intermediate is nucleophilic.)



The lack of reaction of **1** with cyclohexene, its reaction with fumaro- and maleonitrile, and the Hammett study performed on **1** were good evidence that the intermediate is indeed nucleophilic. These results were consistent with a ground state singlet carbene.²³

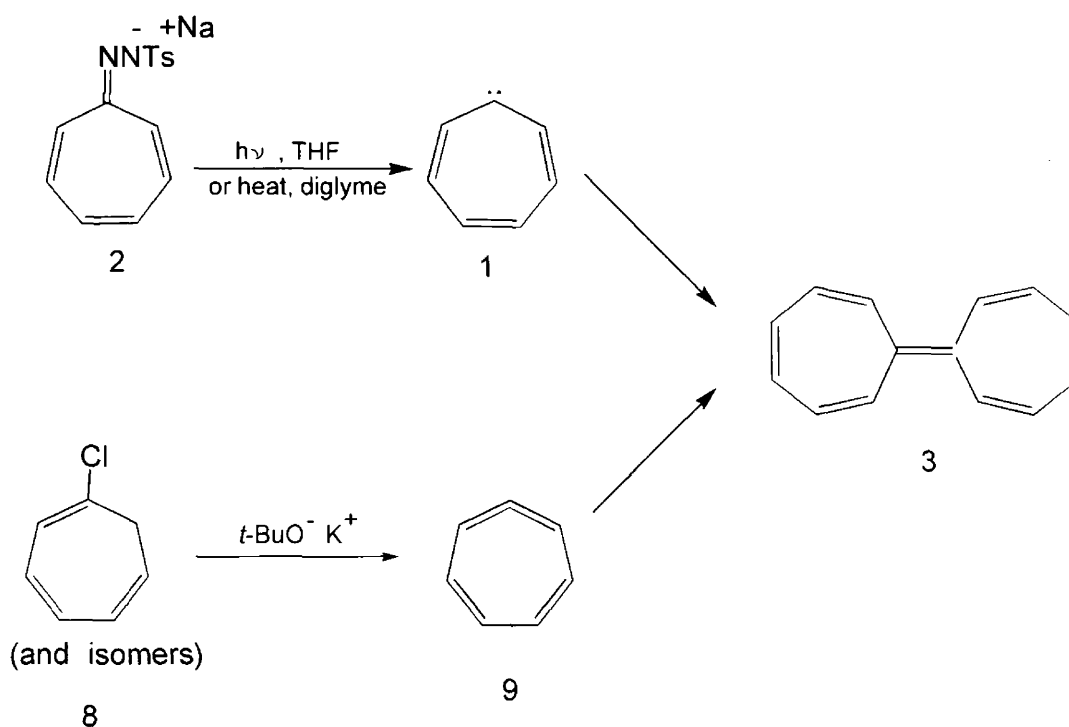
At this point, this reaction mechanism in the decomposition of the sodium salt of tropone tosylhydrazone (**2**) was thought to proceed strictly through a singlet state carbene intermediate.

1.3.3. Allene Intermediate Proposed

Jones first reported the major product heptafulvalene (**3**) upon addition of **2** to

refluxing diglyme. In the suggested mechanism, the salt was thought to convert to the singlet state carbene **1** which in turn dimerized to **3**. Shortly after this, Karl Untch discovered that the dehydrohalogenation of 1-, 2-, and 3-chlorocycloheptatrienes (**8**) with potassium *t*-butoxide also yielded **3** (Scheme 2).²⁴ In addition, Untch's proposed allene intermediate (**9**) showed the same properties as the one resulting from the decomposition of the sodium salt (**2**). Untch's work introduced the possibility that the allene (**9**) might be involved. As such, can all previous chemistry ascribed to carbene intermediate **1** (Section 1.3.2.) be explained by allene intermediate **9**?

Scheme 2. Two Possible Intermediates



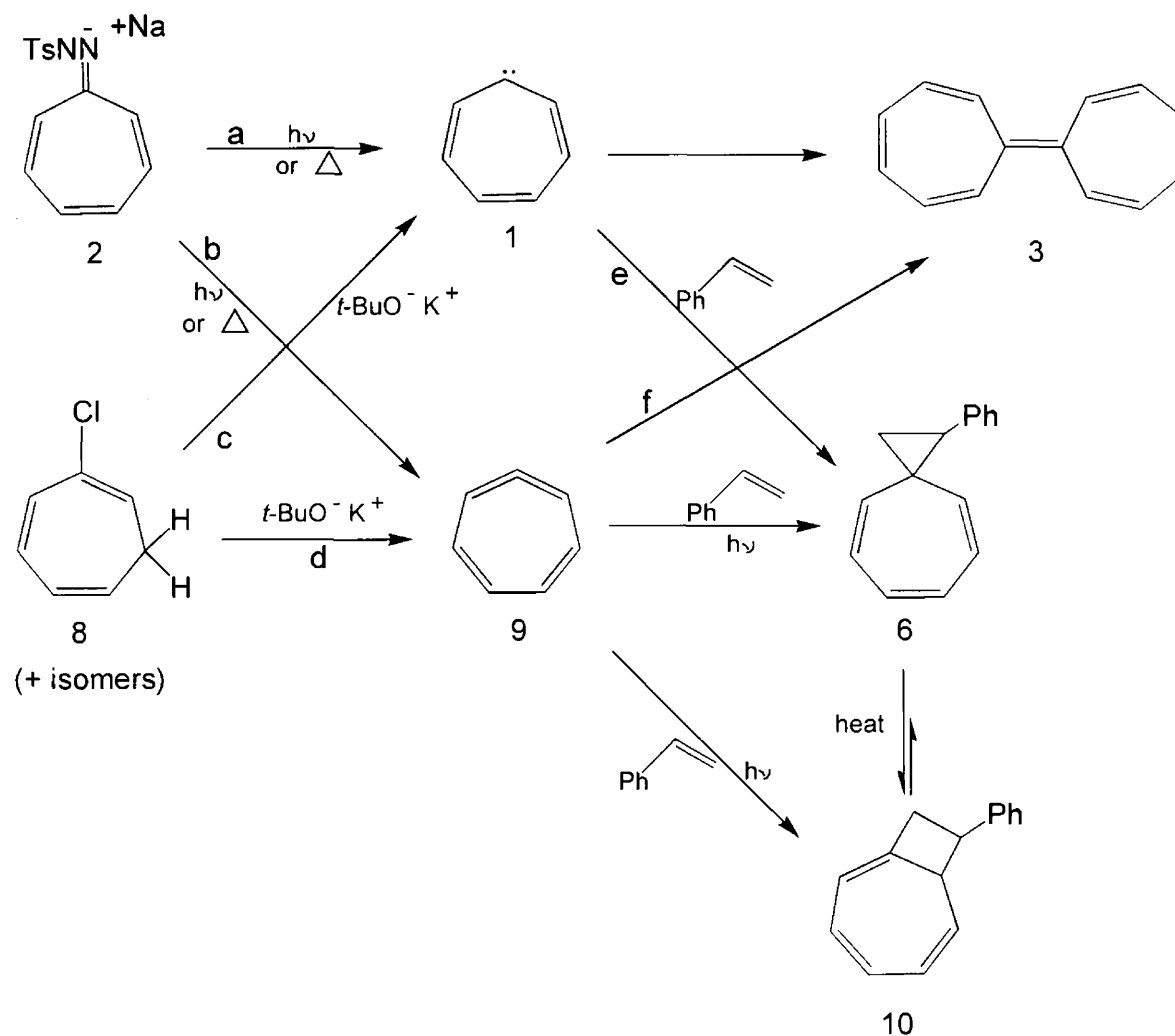
1.3.4. Different Precursors, Same Products

Following the Untch study, it was found that reaction of carbene intermediate **1**

with styrene initially yields the spiroonatriene adduct **6** (Scheme 3; paths a,f). Upon heating, **6** rearranges to the more stable **10** (path j).²⁵ The cyclobutane **10** is also the expected product for the [2+2] cycloaddition of the allene **9** with styrene (path i). Therefore, it becomes apparent that the intermediate reacting with olefins to yield cyclopropanes may not be represented solely by the allene structure.

So the question arises: From which intermediate do the spirocyclopropane (**6**) and heptafulvalene (**3**) result? Reaction **Scheme 3** summarizes the possibilities considered up to this point.

A carbene reaction followed by a rearrangement might give an allene-like product. Conversely, an allene reaction followed by a rearrangement might give a carbene-like product. Reactions of carbenes with alkenes inherently yield cyclopropanes (such as **6**) in which the carbene carbon forms two separate σ -bonds with two other carbon atoms. Reactions of allenes with alkenes tend to yield [2+2] cycloaddition products, such as cyclobutane **10**. Therefore, it is difficult at this point to determine which intermediate exists in the mechanism, based solely on structural analysis of the products.

Scheme 3. Summary of Possible Mechanistic Pathways

1.3.5. Possible Carbene/Allene Equilibrium

Thus far, products **3** or **6** have been seen to result from two entirely different precursors (**2** and **8**). Two different intermediates (**1** and **9**) have been proposed in the mechanism of each reaction. The results of the previous sections were inconclusive as to

which intermediate was present. Evidence was then gathered to either confirm or refute the possibility that both cycloheptatriene (**1**) and allene **9** were present and in equilibrium with one another.

1.3.5.1. Equilibrium Studies

Jones and co-workers performed an INDO molecular orbital calculations on cycloheptatrienyliene (**1**) and allene **9** to determine their conformations.²⁶ Their results showed **1** to be planar (or nearly so) and **9** to have a twisted conformation (Figure 1-7). In addition, allene **9** can be seen to have two possible enantiomeric structures. This study is incorporated in the following MNDO study.

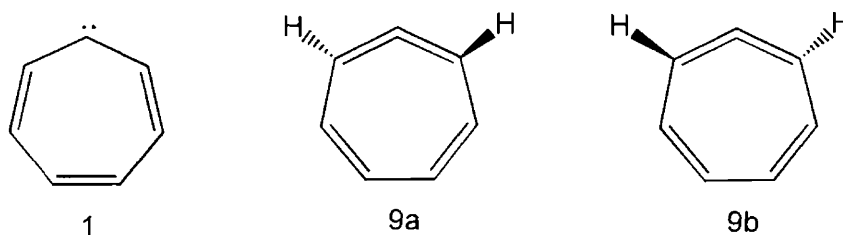


Figure 1-7. Carbene **1** and Two Isomers of **9**

MNDO molecular orbital calculations performed by Waali showed the singlet state allene **9** to be more stable than the singlet state carbene (**1**) by 23 kcal/mole (Figure 1-8).²⁷ His calculations also showed the triplet state carbene to be more stable than singlet allene **9**. What is more important, the calculations suggested the carbene to be a *transition state* for racemization of **9a** and its enantiomer **9b**.

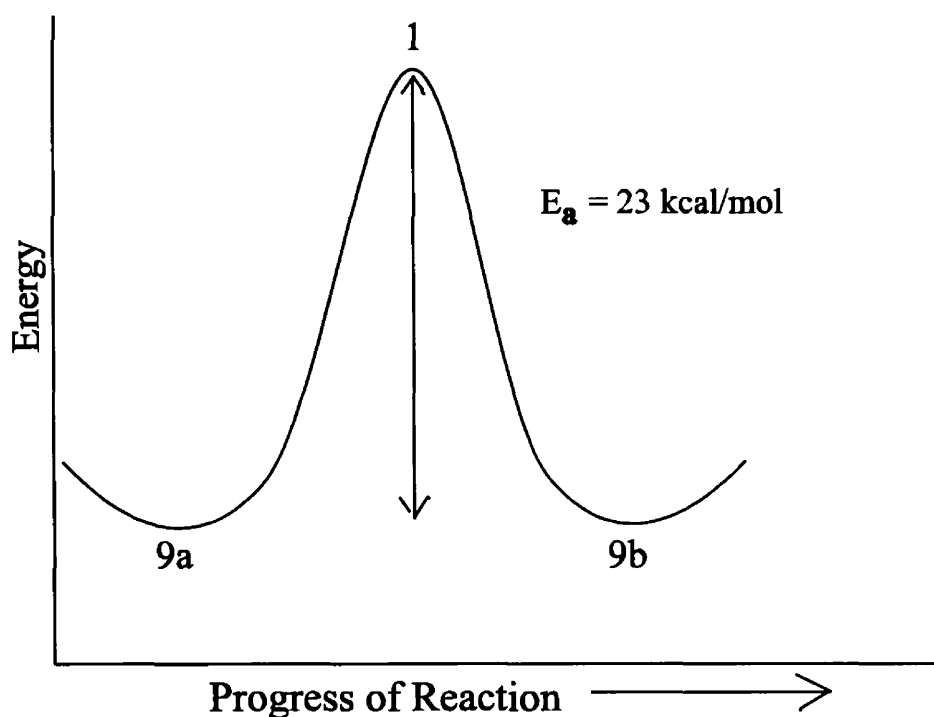


Figure 1-8: Energy Diagram Indicating a Carbene Transition State

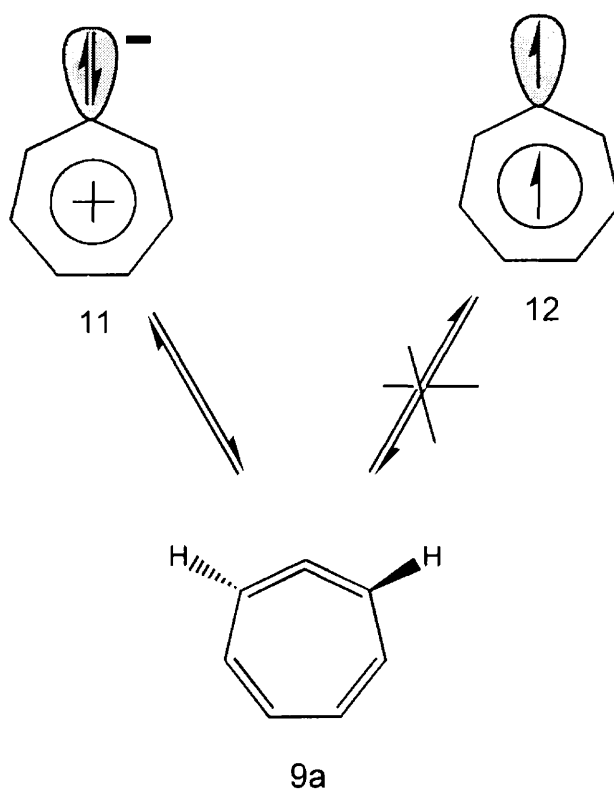
Calculations performed by Schaeffer and co-workers contradicted these results by showing cycloheptatrienyldiene (**1**) to be an intermediate.²⁸ Their calculations showed singlet state carbene **1** to be more stable than the triplet state carbene (thus suggesting a ground state singlet carbene responsible for reaction).

McMahon and Chapman performed an Electron Spin Resonance (ESR) study.²⁹ They observed the triplet state carbene **12** in the decomposition of lithium salt of tropone tosylhydrazone and found no evidence for the isomerization of it to the allene **9** or any other singlet state carbene intermediate. This indicated that triplet **12** was the ground state (Scheme 4). However, an interconversion between the singlet state carbene and the allene remained possible.

Wentrup and co-workers reproduced McMahon and Chapman's results, observing the triplet state carbene **12** by Electronic Spin Resonance (ESR) spectroscopy and suggesting a triplet ground state carbene.³⁰

At this point, evidence strongly indicated **1** and **9** were not in equilibrium.

Scheme 4: Carbene/Allene Isomerization



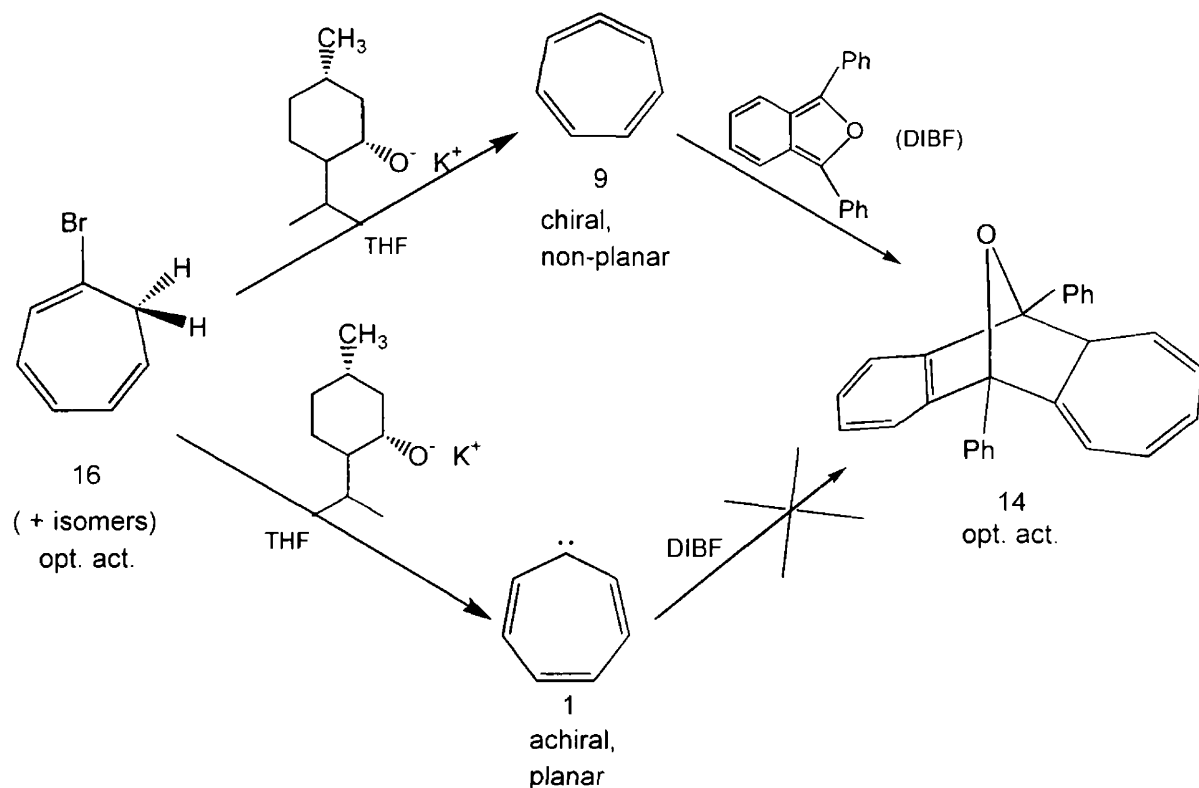
1.3.6. Definite Allene Presence

1.3.6.1. Optical Activity Study

Harris and Jones reported definitive evidence that the allene intermediate must be present in the reactions.³¹ The structure of allene **9** had been calculated to be non-planar

and chiral, and carbene **1** was calculated to be planar and achiral.²⁶ If these calculations were correct, only allene **9** could generate an optically active adduct. The planar carbene was incapable of generating optically active adducts. Harris and Jones created a THF solution of a mixture of 1-, 2-, and 3-bromocycloheptatrienes **16** and allowed it to react with the potassium salt of (+)-menthol (optically active), in the presence of DIBF, in hopes of generating an excess of one of the enantiomeric adducts (Scheme 5). The isolated adducts were indeed found to be optically active, suggesting the allene intermediate was definitely present.

Scheme 5. Optical Activity Study



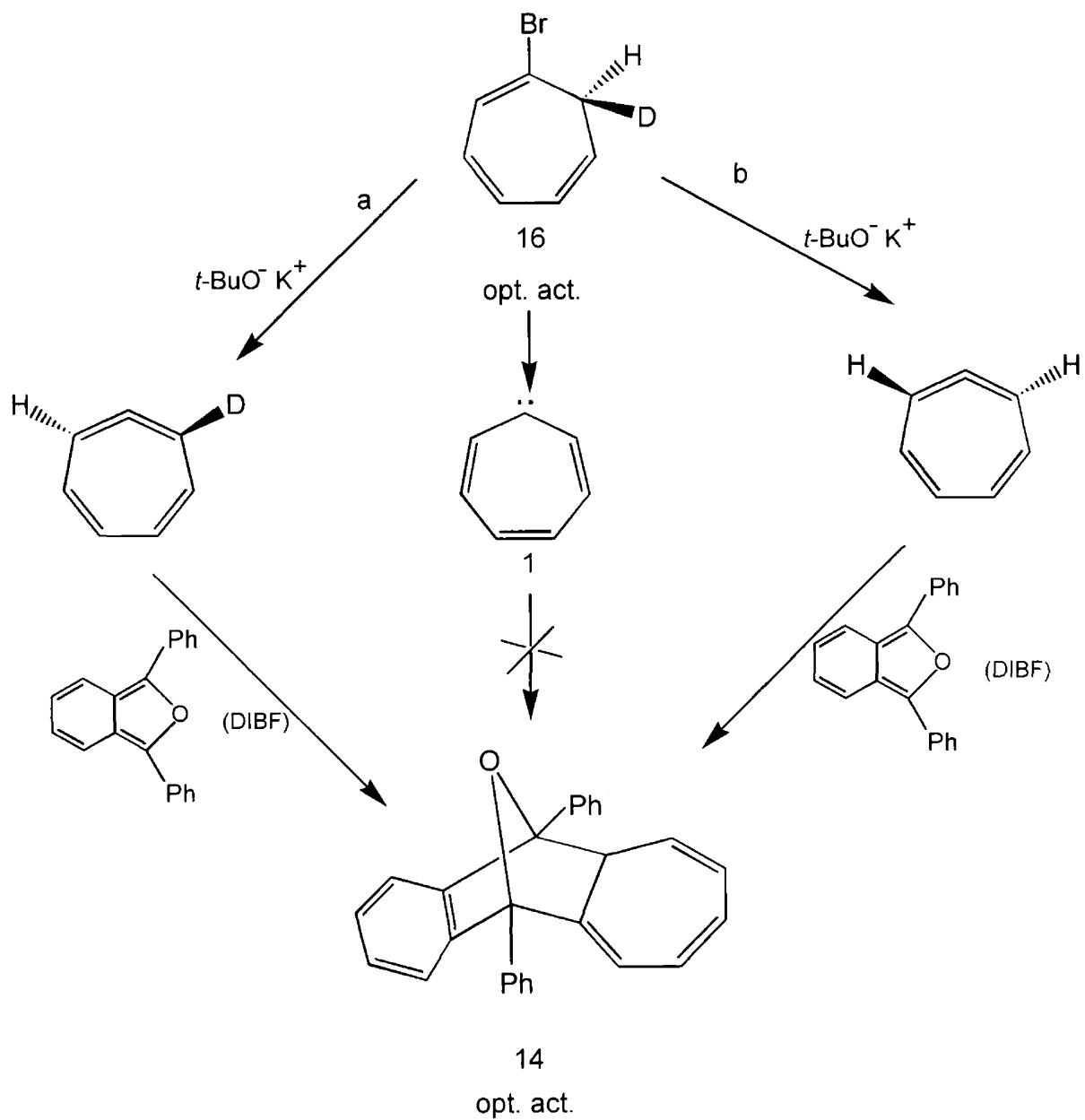
This was not conclusive evidence of an allene presence, however, because the presence of menthol can create a chiral environment during cycloaddition.

1.3.6.2. Isotope Study

In order to obtain unequivocal evidence of the presence of an allene intermediate, Harris and Jones then designed a reaction taking advantage of the primary deuterium isotope effect. Their goal this time was to generate an enantiomeric excess of the intermediate. They prepared a mixture of optically active 1-bromo-7-deuteriocycloheptatriene (deuterated **16**, stereochemistry is assumed) by reducing 7,7-dibromocycloheptatriene with LiAlD_3 ·(-)-quinine (Scheme 6). Following allene formation, an excess of one enantiomer over the other should result since the elimination of HBr from **16** (path a) will yield one enantiomer, and the elimination of DBr would yield the other (path b). This was indeed the case. Reaction of **16** with 1,3-diphenyl-isobenzofuran (DIBF) in potassium *t*-butoxide and tetrahydrofuran (THF) yielded optically active **14** (optical activity was determined qualitatively). Again, the carbene could be disregarded as the possible intermediate because of its planar, achiral structure.

Evidence was now strongly in favor of the allene (**9**) as being the sole intermediate.

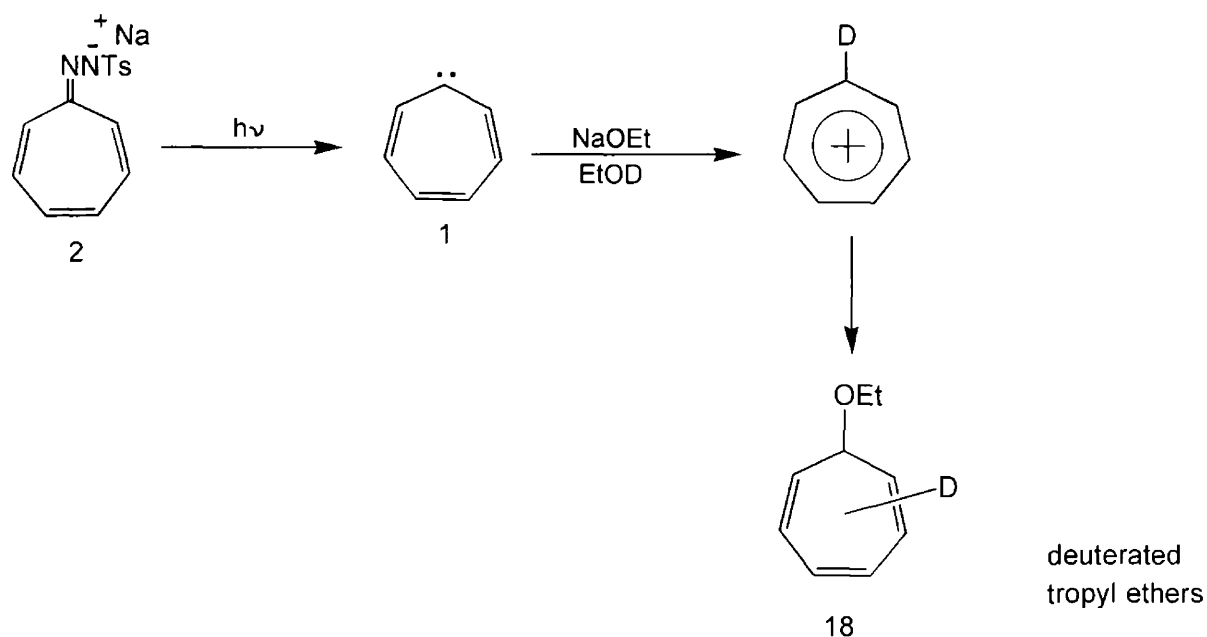
Scheme 6. Isotope Study Results



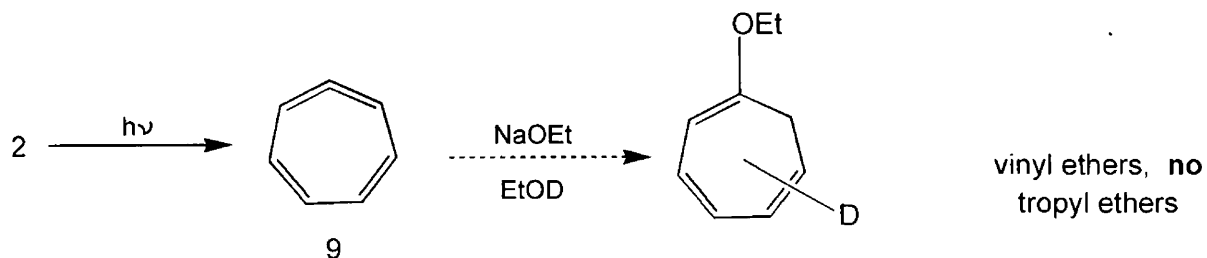
1.3.7. Carbene Makes a Come-Back

Kirmse and Sluma reported evidence that carbene **1** may be present in these reactions after all. They observed that the photolysis of sodium salt of tropone tosylhydrazone (**2**) in the presence deuterated ethanol yielded the deuterated tropyl ether **18** (Scheme 7).³² They suggested that the carbene intermediate proceeded through the tropylium ion and trapped the deuterated alcohols to yield **18**. If allene **9** was present in these reactions, *vinyl* ethers should have also resulted because available evidence indicated vinyl ethers resulted from the reaction of cyclic allenes with alcohols (Scheme 8). It was therefore suggested by Kirmse that "the nucleophilic of the carbene is trapped from an unfavorable equilibrium with the allene by protonation."

Scheme 7. Carbene Intermediate Yielding Tropylium Ions



Scheme 8. Allene Intermediate Yielding Vinyl Ethers



This carbene trapping was questioned by Waali.³³ He suggested that "the nature of the HOMO of **9** is consistent with the observed chemistry" (protonation to yield **14**; Scheme 5). Waali concluded that all of the chemistry previously attributed to the singlet state of **1** should instead be explained in terms of the nonplanar allene **9**.

1.3.8. Summary of the Evidence

The preceding sections (Sections 1.3.1. through 1.3.7.) described how the literature oscillated in its indications as to whether a carbene intermediate or an allene intermediate were present in the decomposition of sodium salt of tropone tosylhydrazone (**2**) and the dehydrohalogenation of 2-chlorocycloheptatriene (**8**) (Scheme 1; Section 1.3.2.). First, only a carbene intermediate (cycloheptatrienylidene **1**) was considered (Section 1.3.2.). An allene intermediate was then proposed (Section 1.3.3.). Next, evidence was gathered under the suspicion that both of these intermediates were present and in equilibrium with one another (Section 1.3.5.). "Definitive evidence" of the presence of allene intermediate **9** in these reactions was then reported (Section 1.3.6.).

Now with this last interpretation from Kirmse and Sluma (Section 1.3.7.), carbene **1** again becomes a possible intermediate in these reactions. More evidence must be obtained to better determine through which intermediate system these reactions proceed.

A kinetic study is needed in order to determine whether these reactions proceed by way of a single intermediate or by two intermediates.

1.4. Objectives

A kinetic study was initiated to reveal the preferred pathway for the tropone tosylhydrazone reaction - by way of one intermediate or two intermediates.

1.4.1. Synthesis of Expected Products

The sodium salt of tropone tosylhydrazone (**2**) was decomposed by thermolysis in the presence of *n*-butyl alcohol. An alcohol was used because of Kirmse and Sluma's interpretation that singlet **1** reacts with alcohols to give tropyl ethers. If cycloheptatrienyliene (**1**) was an intermediate in this reaction, it would trap the alcohol to yield the butyl tropyl ether product **20** (Figure 1-9). The ideal alcohol must have a relatively high boiling point since the thermolysis reaction occurs at 100 °C. It is for this reason *n*-butyl alcohol was selected for this study (other primary alcohols with high boiling points may also have been used).

The sodium salt was then decomposed in the presence of 1,3-diphenylisobenzofuran (DIBF). This reaction has a purported allene intermediate mechanism (Section 1.3.6.), and yields DIBF product **14** (Figure 1-9).

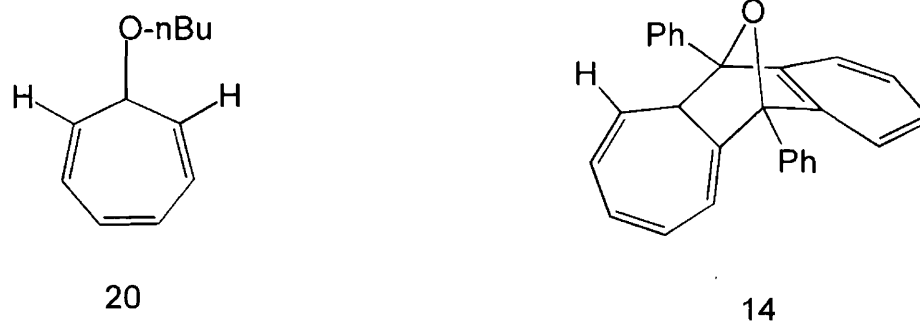


Figure 1-9. Butyl Ether Product **20** and DIBF Product **14**

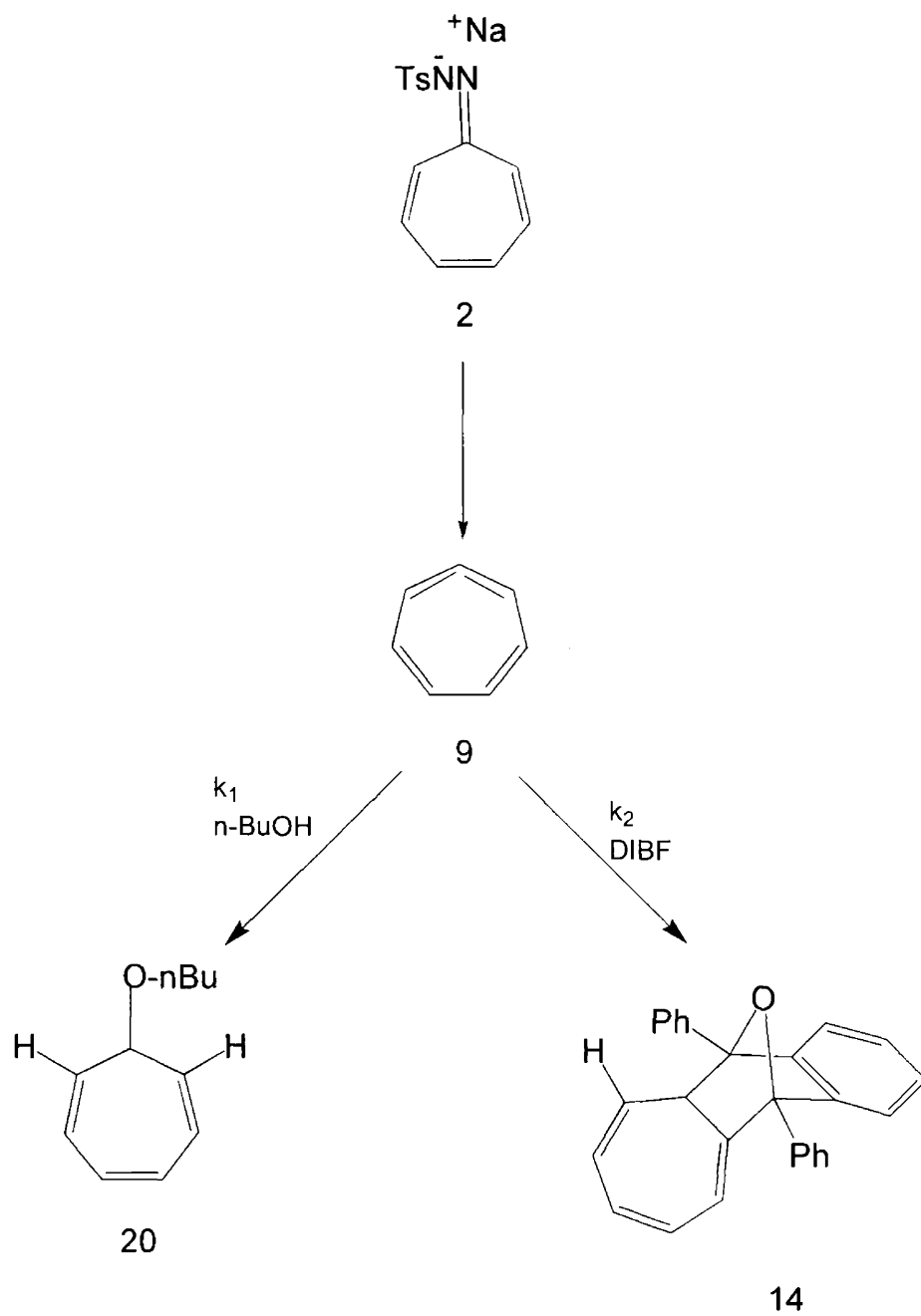
After ^1H NMR of the products in these first two thermolysis reactions confirmed the presence of the expected products, the kinetics reactions were initiated.

1.4.2. Kinetics Reactions

The sodium salt of tropone tosylhydrazone (**2**) was decomposed in the presence of varying concentrations of both the *n*-butyl alcohol and the DIBF. ^1H NMR spectra of the resultant reaction mixture was elucidated and the peaks representing products **20** and **14** were identified. Integration of these peaks yielded the ratio of the butyl ether product **20** to the DIBF product (**14**) (the significance of this will be examined shortly).

1.4.3. Intermediate Reaction Mechanisms

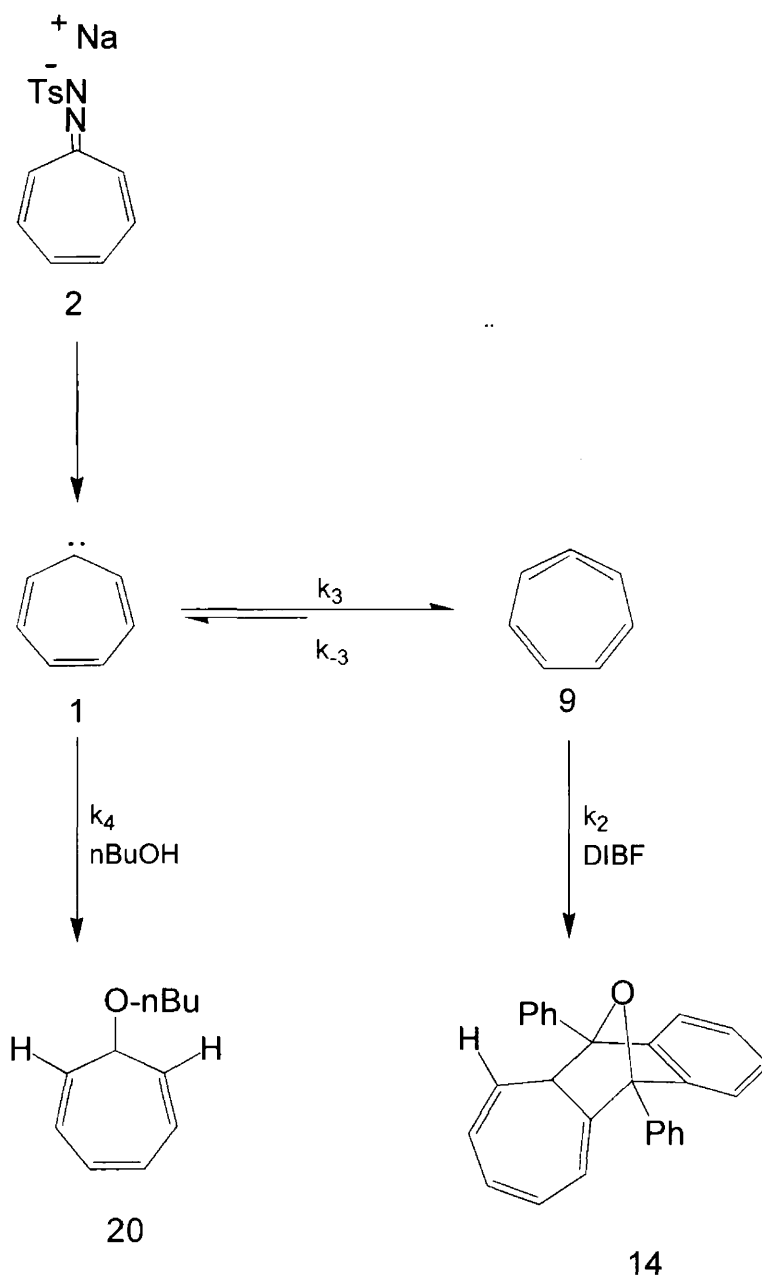
These kinetics reactions proceeded by way of one or two intermediates. The proposed single intermediate and two intermediate reaction mechanisms are depicted in **Scheme 9** and **Scheme 10**, respectively.³⁴

Scheme 9. Proposed Single Intermediate Mechanism

$$[20]/[14] = k_1[\text{BuOH}]/k_2[\text{DIBF}] \quad (22)$$

(Derivation in Appendix I)

Scheme 10. Proposed Two Intermediate Mechanism



$$[\mathbf{20}]/[\mathbf{14}] = (k_{-3}k_4[\text{BuOH}]/k_2k_3[\text{DIBF}]) + (k_4[\text{BuOH}]/k_3) \quad (23)$$

(Derivation in Appendix I)

1.4.4. The Role of Kinetics

After setting up the two possible intermediate mechanisms of the kinetics reactions, the steady state assumption theory of kinetics was employed to determine concentration ratios of butyl ether product **20** and DIBF product **14** (Appendix I). The calculated concentration ratios of the single intermediate mechanism (Equation 22) and the two intermediate mechanism (Equation 23) are shown below their respective schemes (Schemes 9 and 10, respectively).

The kinetics equations could now be put into "equation of a line" format ($y=mx+b$) to create expected graphs representing the two reaction mechanisms (Figure 1-10).

Single Intermediate Mechanism:

$$\frac{[\mathbf{20}]}{[\mathbf{14}]} = (k_1[\text{BuOH}]/k_2) (1/[\text{DIBF}]) \quad (22)$$

$$\mathbf{y} = \mathbf{m} \mathbf{x} + \mathbf{b}$$

Two Intermediate Mechanism:

$$\frac{[\mathbf{20}]}{[\mathbf{14}]} = (k_3k_4[\text{BuOH}]/k_2k_3) (1/[\text{DIBF}]) + (k_4[\text{BuOH}]/k_3) \quad (23)$$

$$\mathbf{y} = \mathbf{m} \mathbf{x} + \mathbf{b}$$

Figure 1-10. Kinetics Equations in Equation of a Line Format

By varying the concentrations of the *n*-butyl alcohol and the DIBF, and by measuring the concentration ratio between the products ($[\mathbf{20}]/[\mathbf{14}]$), data points were then placed on graphs.

In the case of the single intermediate mechanism, no *y*-intercept (**b**) should be observed (Equation 22). The expected graph would appear as in **Figure 1-11**, where all lines have a *y*-intercept of zero. (Slopes are arbitrary in this graph.)

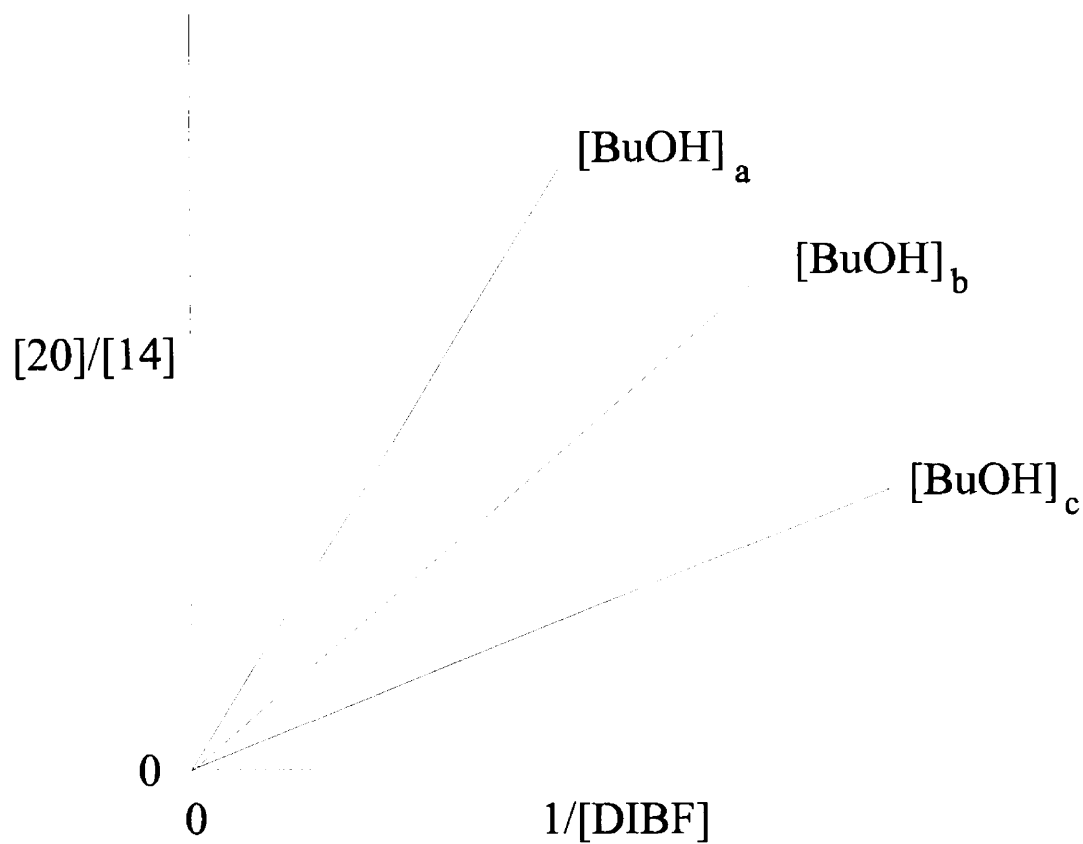


Figure 1-11. Plot of a Single Intermediate Mechanism (Scheme 9)

In the case of a two-intermediate mechanism, all y -intercepts should be non-zero and non-equivalent to one another. The expected graph would appear as in **Figure 1-12**.

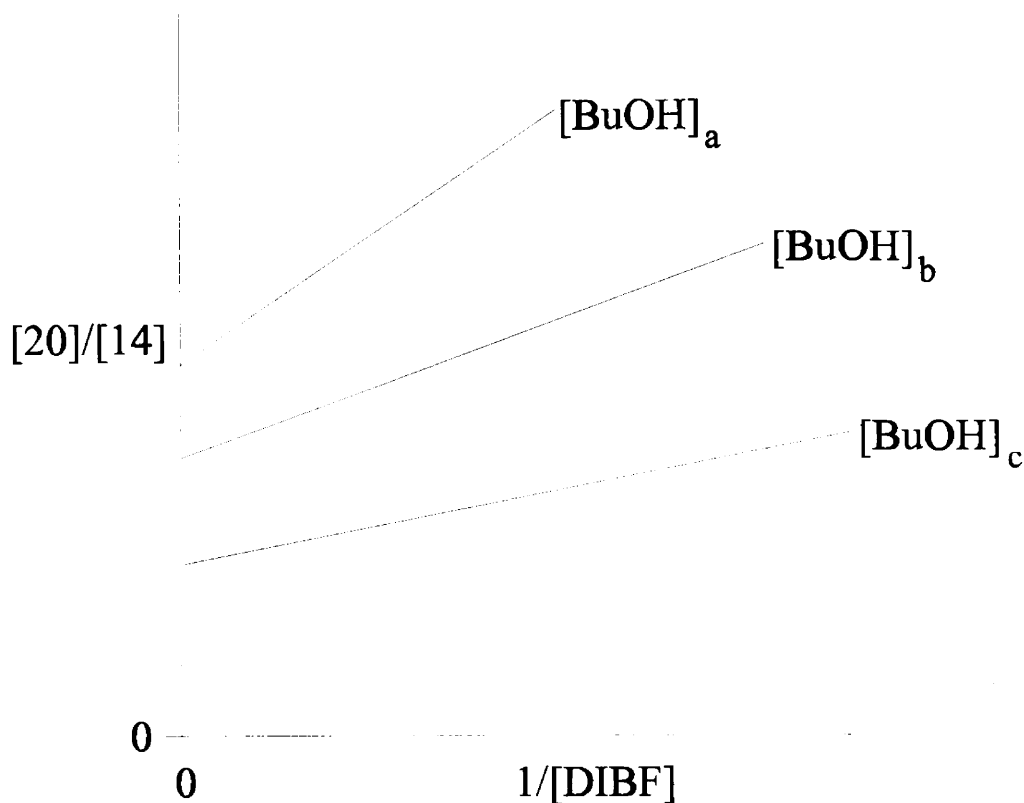


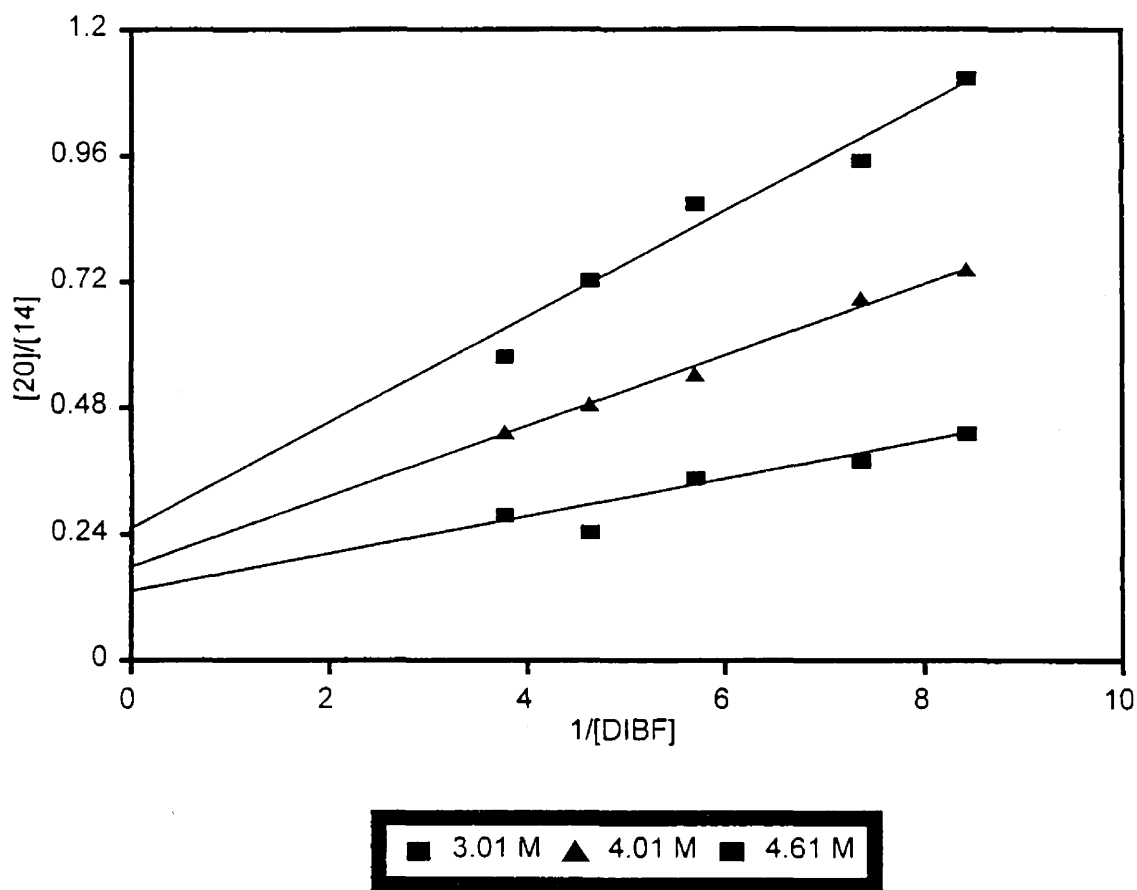
Figure 1-12. Plot of a Two Intermediate Mechanism (**Scheme 10**)

1.5. Preliminary Results of Zepp

Preliminary results of a kinetic study performed by Zepp are shown in **Table 1**, along with the corresponding graph of his data in **Figure 1-13**.³⁴ This data indicated the kinetics reaction proceeded by way of a two-intermediate mechanism. The preliminary results were obtained on an NMR spectrometer that was much less sensitive than the one available currently. Since the results of this kinetic study depended heavily upon spectral identification of the expected products, it became necessary to further the kinetic study in order to gain unequivocal evidence of the presence of a two-intermediate system using a much more sensitive, more reliable spectrometer.

Table 1. Data of Zepp (observing one DIBF product)

<u>[BuOH]</u>			
<u>3.01 M</u>	<u>4.01 M</u>	<u>4.61 M</u>	<u>1/[DIBF]</u>
0.38	0.69	0.95	7.36
0.25	0.49	0.72	4.63
0.43	0.75	1.11	8.42
0.35	0.55	0.87	5.70
0.28	0.44	0.58	3.78

**Figure 1-13.** Preliminary Results of Zepp³⁴

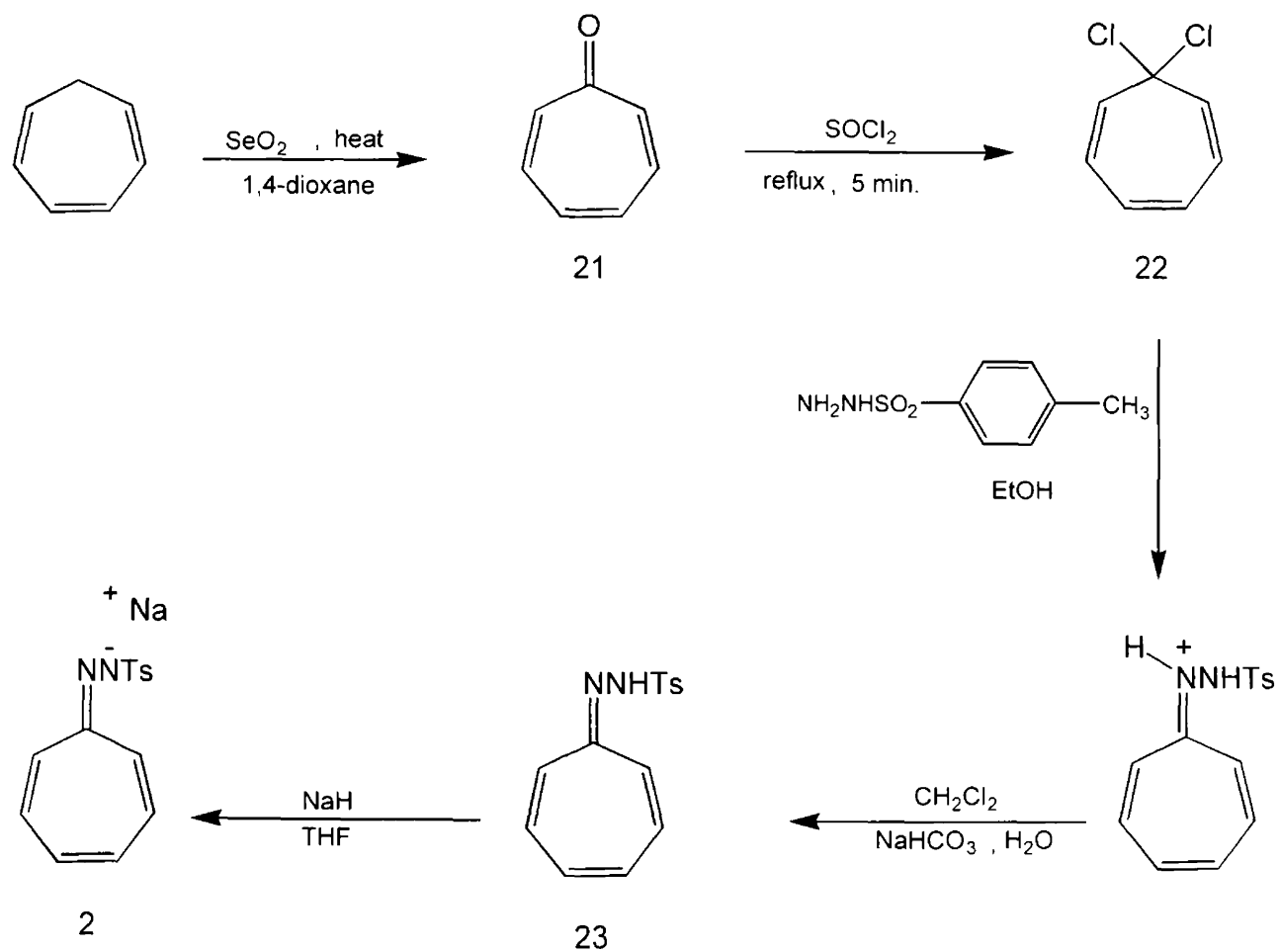
The graph of Zepp's preliminary results was consistent with that of a two-intermediate reaction mechanism.³⁴ The current study was performed in order to support or contradict the suspicion that this reaction did indeed proceed by way of a two-intermediate mechanism.

2. Results and Discussion

2.1. Synthesis of the Sodium Salt of Tropone Tosylhydrazone (2)

The synthetic route to the sodium salt **2** used in this study is shown in **Scheme 11**.^{18,38}

Scheme 11. Synthesis of Sodium Salt of Tropone Tosylhydrazone (**2**)

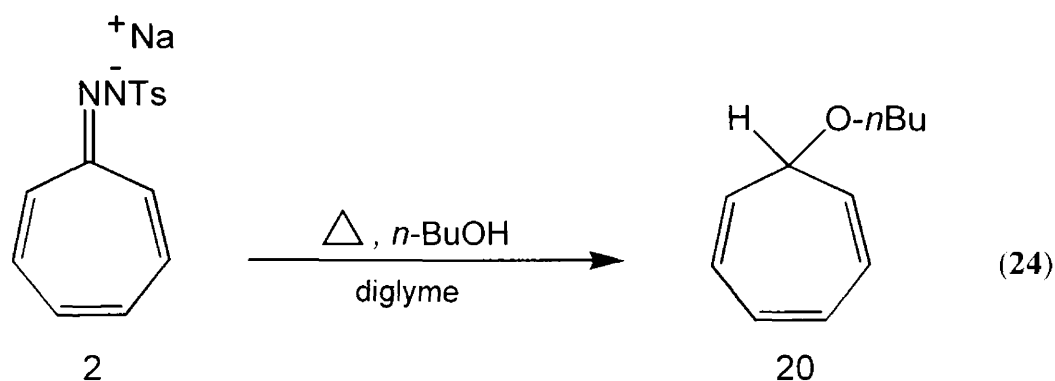


Once **2** was synthesized, the next step required the synthesis of the two expected products in this kinetic study, the butyl ether product **20** and the DIBF product **14**.

2.2. Synthesis of the *n*-Butyl Tropanyl Ether (**20**)

One of the expected products synthesized is the butyl ether product **20**. In order to confirm the reaction mechanisms, this product was prepared using two methods.

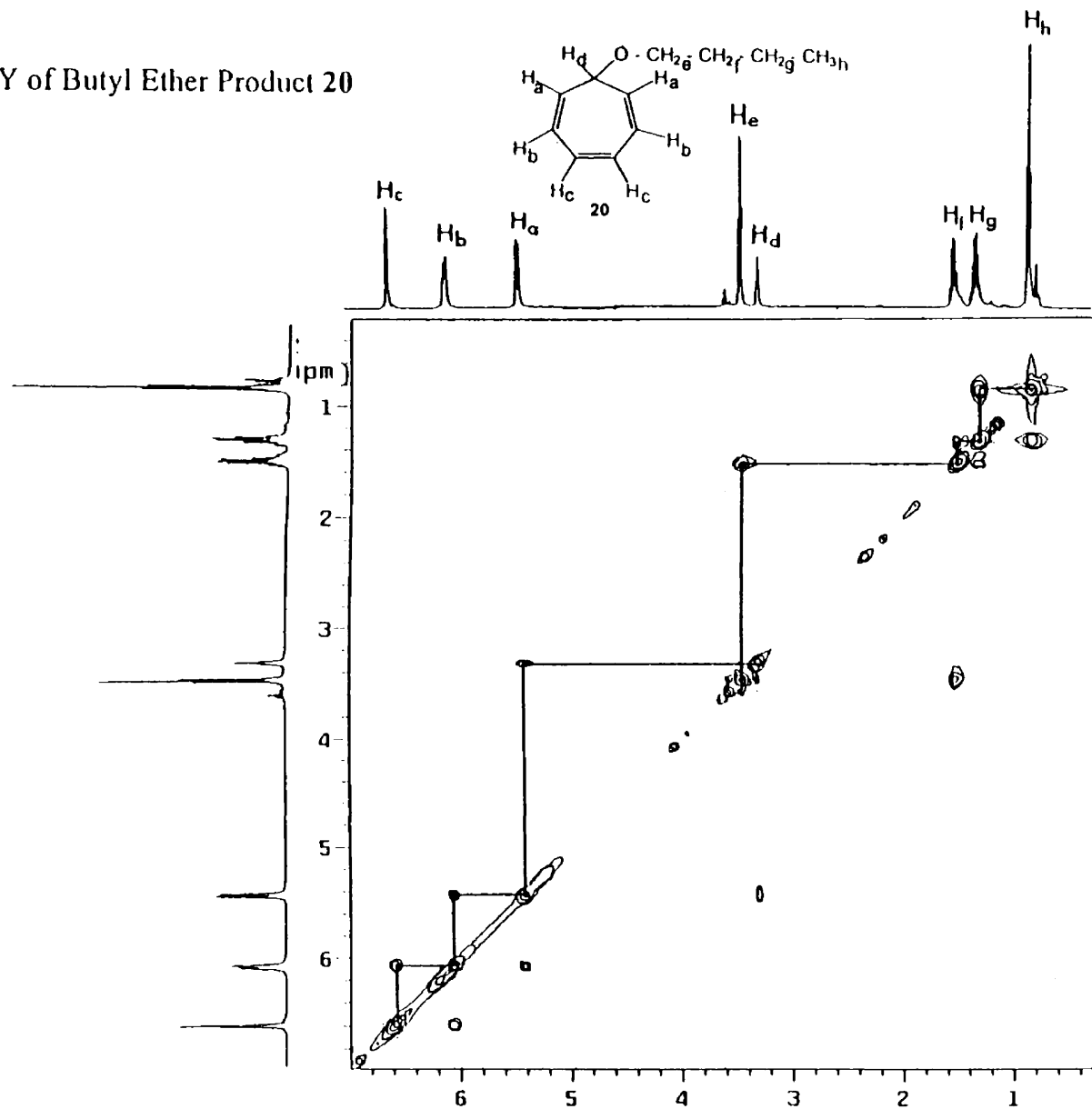
Method 1: Generation of **20** from sodium salt of tropone tosylhydrazone (**2**)³²



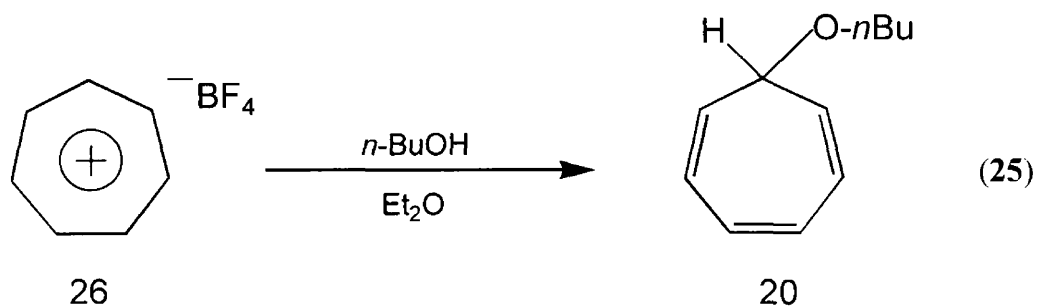
This sample was then purified by column chromatography and thin-layer chromatography (TLC).

In order to confirm the chemical shifts obtained by *Method 1*, **20** was then synthesized by another method known to yield tropanyl ethers (Equation 25). The chemical shift of each proton in this product was determined by 1-D and 2-D COSY NMR (Figure 2-1).

Figure 2-1. COSY of Butyl Ether Product 20



Method 2: Generation of **20** from tropylium tetrafluoroborate (**26**)



The spectra of both butyl ether products, generated from different precursors, were identical (Figure 2-3).

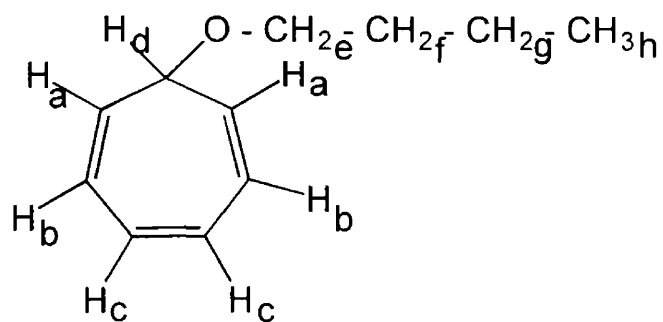
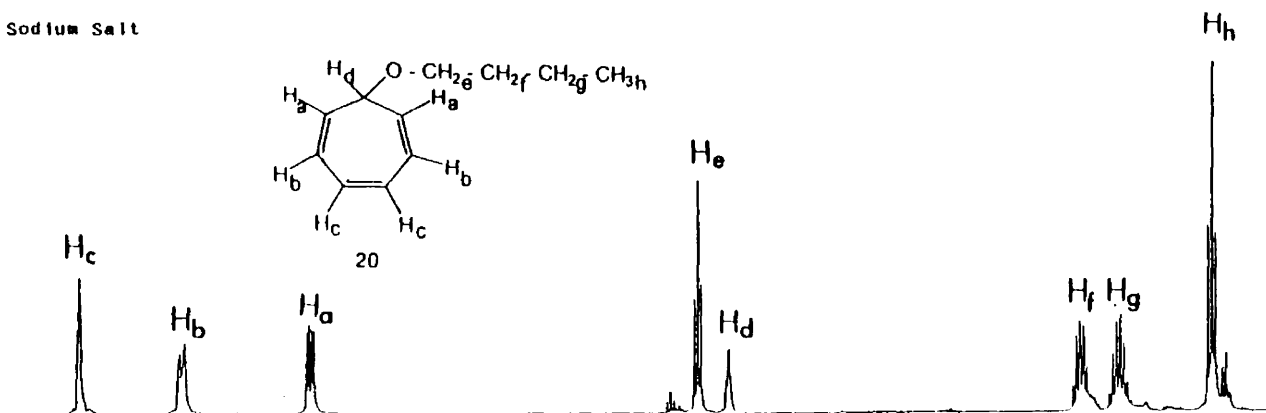


Figure 2-2. Butyl Ether Product **20**

The proton chemical shifts of **20** are listed in **Table 2**.

Figure 2-3. Spectra of Butyl Ether Product 20 from Two Precursors

Butyl Ether Product from Sodium Salt



Butyl Ether Product from TrBF₄

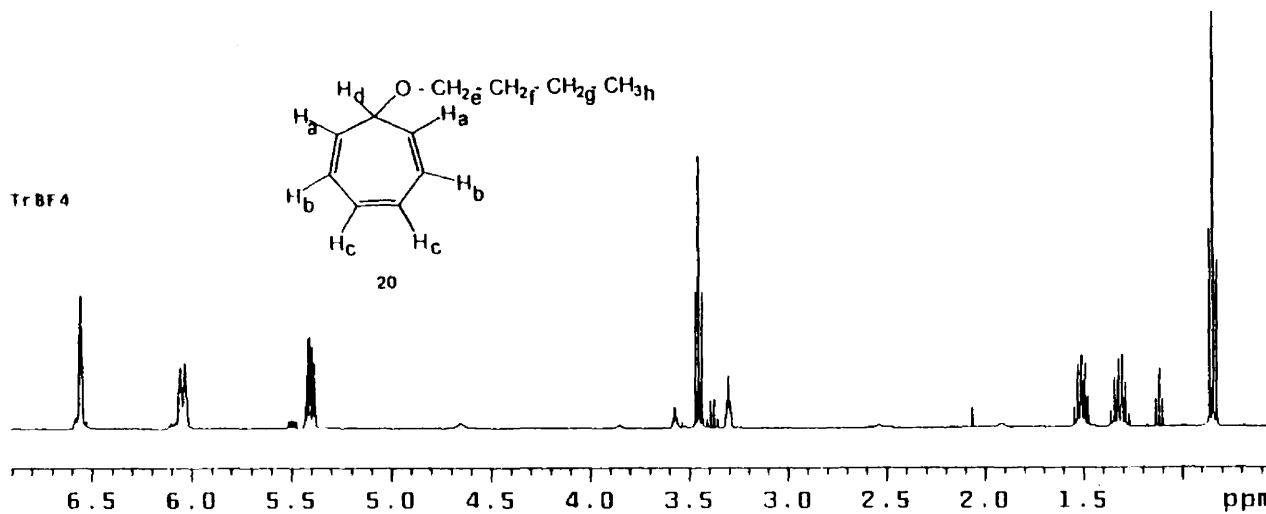


Table 2. Chemical Shifts of Butyl Ether Product **20**

<u>proton</u>	<u>δ(ppm)</u>	<u>pattern</u>	<u>coupling constant</u>
H _a	5.40	d of d	$J_{ab} = 9.50$
H _b	6.05	d of d	$J_{bc} = 9.62$
H _c	6.56	m	
H _d	3.30	m	
H _e	3.44	t	$J = 6.57$
H _f	1.50	p	$J = 7.46$
H _g	1.31	h	$J = 7.51$
H _h	0.84	t	$J = 7.50$

2.3. Bitropyl Formation

Analysis of the 1-D spectrum of the butyl ether product **20** produced from **2** (Equation 24) indicated the presence of a by-product. This by-product was theorized to be bitropyl. Bitropyl (**24**) was synthesized through an alternative, known method (Figure 2-4).³⁵ Its spectrum was compared to that of **20**. The chemical shifts of the by-product evident in the spectrum of **20** were consistent with those of **24** (Figure 2-5).

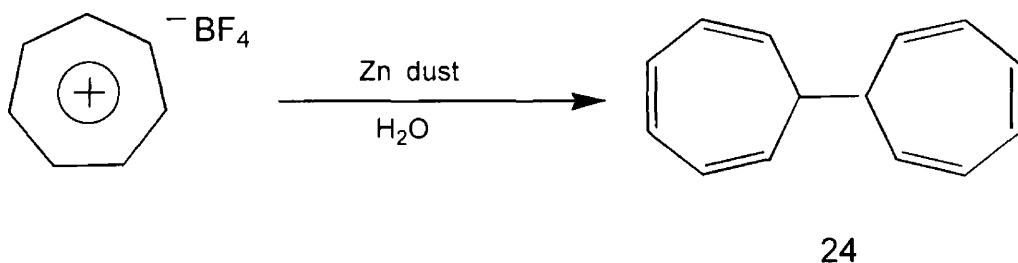
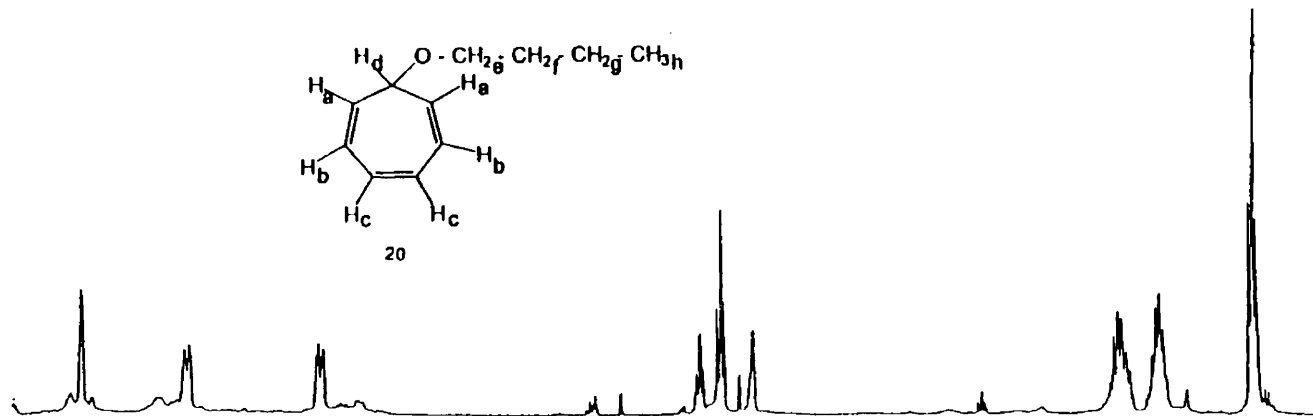
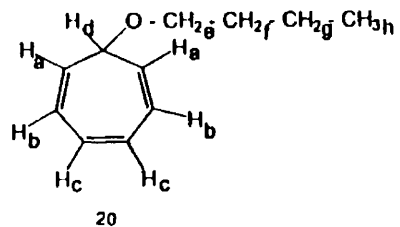
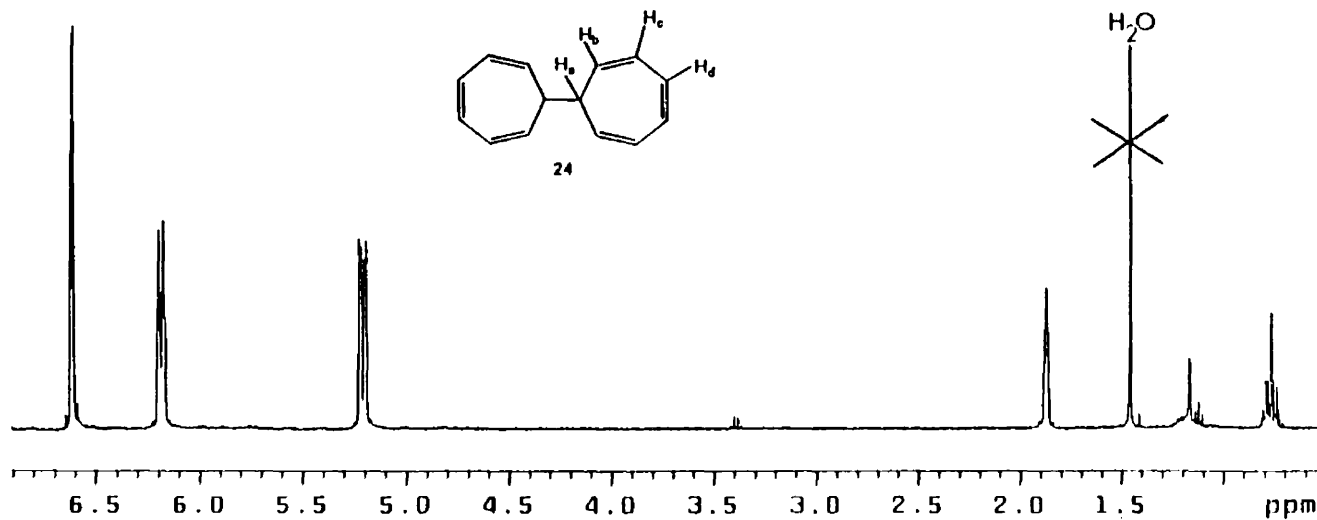
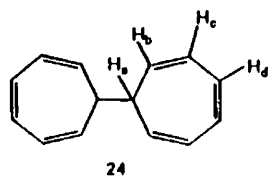
**Figure 2-4.** Alternative Bitropyl Synthesis

Figure 2-5. Spectra of Butyl Ether Product 20 and Bitropyl (24)

Butyl Ether Product



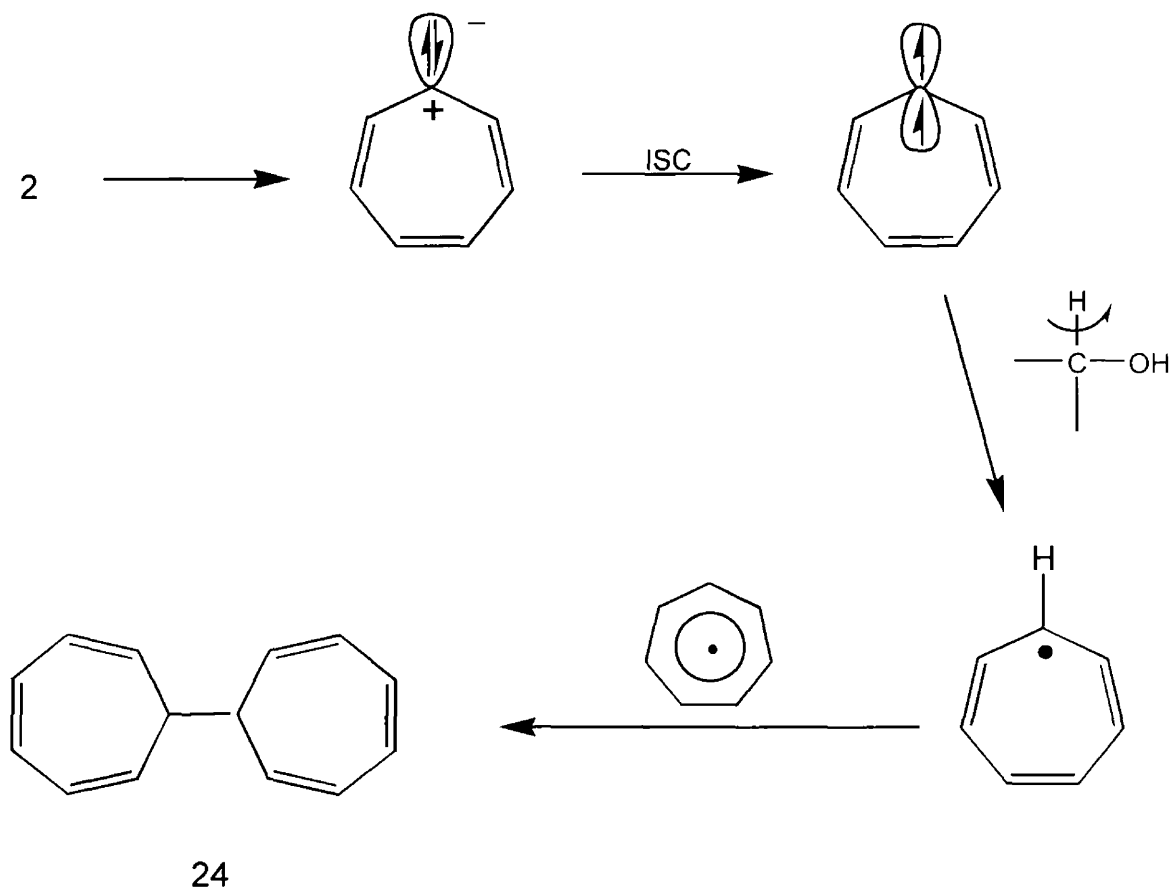
Bitropyl



A COSY spectrum was also obtained for bitropyl (**24**) and is shown in **Figure 2-6**.

The most likely mechanism of the formation of the bitropyl is shown in **Scheme 12**.

Scheme 12. Bitropyl Formation

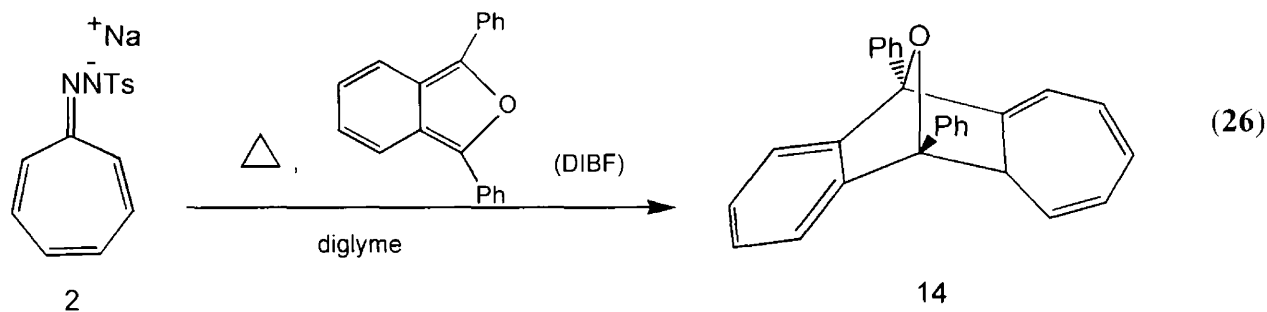


The singlet state carbene intersystem crosses (ISC) to the triplet state, which in turn abstracts a hydrogen atom from the *n*-butyl alcohol to form the tropanyl radical. This free radical dimerizes to bitropyl (**24**). The chemical shifts for the protons in bitropyl are reported in **Section 4.7**.

2.4. Elucidation of the Structures of the DIBF Product (14)

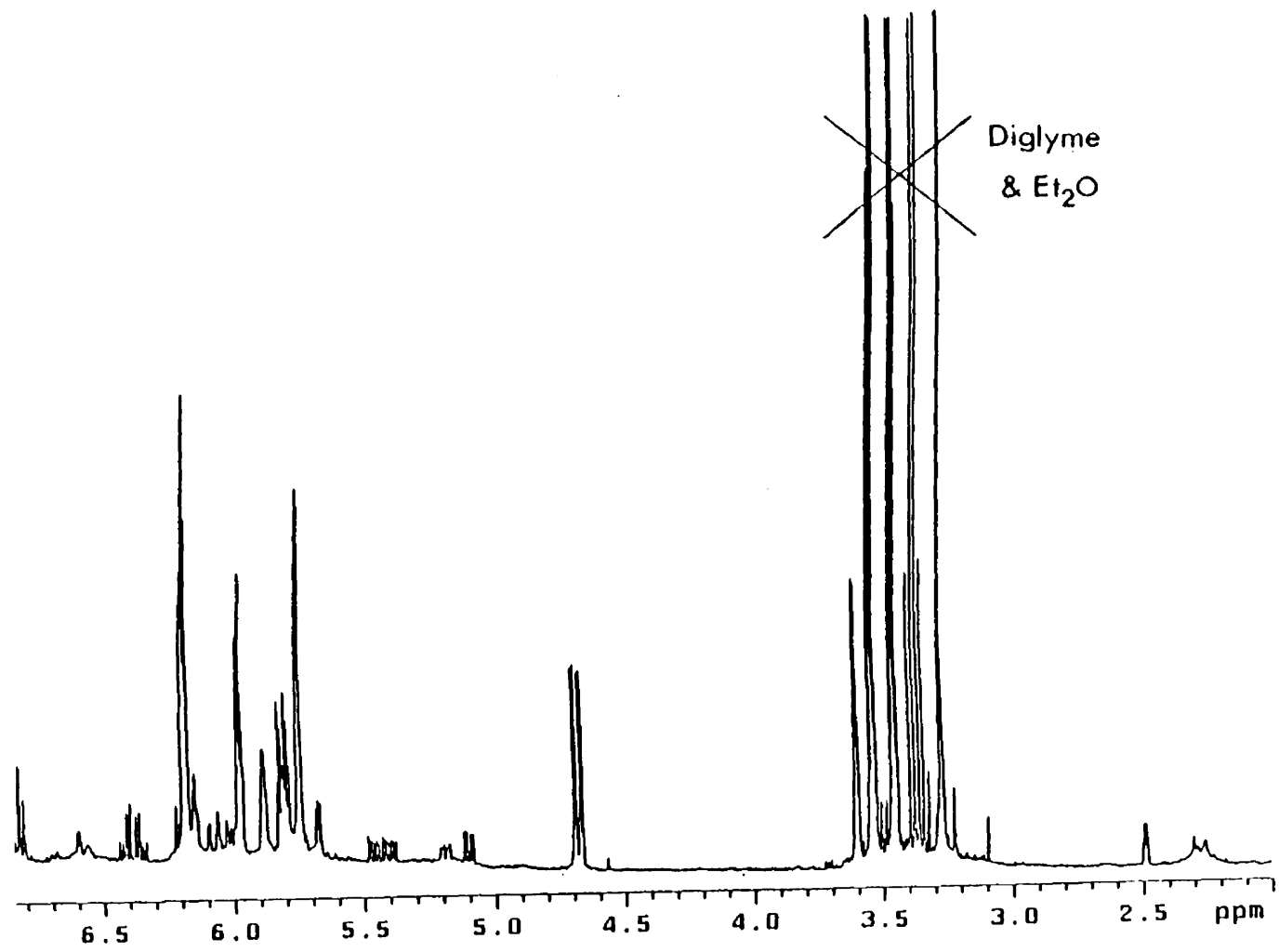
2.4.1. Isomers Discovered

The other expected product in this study is the DIBF adduct (**14**). This was synthesized by thermolysis of **2** in diglyme in the presence of 1,3-diphenylisobenzofuran (DIBF).



A 1-D ^1H NMR spectrum was obtained for the crude product (Figure 2-7). This spectrum indicated the presence of at least three products in this reaction. The protons at δ 4.7, 5.1, and 5.2 ppm did not exhibit a 1:1:1 ratio. Given the structure of **14**, there should have been five protons in the alkene region of the spectrum exhibiting equal areas. The fact that there are additional unexpected peaks in the alkene region (not in an equivalent ratio with the expected peaks) leads to the conclusion that there was more than one product generated in this reaction. **Figure 2-7** was not consistent with the spectrum that would have been expected if only one product was present.

Figure 2-7. 1-D Spectrum of the Crude DIBF Reaction Mixture



The 2-D COSY spectrum of the crude product (Figure 2-9) was also consistent with the presence of three separate compounds in the DIBF reaction.

The DIBF products then underwent column chromatography and TLC. The compounds containing the protons at δ 4.7 ppm and δ 5.1 could not be separated. The third product at δ 5.4 ppm was unstable and not seen after chromatography. Since the two surviving compounds were not separable by column chromatography and TLC, it was hypothesized that they were isomers of **14**. As can be seen in **Figure 2-8**, isomers of **14** are possible (exo and endo structures, depending upon the position of H_a).

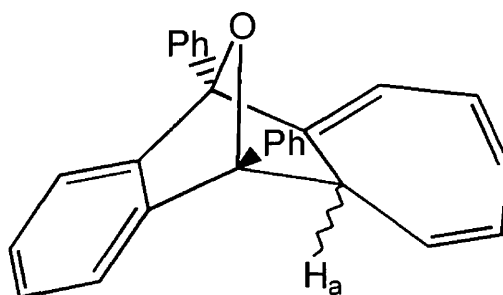


Figure 2-8. Isomers of **14** Possible

The products **14a** and **14b** were successfully separated by HPLC. A chromatogram of this separation is shown in **Figure 2-10**. Hydrogen 1-D spectra of the isomers before and after separation by HPLC are shown in **Figure 2-11**.

Figure 2-9. COSY Spectrum of the Crude DIBF Reaction Mixture Before Chromatography

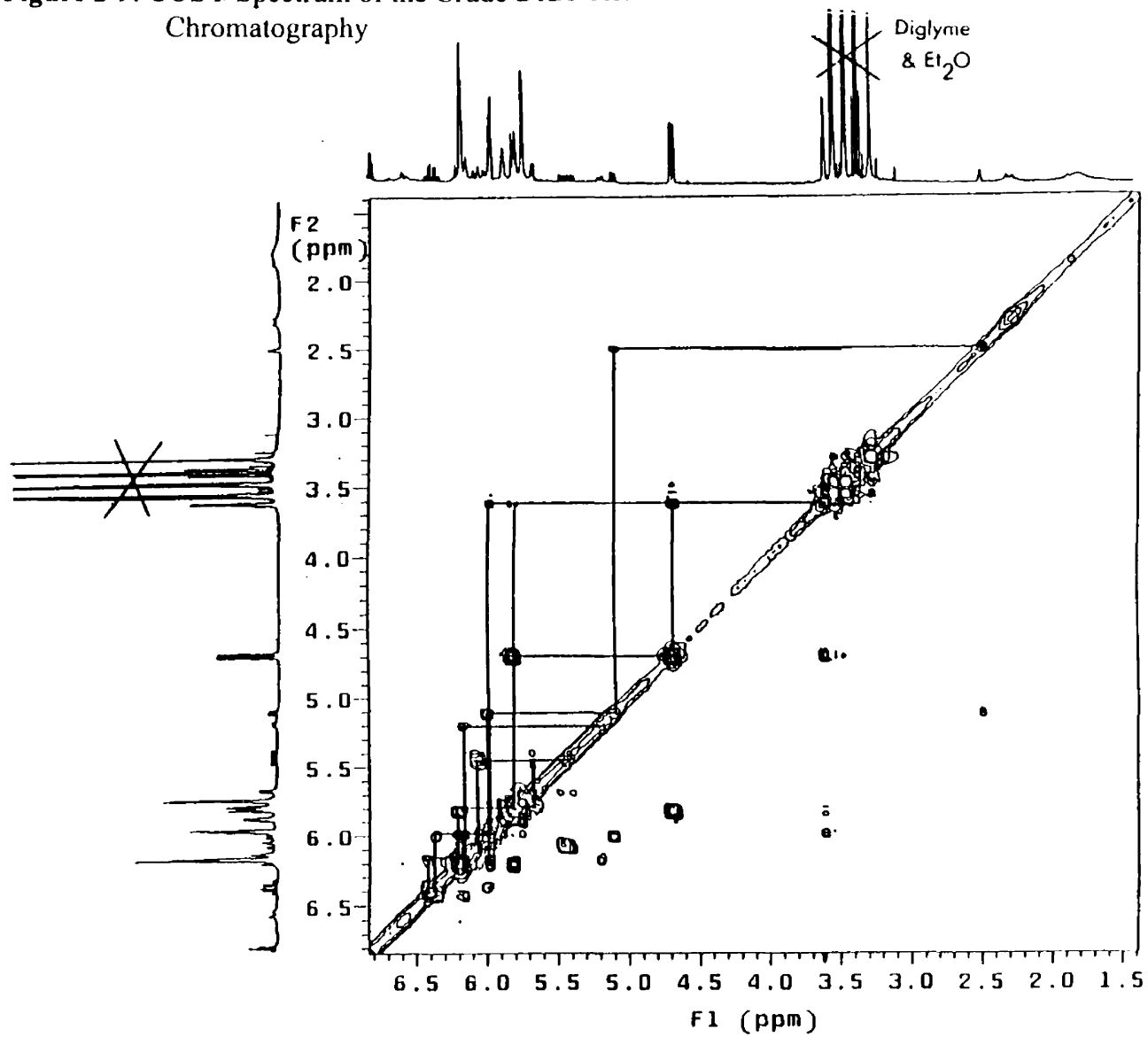


Figure 2-10. HPLC Chromatogram of Isomer Separation

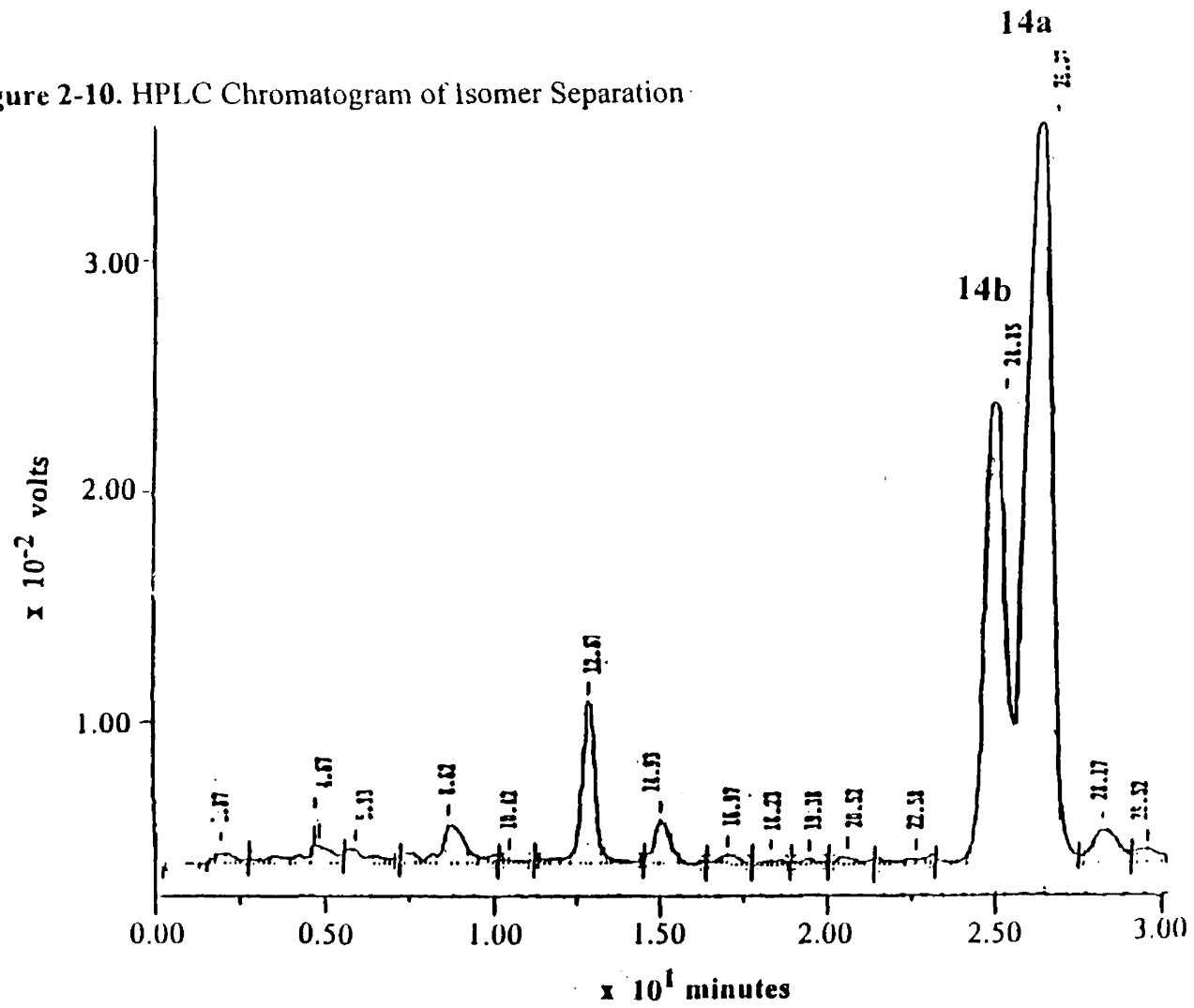
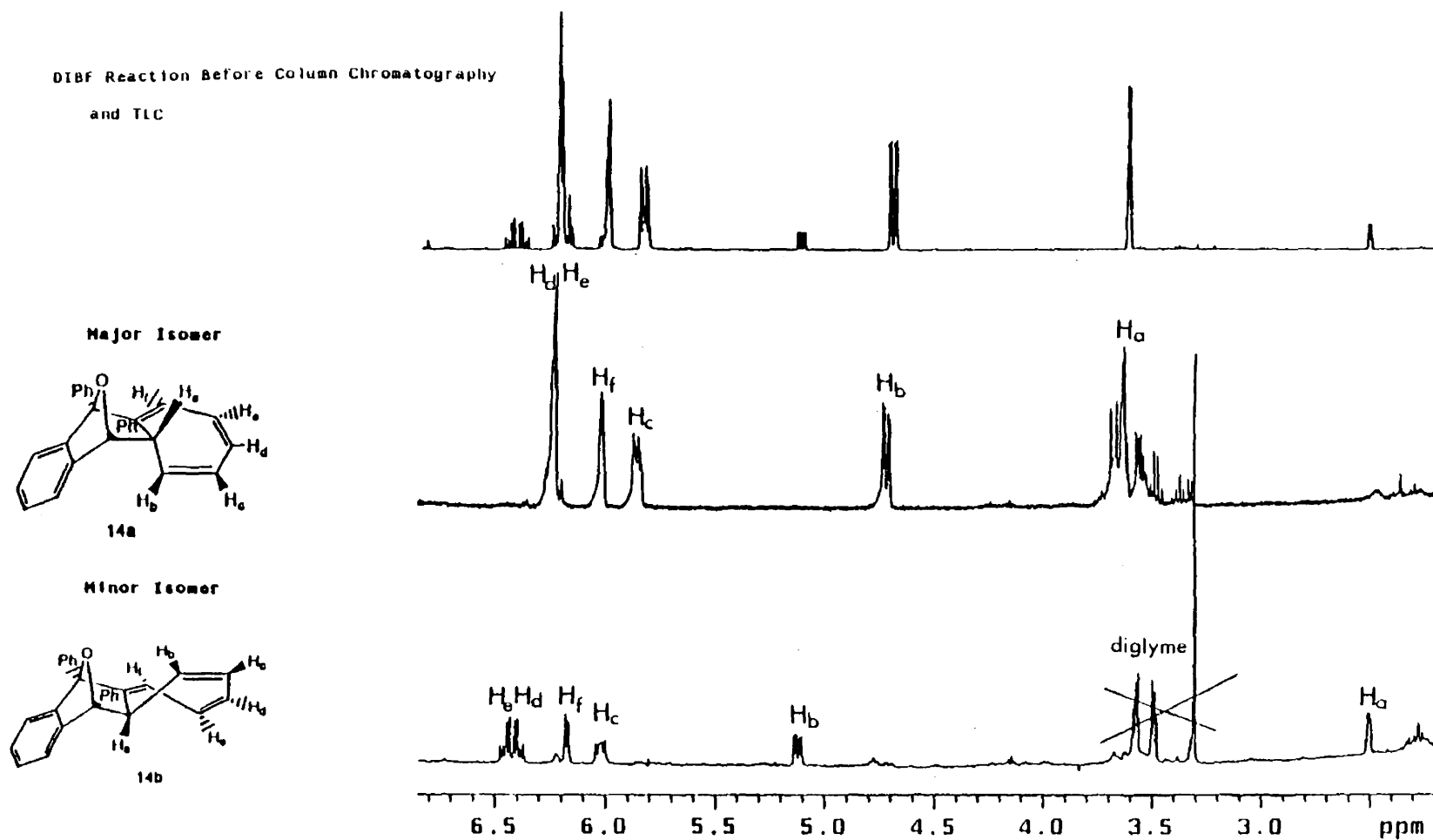


Figure 2-11. Spectra of the DIBF Isomers



A COSY spectrum of the isomers after column chromatography and TLC was obtained and is shown in **Figure 2-12**. A COSY spectrum of the minor isomer (**14b**) was obtained after HPLC and is shown in **Figure 2-13**.

The chemical shifts of the protons of each isomer were determined and placed in **Table 3**.

Table 3. Chemical Shifts of the Major and Minor Isomers

Major Isomer (14a): (d = doublet, d of d = doublet of doublets, m= multiplet)

<u>proton</u>	<u>δ (ppm)</u>	<u>pattern</u>	<u>coupling constant (Hz)</u>
H _a	3.64	d	$J_{ab} = 3.69$
H _b	4.73	d of d	$J_{bc} = 9.72$
H _c	5.85	m	$J_{cd} = 9.87$
H _d	6.23	m	
H _e	6.22	m	
H _f	6.01	m	

Minor Isomer (14b):

H _a	2.54	d	$J_{ab} = 4.35$
H _b	5.14	d of d	$J_{bc} = 9.58$
H _c	6.02	d of d	$J_{cd} = 10.78$
H _d	6.41	d of d	$J_{de} = 10.93$
H _e	6.44	d of d	$J_{ef} = 11.06$
H _f	6.20	d	

As can be seen in **Table 3**, these two isomers became known as the major and minor isomer (**14a** and **14b**, respectively). These designations were assigned in lieu of the fact that the proton belonging to **14a** (δ 4.7 ppm) exhibited the larger peak area in the 1-D NMR spectrum. The transient signal at δ 5.4 ppm will be discussed shortly.

Figure 2-12. COSY Spectrum of DIBF Product's Isomers after Column Chromatography and TLC

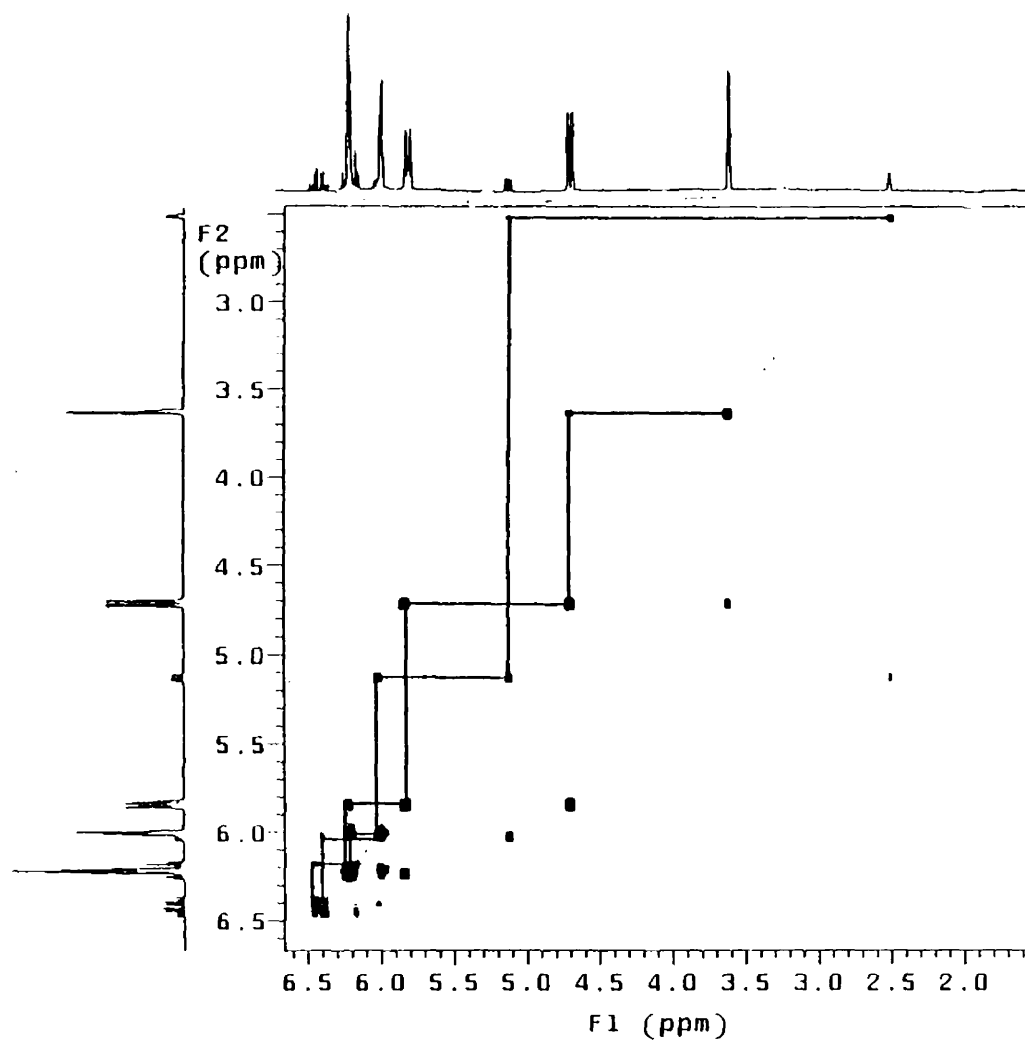
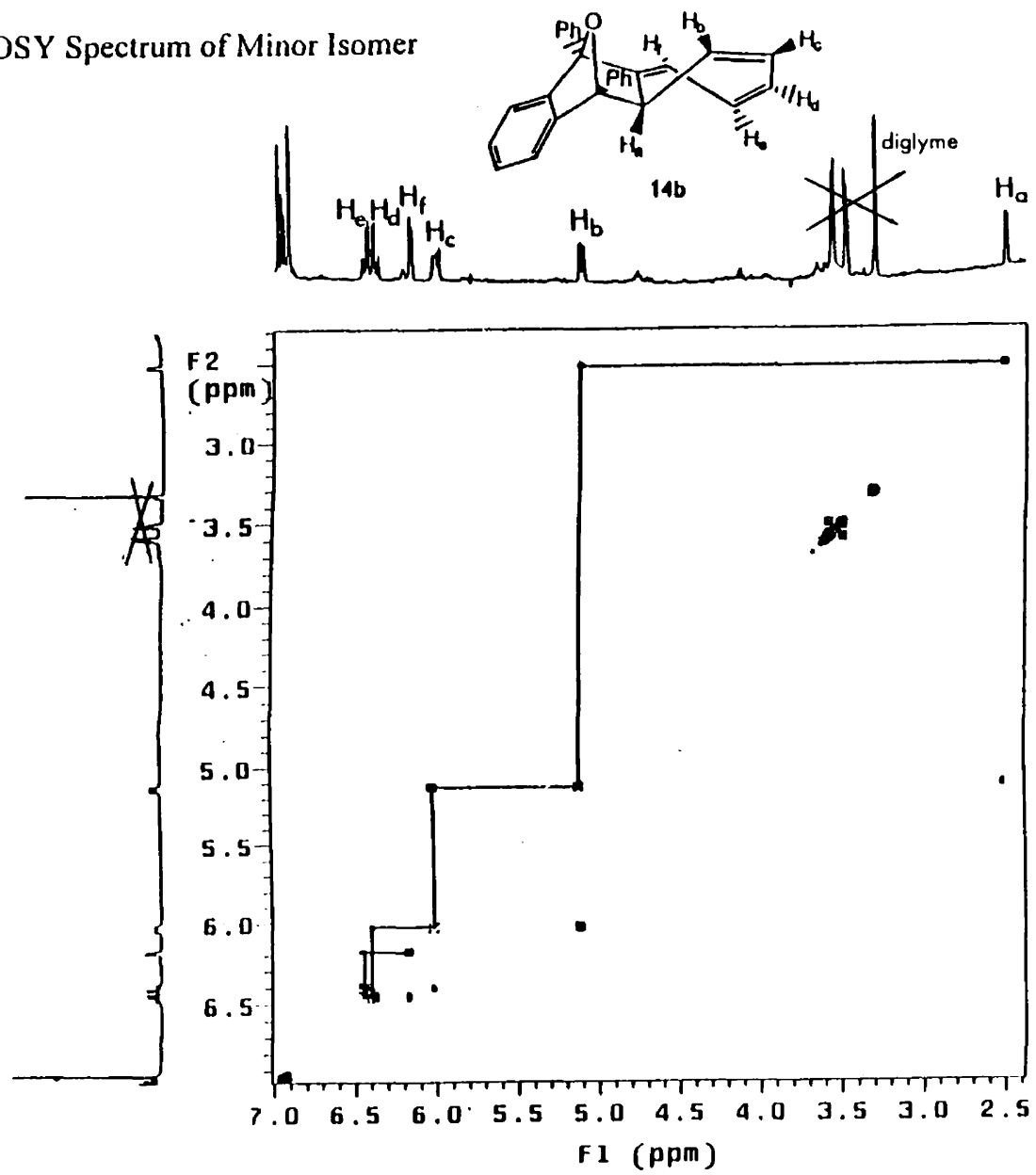


Figure 2-13. COSY Spectrum of Minor Isomer



The relative energies of **14a** and **14b** were estimated by force field calculations (SYBYL and Alchemy III).³⁶ The results of the SYBYL calculations, determining the most stable configurations of the isomers, are shown in **Figure 2-14**.

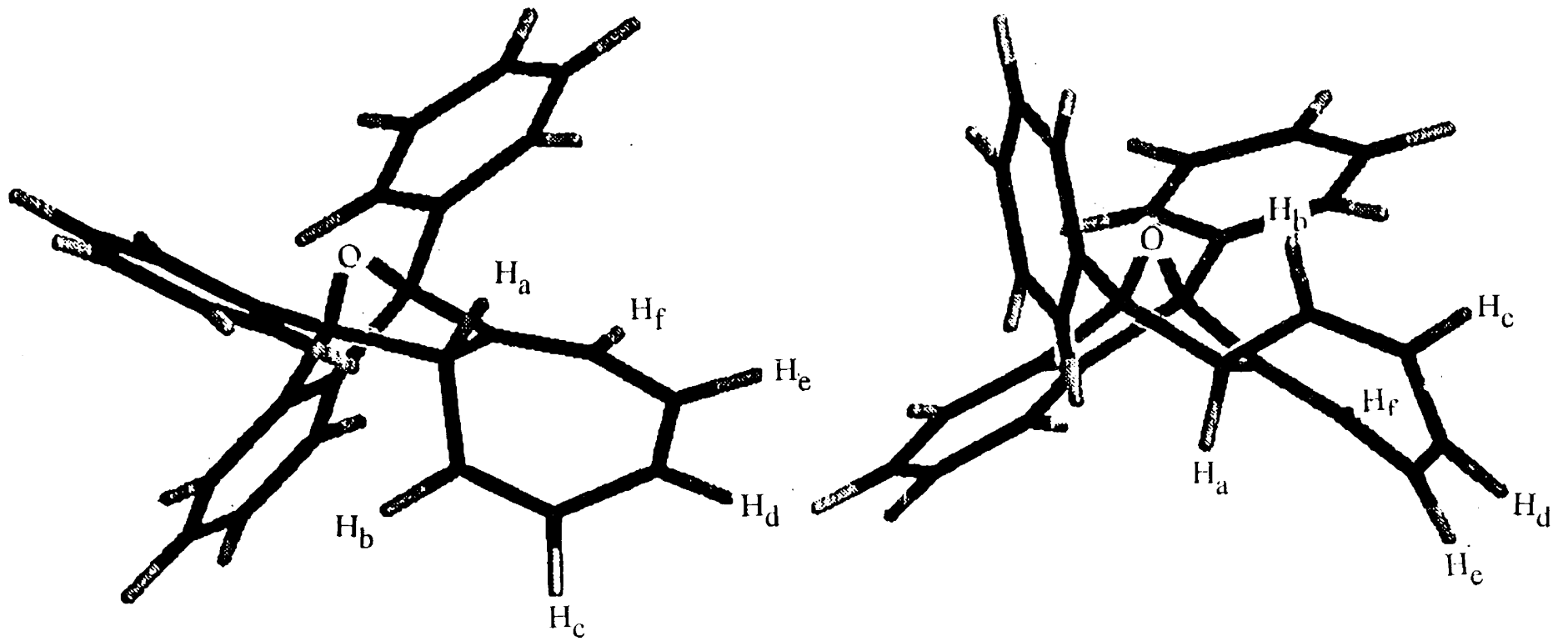
Table 4 lists the numerical SYBYL results. These values supported the nomenclature of the isomers, which was initially based upon peak areas. The major isomer was calculated to be more stable (lower strain energy) than the minor isomer. (The difference was only 0.06 kcal/mol, which was within the limits of the calculation.)

Table 4. SYBYL Force Field Results

	<u>DIBF Isomer</u>	
	<u>Minor</u>	<u>Major</u>
Strain Energy	26.5565	26.4934
Gradient	0.3862	0.1571
Stretching	0.4732	0.4399
Bending	23.8921	23.0887
Torsion	8.0486	8.8910
VdW Energy	-5.9493	-6.0324
Out-of-Plane	0.0918	0.1062

The chemical shifts of the protons in the isomers were then assigned to the structures in **Figure 2-14** using the following logic. As can be seen in **Table 3**, the chemical shift of proton H_b in **14a** is further upfield in the spectrum than proton H_b in **14b**. This can be explained by proximal effects on this proton. The benzo group and one of the phenyl groups are shielding H_b in the major isomer to a certain extent. In **14b**, H_b is in the vicinity of one of the phenyl groups but should not be shielded to the extent that H_b is in **14a**.

Figure 2-14. Calculated Stereochemistry of the Isomers



Major Isomer (14a)

Minor Isomer (14b)

The converse is true for proton H_a in both structures. Proton H_a in **14b** should be found further upfield in the spectrum than in **14a** due to shielding effects from the benzo and phenyl groups.

Further evidence that the two products were isomers was provided by high resolution mass spectroscopy (HRMS). After HPLC separation, the samples of the isomers underwent HRMS.³⁷ **Table 5** lists the results. (Complete analyses given in Appendix II).

Table 5. HRMS Results of the DIBF Product's Isomers³⁷

	<u>Mass, found</u>	<u>Mass, calculated</u>
Major Isomer (14a):	360.149651	360.151415
Minor Isomer (14b):	360.150482	360.151415

The masses found for each isomer were in good agreement with their calculated masses, and the empirical formulas of both were calculated to be $C_{27}H_{20}O$. The two isolated DIBF products were therefore considered to be isomers, having structures **14a** and **14b** seen in **Figure 2-14**.

2.4.2. The Third DIBF Product

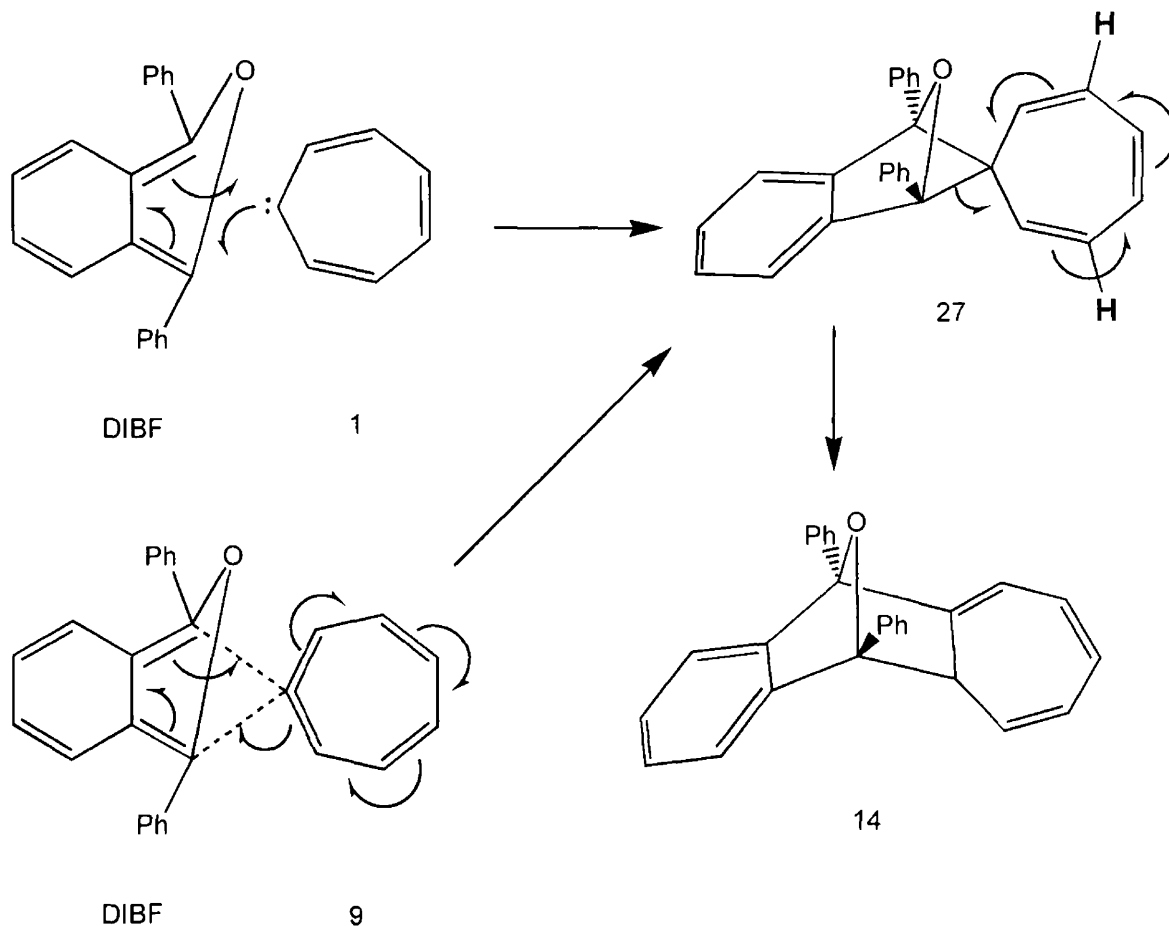
The third product generated in this reaction was unstable and disappeared rather rapidly in the spectra of the DIBF reaction mixtures. It exhibited an unusual splitting pattern in the 1-D spectrum at δ 5.4 ppm. At first glance it appeared to have one proton being split by four non-equivalent protons into a doublet of doublet of doublet of doublets (d of d of d of d) pattern. If this was the case, the largest coupling constant would have been 22 Hz. It would have been highly unlikely that any product generated in this synthesis would have exhibited this coupling constant. Upon closer inspection, the splitting pattern was seen to be two doublet of doublet of

doublets (d of d of d). Due to its instability, this product was not isolated, and its structure was not identified

This product was only observed in the DIBF syntheses. It was not observed in the competition reactions, perhaps augmenting the likelihood of a rearrangement during reaction.

Scheme 13 shows one feasible structure of the unknown product (**27**) using both **1** and **9** as potential intermediates.

Scheme 13. Possible Formation and Structure of the Unknown DIBF Product



The carbene intermediate **1** or allene **9** may react with the DIBF to generate spiro compound **27**. This spiro compound could then rearrange to **14**. The splitting pattern at δ 5.4 ppm (Figure 2-7.) is consistent with the pattern expected for the highlighted protons in **27**.

2.5. Reaction Time vs. DIBF Product Generation

In an attempt to see what effect the reaction time had on the generation of the three observed DIBF products, a series of six DIBF reactions were performed and terminated at designated time intervals. **Table 6** lists the DIBF products' reaction durations and the percentage of each product's peak area in proportion to the combined peak area of all three products. Concentration effects were avoided by adding the same volume of sample (~ 0.1 ml) from the reaction vessel to the NMR tubes containing equivalent amounts of the standard (TMS).

Table 6. Stabilization of the DIBF Products Over Increasing Reaction Time

		<u>Time of Reaction</u>		
		<u>15 min.</u>	<u>30 min.</u>	<u>45 min.</u>
% Peak Area:	Major Isomer (14a):	46	46	54
	Minor Isomer (14b):	25	25	27
	Unknown:	29	29	19
		<u>1 hr.</u>	<u>2 hrs.</u>	<u>3 hrs.</u>
	Major Isomer (14a):	54	53	56
	Minor Isomer (14b):	31	31	32
	Unknown:	15	16	12

The **14a:14b** ratio is about 1.8:1 throughout. the relative amount of the third (unknown) product decreases with time. If the unknown product rearranges to **14a** and/or **14b** or

decomposes in some other way, it seriously impacts the kinetic study.

2.6. Competition Reactions

2.6.1. Preparation for the Kinetic Study

The competition reactions were then undertaken. The sodium salt of tropone tosylhydrazone was decomposed in diglyme in the presence of specific concentrations of *n*-butyl alcohol and DIBF concentrations. The 1-D ^1H NMR spectra were obtained. Due to slight variations in chemical shifts with NMR concentration, it was then necessary to "spike" the NMR samples containing the kinetics products. First, additional butyl ether product **20** was added to the kinetics NMR samples, allowing the chemical shifts of the protons belonging to **20** to be more easily identified. The same was then done for the DIBF products (**14a** and **14b**) and their corresponding proton chemical shifts.

Figure 2-15 shows spectra of a competition reaction (before HPLC) which had been spiked with first additional butyl ether product **20**, then with additional DIBF products (**14a** and **14b**). The peaks are labeled by the number of the product they represent. For example, the pattern at δ 5.66 ppm increased in size after butyl ether product **20** was added to the competition reaction sample. The other patterns, not representing **20**, decreased in size. The converse was true upon addition of more DIBF product. The peaks of the protons contained in the isomers increased upon addition of the DIBF product and the peaks of **20** decreased.

Figure 2-15. Spectra of the Competition Reaction Sample with Spiking

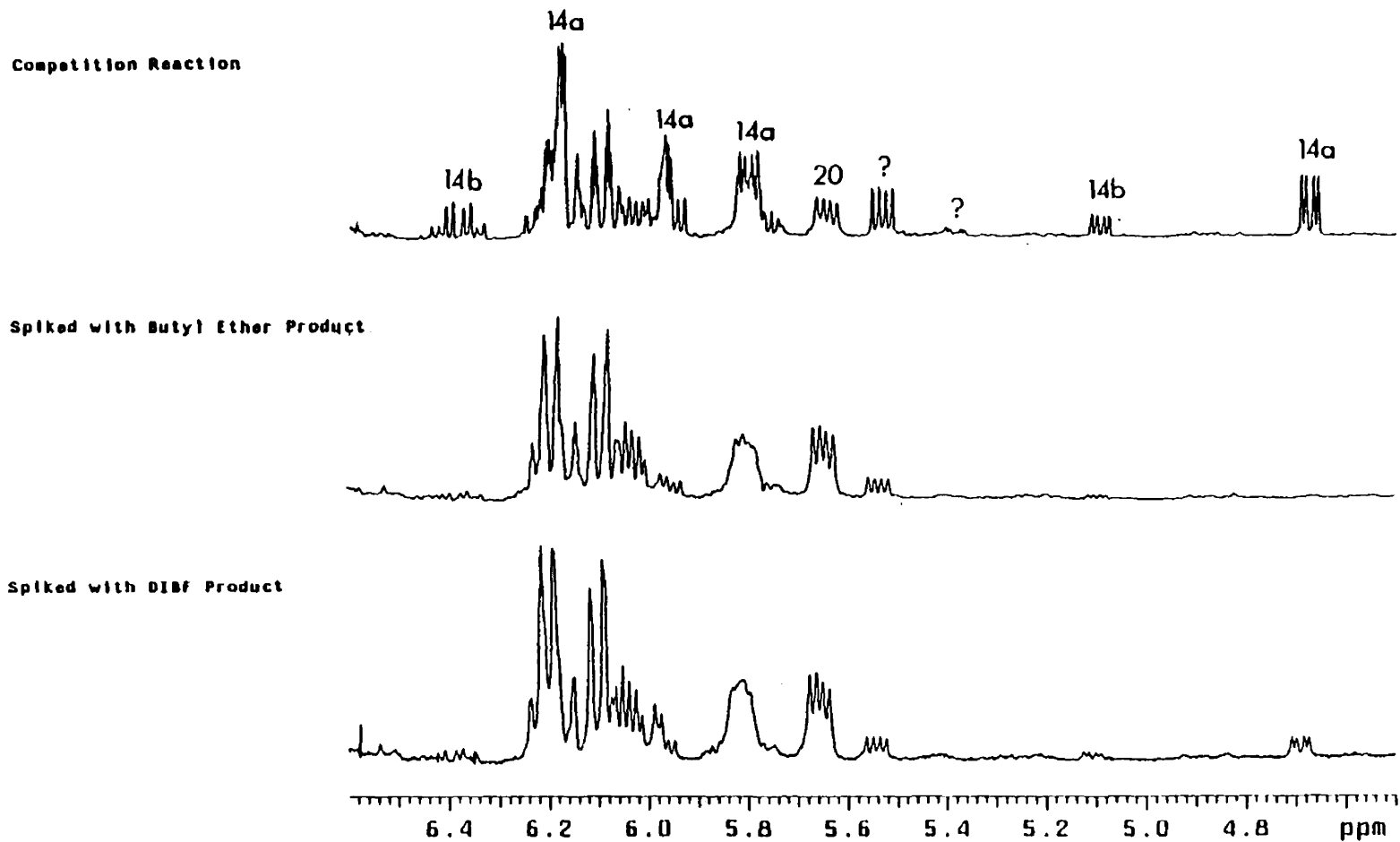
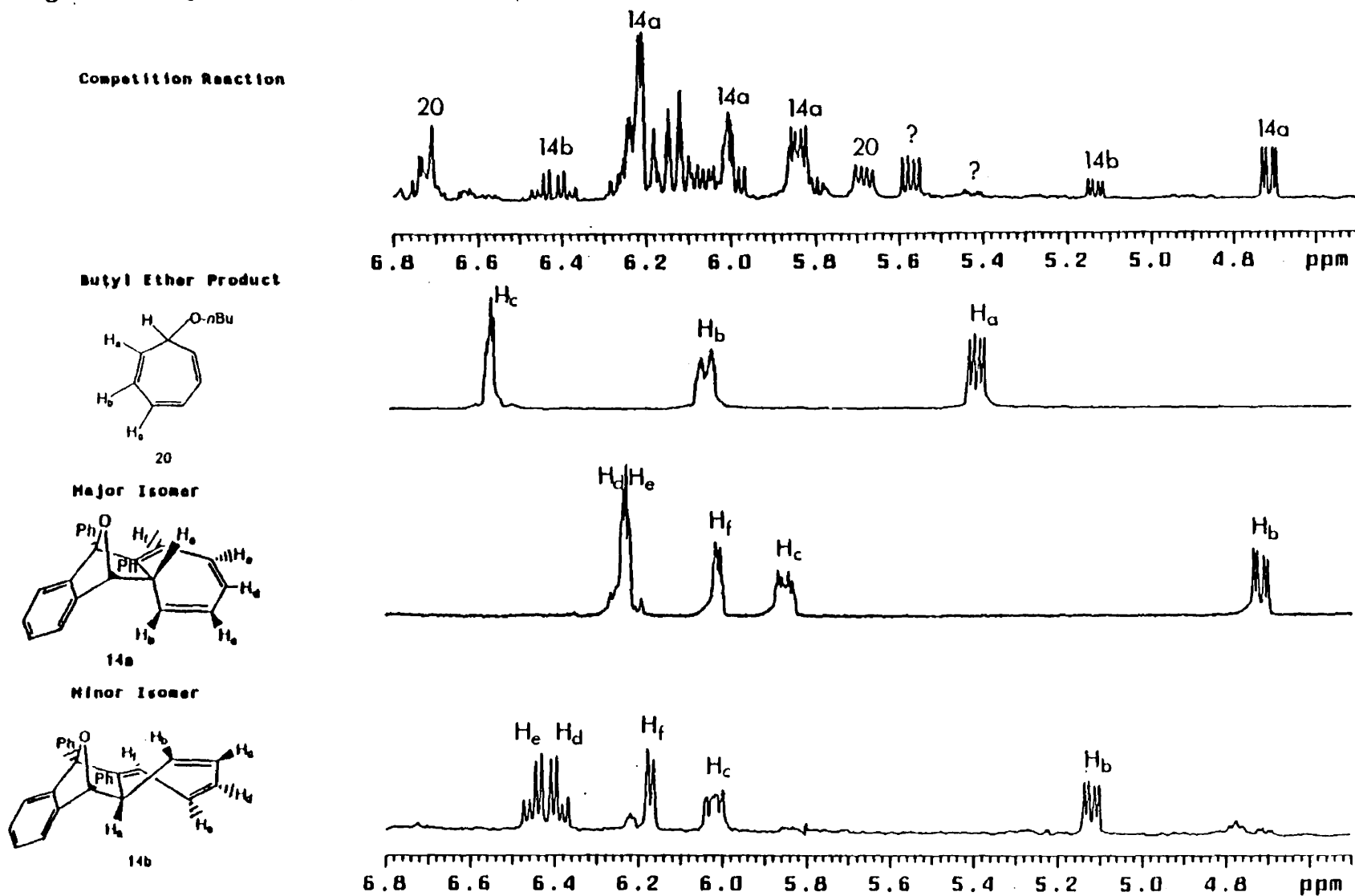


Figure 2-16 shows the spectra of a competition reaction and three of the products prepared independently. Slight chemical shift differences appeared with concentration differences. The proton at δ 5.68 ppm belonged to the butyl ether product **20** (as seen in Figure 2-15). In comparison to the butyl ether spectrum, it is likely this proton is H_a , due to the similarity in the splitting patterns. It is observed almost 2.5 ppm downfield of H_a in the butyl ether spectrum, however. The protons at δ 5.42 and 5.56 ppm are seen with question marks because it is unknown what is responsible for their presence. At first glance it appears the proton at δ 5.42 ppm is H_a in the butyl ether product. Results of the spiking (Figure 2-15) showed that this was not the case. The pattern at δ 6.7 ppm was designated as arising from **20**. This was because of its similarity to H_c in the spectrum of **20**, both in chemical shift and splitting pattern. With the exception of H_c and H_f in the minor isomer, the protons belonging to both isomers are more easily identified in the competition reaction. The same splitting patterns and similar chemical shifts were observed in the protons of the major isomer (**14a**) and the minor isomer (**14b**).

2.6.2. Competition Kinetics

Once the NMR peaks were identified, competition reactions were performed. Once the spectra of these competition reactions were obtained, the relative areas of the butyl ether product (**20**; δ 5.68 ppm), the minor isomer (**14b**; δ 5.14 ppm), and the major isomer (**14a**; δ 4.72 ppm) were measured by integration in each spectrum in order to obtain a ratio of the products.

Figure 2-16. Spectra of Competition Reaction with Its Component Products



The data obtained in the preliminary results were not reproducible. Due to incomplete NMR data, only one DIBF product was observed in the preliminaries.³⁴ The present study observed at least three DIBF products, one of which was unstable. This seriously affects the kinetics. There were also other products which were not identifiable in the competition reactions (specifically those whose protons are at δ 5.40 and 5.54 ppm; Figure 2-16). The inability to account for all products generated in these competition reactions made a kinetic treatment of the data impossible.

3. Summary and Conclusions

This study was valuable in that it helped to assess the validity of the proposed kinetic treatment. It served a purpose in showing that the preliminary results performed by Zepp were based upon incomplete NMR data.³⁴ The following is a list of reasons why this kinetic study failed to shed light on the mechanism of the thermolytic decomposition of the sodium salt of tropone tosylhydrazone (**2**):

1. The reaction system was much more complex than it was originally assumed. Several products were generated in these kinetic reactions. Several DIBF products, previously unobserved, were discovered.

2. Some of the products were unstable. One of the DIBF products disappeared rather rapidly. Thus, it was not possible to account for all of the products generated in the competition reactions. This inability to integrate all of the products nullified the kinetic treatment.

3. A heterogeneous mixture was unavoidable in this reaction. The solid precursor (**2**) was only slightly soluble in the reaction solution. The by-product, sodium *p*-toluenesulfinate, was also insoluble. This may have led to solid surface problems during the reaction, and may account for the lack of reproducibility of the preliminary results.

4. A third intermediate, the triplet state carbene, may have been present. Bitropyl (**24**) was reported in the synthesis of the butyl ether product **20** (Section 2.3.). This suggests that a triplet state carbene was present at some point in that reaction. The presence of a triplet state carbene in the competition reactions would mean the proposed kinetic schemes are questionable.

4. Experimental Section

General Experimental

NMR spectra were recorded on a Varian Unity Plus 400 spectrometer at 399.953 MHz (^1H) and 100.568 MHz (^{13}C) using deuteriochloroform (CDCl_3 , 7.26 ppm, ^1H ; 77.0 ppm, ^{13}C) as an internal reference. Data are reported in the following order: chemical shifts are given (δ); multiplicities are indicated as s (singlet), d (doublet), t (triplet), pent (pentet), hex (hextet), d of d (doublet of doublets), d of t (doublet of triplets), m (multiplet); coupling constants, J , are reported in Hz. High performance liquid chromatography (HPLC) chromatograms were recorded using a Waters 501 solvent delivery pump and Waters 486 Tunable Absorbance Detector on Baseline 810 software.

Thin layer chromatography (TLC) was performed on preparative glass plates (8x8 cm) using Silica Gel 60 PF 254 + 366 indicator (Merck). Visualization of developed plates was accomplished by UV light. The following reagents and solvents were distilled before use: *n*-butyl alcohol was distilled from sodium metal; THF was distilled from Na/benzophenone ketyl; diglyme was distilled from CaH; petroleum ether and methylene chloride were distilled neat; diethyl ether was reagent grade and used as received.

All thermolysis reactions were performed under a dry nitrogen atmosphere.

4.1. Synthesis of Tropone (**21**)³⁸

To a solution of potassium dihydrogen phosphate monohydrate (27.75g, 0.20 mol) in water (67.8 mL) in a 1L 3-necked round bottom flask was added 1,4 dioxane (700 mL, 7.9 mol), cycloheptatriene (98 mL, 0.94 mol), and selenium (IV) oxide (103.88 g, 0.94 mol). The mixture was refluxed under nitrogen for 15 h at 88 °C. The mixture was allowed to cool to room temperature and was then vacuum filtered. The filtrate was divided into two halves (due to the large volume). The first half was placed into a 2000 mL separatory funnel containing 750 mL of water and extracted with methylene chloride (3 x 200 mL). The organic layer was washed with a 3:2 mixture of saturated sodium bisulfite:diethyl ether (8 x 400 mL). The organic layer was then dried over anhydrous magnesium sulfate. The drying agent was separated from the tropone via vacuum filtration. The methylene chloride was removed by rotary evaporation until all of the desired crude tropone remained in that one flask. The second half of the filtrate was then put through the same procedure and added to the other half of the recovered tropone.

The 1,4 dioxane was then removed by direct mechanical vacuum distillation (pressure = 9.48 torr, 45 °C). The tropone was then removed from the remaining inorganics (e.g. selenium) by direct mechanical vacuum (3 torr, 77 °C). Data for **21**: $n_D^{20} = 1.6164$; $^1\text{H NMR}$ (400 MHz, CDCl_3); δ 6.92 (d of d, 2H, $\text{H}_c, \text{H}_d, J_{cd}=9.09$ Hz), 6.96 (m, 2H, H_a, H_f), 7.05 (m, 2H, H_b, H_e).

4.2. Synthesis of 7,7-dichlorocycloheptatriene (**22**)¹⁸

Thionyl chloride (143 mL, 1.98 mol) was placed in a 300 mL, 3-necked round bottom flask equipped with a magnetic stir bar and cooled to 0 °C in an acetone/ice bath. Tropone **21** (24.9 mL, 0.26 mol) was added *dropwise* to the thionyl chloride over a 5 min period.

The mixture was then refluxed for 5 min (reflux began at 57 °C) in an oil bath under nitrogen. The excess thionyl chloride was removed from the 7,7-dichlorocycloheptatriene (theoretical yield: 41.37 g, 0.26 mol) by simple distillation, using a water aspirator as the source for the vacuum. Data for **22**: ^1H NMR (400 MHz, CDCl_3); δ 5.99 (m, 2H, H_c , H_d), 6.11 (m, 2H, H_b , H_e), 6.44 (d, 2H, H_a , H_f , $J=8.77$).

4.3. Synthesis of Tropone Tosylhydrazone (**23**)¹⁸

7,7-Dichlorocycloheptatriene (**22**) was placed in a 1000 mL Erlenmeyer flask equipped with a magnetic stir bar. A solution of *p*-toluenesulfonylhydrazide (47.84 g, 0.26 mol) in ethanol (642 mL, 11.0 mol) was added to the 7,7-dichlorocycloheptatriene. The mixture was stirred for 2 h at room temperature, and the crude tropone tosylhydrazone (yellow precipitate) was removed by vacuum filtration. The crude product was placed in a 1500 mL Erlenmeyer flask containing 350 mL of methylene chloride and 649 mL of saturated sodium bicarbonate and stirred for 30 min. In three aliquots, this mixture was transferred to a 1000 mL separatory funnel and the organic layer was drained into a 500 mL Erlenmeyer flask. The aqueous layer was washed with methylene chloride (3 x 50 mL). After all of the crude product in solution was once again in the same flask, the methylene chloride was separated by rotary evaporator. The tropone tosylhydrazone (82% yield, 57.77 g, 0.21 mol, m.p. range = 137.9-139.0 °C) was recrystallized with 95% ethanol. Data for **23**: melting point = 140.5-141.1 °C (lit. = 142.5-143.5 °C);¹⁷ yield = 61.8%; ^1H NMR (400 MHz, CDCl_3) δ 2.41 (s, 1H), 6.30 (m, 2H, H_a , H_f), 6.53 (m, 2H, H_b , H_e), 6.59 (m, 2H, H_c , H_d), 7.30 (d, 2H, $J=8.14$, arom.), 7.84 (d, 2H, $J=8.30$, arom.).

4.4. Synthesis of Sodium Salt of Tropone Tosylhydrazone (**2**)¹⁸

A solution of tropone tosylhydrazone **23** (40.0 g, 0.15 mol) in THF (252 mL, 3.11 mol) was prepared in a 500 mL, 3-necked round bottom flask equipped with a stir bar. To this was added sodium hydride (60% dispersion in oil, 7.05 g, 0.176 mol). This mixture was stirred for 40 min under nitrogen and the sodium salt of tropone tosylhydrazone (brown solid, 51.28 g) was vacuum filtered in a fritted funnel using the water aspirator as the vacuum source. The salt was washed with THF (4 x 25 mL) and the salt was transferred into a brown bottle and placed upright into a vacuum dessicator. The salt was subjected to direct mechanical vacuum (to rid it of any residual tetrahydrofuran) for 15 h. The bottle containing the sodium salt was capped, nitrogen was introduced into the dessicator, and the product was stored until used in the kinetics reactions. Data for **2**: ¹H NMR (400 MHz, CDCl₃) δ 6.77 (m, 1H), 6.88 (m, 1H), 7.09 (m, 1H), 7.32 (m, 2H), 7.63 (m, 1H), 7.91 (d, 2H, *J*=8.37, arom.), 7.99 (d, 2H, *J*=8.54, arom.), 8.61 (s, 1H, arom.)

4.5. Synthesis of 1-Butoxy-2,4,6-Cycloheptatriene (Butyl Ether Product) (**20**)³²

Data for **20**: $n_D^{20}=1.6173$; ¹H NMR (400 MHz, CDCl₃) δ 0.84 (t, 3H, H_h, *J*=7.50), 1.31 (hex, 2H, H_g, *J*=7.51), 1.50 (pent, 2H, H_f, *J*=7.46), 3.30 (m, 1H, H_d), 3.44 (t, 2H, H_e, *J*=7.35), 5.40 (d of d, 2H, H_a, *J*_{ab}=9.50), 6.05 (d of d, 2H, H_b, *J*_{bc}=9.63), 6.56 (m, 2H, H_c).

*Synthetic Route 1:*³²

The sodium salt of tropone tosylhydrazone (0.5 g, 1.7 mmol), diglyme (8.8 mL), and *n*-butyl alcohol (7.5 mL, 0.082 mol) were placed into a 50 mL, 3-necked round bottom flask and stirred for 1 h at 98.5 °C. The mixture was allowed to cool and transferred to a 250 mL

separatory funnel with 60 mL pet ether. The organic layer was washed with water (5 x 20 mL). The crude product was transferred to a 250 mL round bottom flask and the solvent was removed by rotary evaporation. The residual diglyme was removed by direct mechanical vacuum. The resulting crude butyl ether product **20** was purified by silica gel column chromatography (100% pet ether) and silica gel thin layer chromatography (100% diethyl ether).

*Synthetic Route 2:*³⁵

Reagent grade tropylium tetrafluoroborate (Aldrich)(0.50 g, 0.003 mol) was dissolved in 20 mL anhydrous diethyl ether in a 125 mL Erlenmeyer flask equipped with a magnetic stir bar. With stirring, *n*-butyl alcohol (0.38 mL, 0.004 mol) was added slowly over a period of 3 min. After the addition was complete, the reaction mixture was transferred to a 60 mL separatory funnel containing 20 mL of diethyl ether. The organic layer was separated and washed with saturated sodium bicarbonate (7 x 140 mL). The ether was removed from the crude product by rotary evaporation. The crude product was purified by silica gel, thin-layer chromatography (100% diethyl ether) to yield 0.035 g (7.6%) of the butyl ether product **20**.

Synthetic Route 3:

Tropylium tetrafluoroborate (0.50 g, 0.003 mol) was dissolved in 20 mL anhydrous diethyl ether in a 125 mL Erlenmeyer flask equipped with a magnetic stir bar. With stirring, *n*-butyl alcohol was added slowly over 3 min. Saturated sodium bicarbonate (10 mL) was then added slowly to the reaction mixture with stirring in order to keep it basic (basicity was tested with red litmus paper). The diethyl ether was evaporated from the product to yield 0.31 g, (68%)

of the crude butyl ether product **20**.

Synthetic Route 4:

Tropylium tetrafluoroborate (0.50 g, 0.003 mol) was placed in a 50 mL Erlenmeyer flask to which *n*-butyl alcohol (0.38 mL, 0.004 mol) was added slowly with stirring. After the addition was complete, solid sodium bicarbonate (excess) was added to the mixture. Water (~ 1 mL) was added to the mixture to neutralize the mixture. Diethyl ether (10 mL) was added to the mixture, as well as more solid sodium bicarbonate (to keep it in excess). The solid sodium bicarbonate was separated from the organic layer by gravity filtration. The ether was separated from the product by rotary evaporator to yield 0.379 g (82.6%) of the butyl ether product **20**.

4.6. Synthesis of the DIBF Product (**14**)³¹

The sodium salt of tropone tosylhydrazone (0.10 g, 0.3 mmol), 1,3-diphenylisobenzofuran (Aldrich) (DIBF, 0.091 g, 0.3 mmol), and diglyme (3.0 mL) were placed into a 15 mL test tube equipped with a magnetic stir bar. The mixture was stirred for 1 h at 100 °C. The organic layer was transferred to a 125 mL separatory funnel with 30 mL of diethyl ether, washed with water (5 x 60 mL), and dried over anhydrous magnesium sulfate. The ether was removed by rotary evaporation and the crude product was purified twice by preparative silica gel thin-layer chromatography (100% pet ether). The isomers were separated by HPLC (3:1 acetonitrile/H₂O) yielding a yellow crystalline solid (major isomer) and an opaque liquid (minor isomer).

Data for Major Isomer (**14a**):³⁹ ^1H NMR (400 MHz, CDCl_3) 3.64 (d, 1H, H_a , $J_{ab}=3.69$), 4.73 (d of d, 1H, H_b , $J_{bc}=9.72$), 5.85 (d of d, 1H, H_c , $J_{cd}=9.87$), 6.01 (m, 1H, H_f), 6.22 (m, 1H, H_e), 6.23 (m, 1H, H_d).

Data for Minor Isomer (**14b**):³⁹ ^1H NMR (400 MHz, CDCl_3) 2.54 (d, 1H, H_a , $J_{ab}=4.35$), 5.14 (d of d, 1H, H_b , $J_{bc}=9.58$), 6.02 (d of d, 1H, H_c , $J_{cd}=11.06$), 6.20 (m, 1H, H_f), 6.41 (d of d, 1H, H_d , $J_{de}=10.93$), 6.44 (d of d, 1H, H_e , $J_{ef}=11.06$).

4.7. Synthesis of Bitropyl (**24**)³⁵

Zinc dust (0.200 g, 0.003 mol), tropylium tetrafluoroborate (0.53 g, 0.003 mol), and water (6 mL) were placed into a 15 mL centrifuge tube. The centrifuge tube was corked with a rubber stopper, and the mixture was shaken thoroughly for 4 min. The product was washed with pentane (4 x 5 mL). The pentane was removed by rotary evaporation leaving the yellow crystalline product. Data for **24**: ^1H NMR (400MHz, CDCl_3) 1.87 (m, 2H, H_a), 5.21 (d of d, 4H, H_b , $J_{bc}=9.02$), 6.19 (d of t, 4H, H_c , $J_{cd}=9.24$), 6.62 (m, 4H, H_d).

4.8. Competition Reaction (synthesis of **20** and **14**)⁴⁰

DIBF (0.429 g, 1.6 mmol), *n*-butyl alcohol (3 mL, 0.0328 mol), and diglyme (6 mL) were placed into a 15 mL test tube equipped with a magnetic stir bar and stoppered with a rubber septum. The mixture was heated at 100 °C for 10 min. The sodium salt of tropone tosylhydrazone (0.075 g, 0.3 mmol) was added immediately thereafter and this mixture was heated for an additional 50 min at 100 °C. The solution was allowed to cool. The solution was

transferred to a 250 mL separatory funnel with 50 mL pet ether. The organic layer was washed with water (2 x 125 mL). The DIBF products and butyl ether product were separated by Grade III alumina column chromatography (100% pet ether). The DIBF products were purified by silica gel thin-layer chromatography (7:3 pet ether/methylene chloride) and separated by HPLC (RP-18 column, 3:1 acetonitrile/water). Data for Competition Reactions: reported in **Section 4.5.** (butyl ether product **20**) and **Section 4.6.** (DIBF products **14a** and **14b**).

Appendix I

Scheme A1: Single intermediate kinetics (see Scheme 9, pg. 30)

$$d[9]/dt = -k_1[9][\text{BuOH}] - k_2[9][\text{DIBF}]$$

$$d[14]/dt = k_2[9][\text{DIBF}]$$

$$d[20]/dt = k_1[9][\text{BuOH}]$$

$$d[20]/d[14] = k_1[9][\text{BuOH}]/k_2[9][\text{DIBF}]$$

$$[20]/[14] = k_1[\text{BuOH}]/k_2[\text{DIBF}]$$

Scheme A2: Two-intermediate kinetics (see Scheme 10, pg. 31)

$$d[1]/dt = k_3[1] - k_{-3}[9] + k_4[1][\text{BuOH}]$$

$$d[9]/dt = -k_3[1] + k_{-3}[9] + k_2[9][\text{DIBF}]$$

$$d[14]/dt = k_2[9][\text{DIBF}]$$

$$d[20]/dt = k_4[1][\text{BuOH}]$$

$$[20]/[14] = k_4[1][\text{BuOH}]/k_2[9][\text{DIBF}]$$

$$k_{-3}[9] + k_2[9][\text{DIBF}] = k_3[1]$$

$$[9] = k_3[1]/(k_{-3} + k_2[\text{DIBF}])$$

$$[20]/[14] = k_4[1][\text{BuOH}]/\{k_2[\text{DIBF}](k_3[1]/(k_{-3} + k_2[\text{DIBF}]))\}$$

$$= k_4[\text{BuOH}]/\{(k_2k_3[\text{DIBF}])/(k_{-3} + k_2[\text{DIBF}])\}$$

$$= k_4[\text{BuOH}] + (k_{-3} + k_2[\text{DIBF}])/(k_2k_3[\text{DIBF}])$$

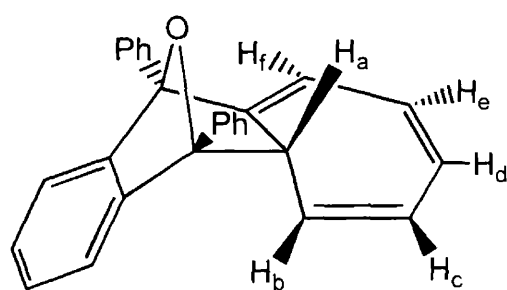
$$= \{(k_{-3}k_4[\text{BuOH}])/(k_2k_3[\text{DIBF}])\} +$$

$$\{(k_2k_4[\text{BuOH}][\text{DIBF}])/(k_2k_3[\text{DIBF}])\}$$

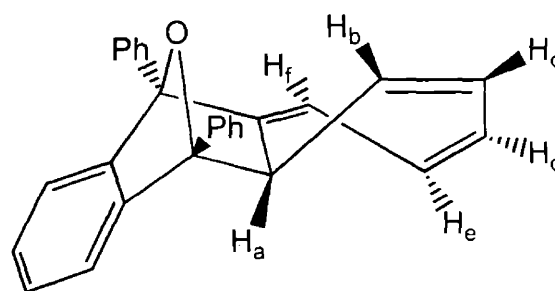
$$[20]/[14] = \{k_{-3}k_4[\text{BuOH}]/k_2k_3[\text{DIBF}]\} + \{k_4[\text{BuOH}]/k_3\}$$

Appendix II

HRMS results of the DIBF products **14a** (major isomer) and **14b** (minor isomer).



14a
Major Isomer



14b
Minor Isomer

Structures of the isomers were determined by SYBYL and Alchemy III.

Computer generated drawings are seen in **Figure 2-14**, page 56.

Major Isomer (14a)

Elemental Composition

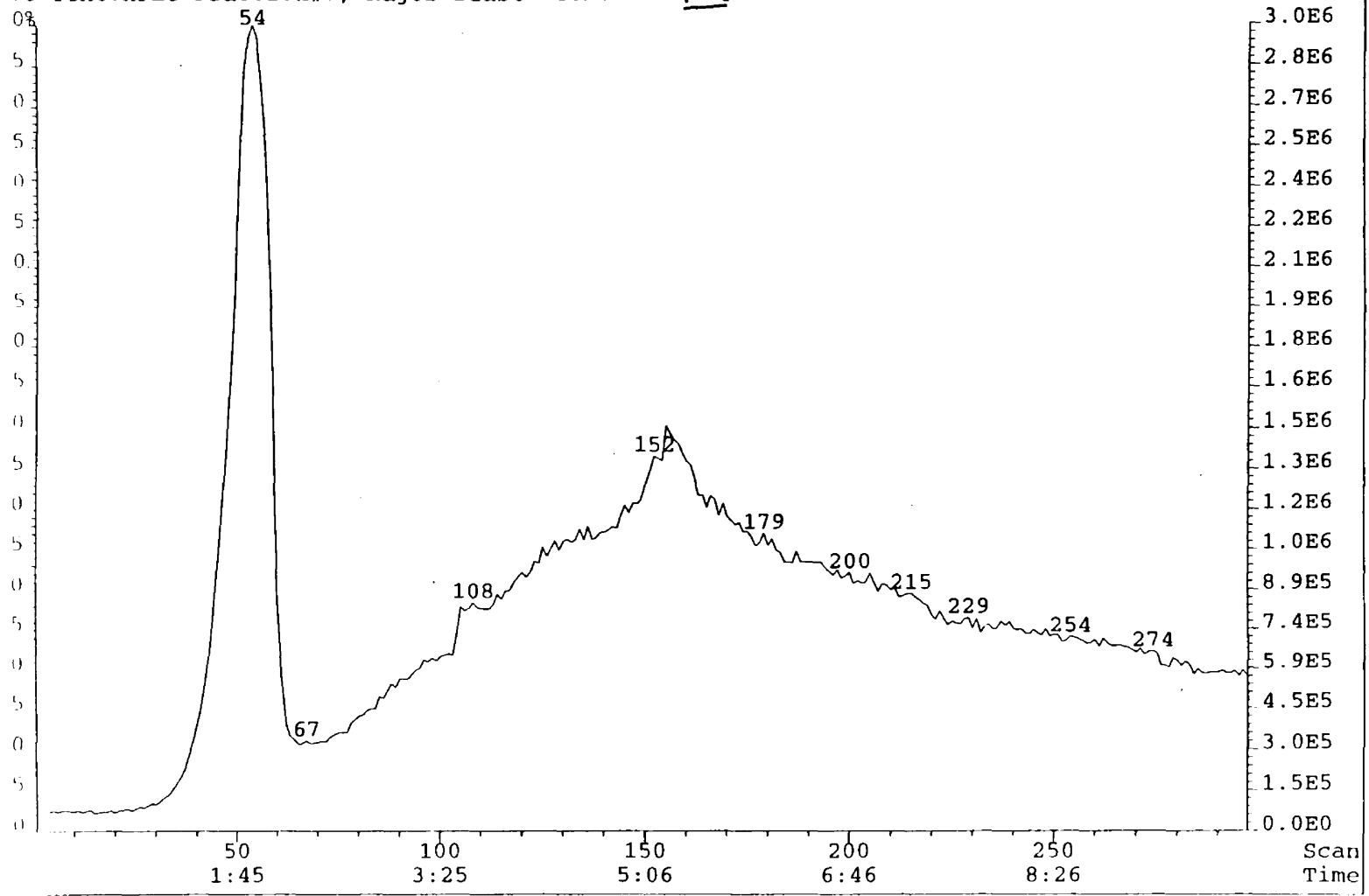
File:10OCT95A1 Ident:1 Acq:10-OCT-1995 07:19:43 +3:35 Cal:10OCT95A1
70S EI+ Voltage BpM:331 BpI:2624512 TIC:9293224 Flags:NORM
File Text:ew; major diastereomer Created from 10OCT95A 33_39+52_60 SMO(1,7)
Heteroatom Max: 20 Ion: Both Even and Odd
Limits:

360.149651	10.0			-0.5	5	10	0
				20.0	30	50	3
Mass	mDa	PPM	Calc. Mass	DBE	C	H	O
360.149651	1.8	4.9	360.151415	18.0	27	20	1

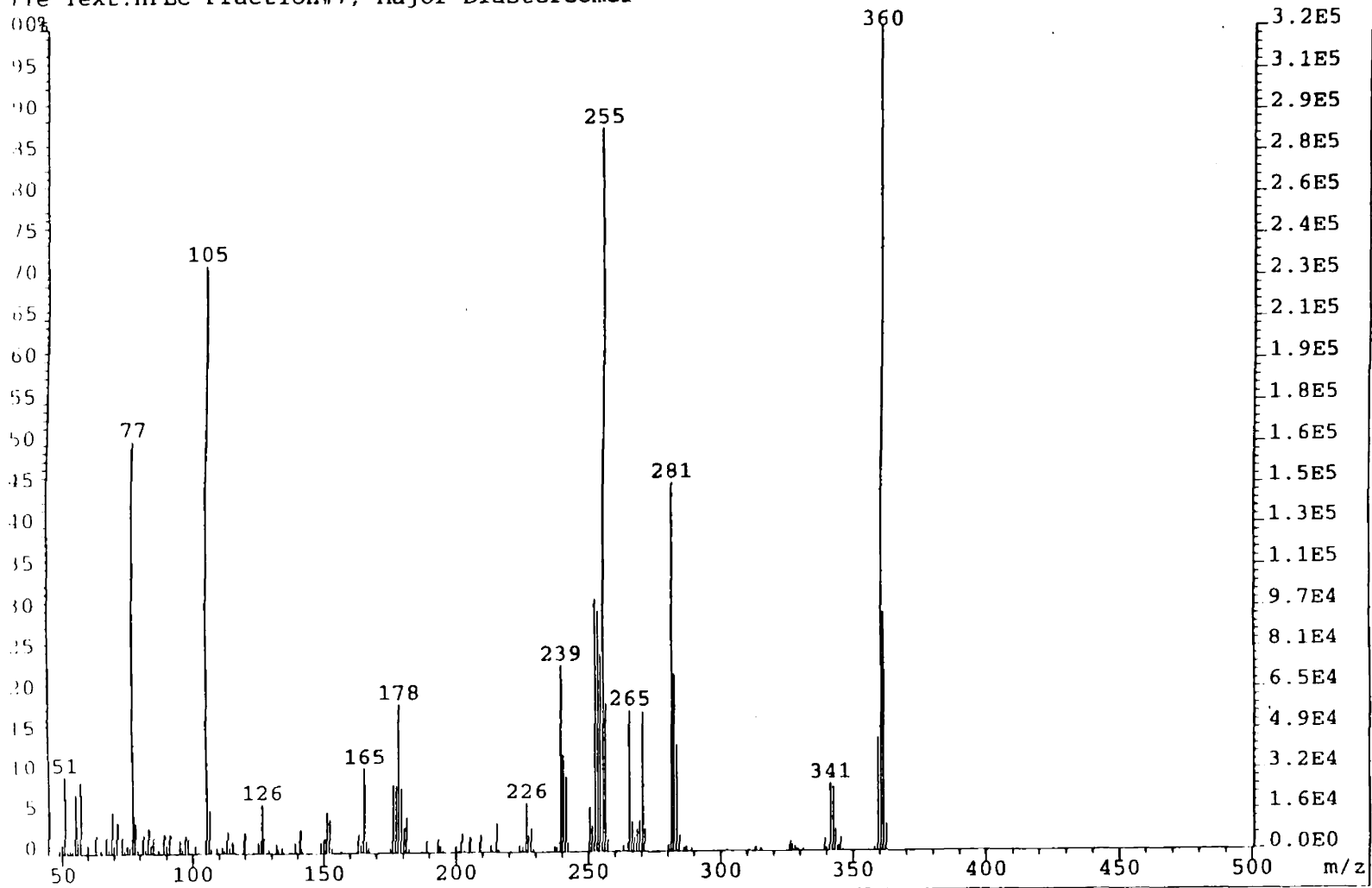
le:28SEP95O #1-297 Acq:28-SEP-1995 13:24:09 Septum EI+ Magnet 70S

C (+RP) Exp:PROBE

le Text:HPLC Fraction#7, Major Diastereomer - 14a



file:28SEP950 Ident:53_55 Mer Def 0.25 Acq:28-SEP-1995 13:24:09 +1:53 Cal:28SEP95N_1
MS EI+ Magnet BpM:360 BpI:323951 TIC:2940714 Flags:HALL
file Text:HPLC Fraction#7, Major Diastereomer

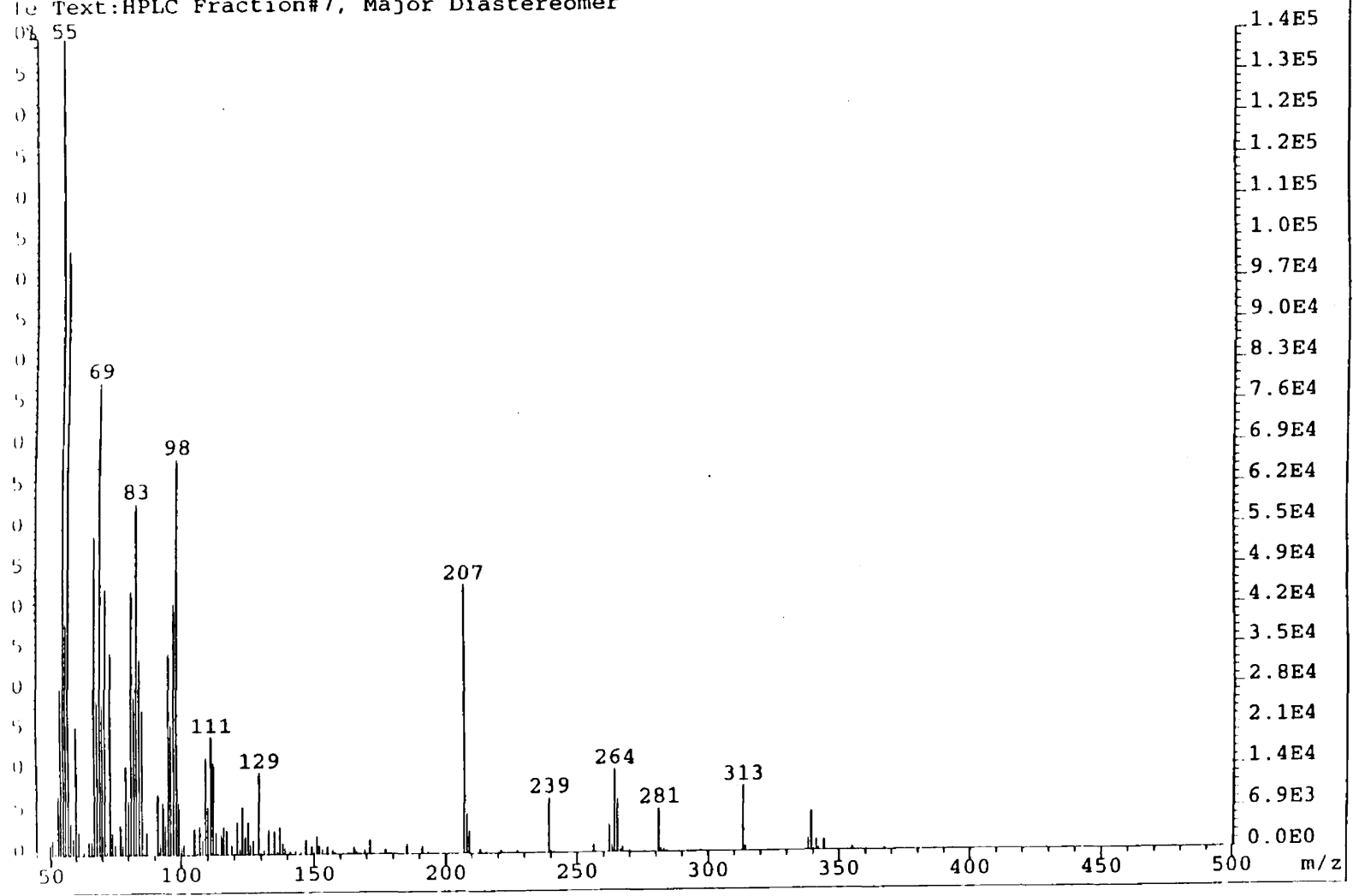


MS_USER:SPE_DEFAULT.LIS 29-SEP-1995 08:11
 Listing of raw data for -
 data file 28SEP950
 data ident 53_55 Mer Def 0.25
 Axis display range X_MASS (45.00, 500.11)
 Normalising intensity 3.21951E+05
 Data threshold 0.17% of normalising intensity

MASS	TIME	ABS HEIGHT	REL HEIGHT(%)	FLAGS
48.9832	79271.7738	2.123667E+03	0.66	
50.0162	78654.7065	4.086667E+03	1.26	
51.0268	78063.1972	3.108800E+04	9.60	
52.0350	77484.6275	1.609000E+03	0.50	
53.0439	76916.8188	1.637333E+03	0.51	
54.0517	76360.2634	1.722667E+03	0.53	
55.0606	75813.4202	2.404367E+04	7.42	
56.0709	75275.7971	6.660000E+03	2.06	
57.0786	74749.0755	2.876900E+04	8.88	
59.0529	73743.5897	6.163334E+02	0.19	
60.0293	73258.6750	3.514667E+03	1.08	
63.0318	71815.4956	7.259333E+03	2.24	
65.0467	70885.0894	1.535667E+03	0.47	
67.0639	69981.9996	6.978000E+03	2.15	
68.0696	69541.8742	2.084333E+03	0.64	
69.0761	69107.8665	1.672000E+04	5.16	
70.0822	68680.3016	3.761333E+03	1.16	
71.0887	68258.6531	1.268400E+04	3.92	
73.0358	67459.8162	6.758000E+03	2.09	
74.0281	67060.8891	1.911333E+03	0.59	
75.0233	66666.2302	3.598333E+03	1.11	
76.0284	66272.9913	3.006000E+03	0.93	
77.0386	65883.0199	1.633707E+05	50.43	
78.0440	65500.0444	1.233600E+04	3.81	
79.0511	65121.4439	1.859333E+03	0.57	
81.0695	64377.2314	7.602667E+03	2.35	
82.0754	64013.4163	2.484000E+03	0.77	
83.0856	63652.5815	1.026667E+04	3.17	
84.0475	63313.1634	3.635000E+03	1.12	
85.0995	62946.4087	6.436000E+03	1.99	
87.0330	62284.0914	1.847667E+03	0.57	
89.0450	61610.4021	8.010667E+03	2.47	
90.0550	61277.9117	3.779333E+03	1.17	
91.0638	60949.4903	7.560000E+03	2.33	
93.0838	60302.5811	6.443334E+02	0.20	
95.0838	59675.5373	5.155000E+03	1.59	
96.1005	59361.7219	1.930000E+03	0.60	
97.1115	59052.9167	7.255333E+03	2.24	
98.0868	58757.9741	5.997333E+03	1.85	
99.1041	58453.3917	8.430000E+02	0.26	
101.0507	57879.0484	3.361000E+03	1.04	
102.0551	57586.9801	8.113334E+02	0.25	
105.0400	56735.6298	2.314027E+05	71.43	
106.0408	56455.6486	1.730933E+04	5.34	
106.9938	56191.5018	1.997667E+03	0.62	
109.0956	55617.4242	2.263333E+03	0.70	
111.1082	55078.3350	2.537667E+03	0.78	
112.0792	54821.8730	1.228667E+03	0.38	
113.0425	54569.7587	8.520000E+03	2.63	
113.9819	54326.0094	2.415667E+03	0.75	
115.0590	54049.0719	4.569000E+03	1.41	
116.0582	53794.4958	5.670000E+02	0.18	
118.9612	53067.0772	9.266667E+02	0.29	
119.6542	52896.0058	8.383667E+03	2.59	
123.1281	52052.6602	8.156667E+02	0.25	
125.0673	51591.9266	4.528667E+03	1.40	
126.0550	51359.9592	1.949200E+04	6.02	
126.8758	51168.5487	6.268333E+03	1.93	
128.0384	50899.4877	5.866667E+02	0.18	
129.0816	50660.1375	1.887000E+03	0.58	
131.8541	50033.1784	3.789000E+03	1.17	
132.6901	49846.6954	1.471333E+03	0.45	
134.0621	49543.2005	2.509667E+03	0.77	
137.0811	48886.2333	6.513334E+02	0.20	
139.0589	48463.7297	4.039667E+03	1.25	
140.9262	48070.4169	3.401667E+03	2.90	
141.8757	47934.3506	1.727333E+03	0.53	
149.0467	46419.1302	4.032000E+03	1.24	
150.0833	46213.4237	5.575333E+03	1.72	
151.0833	46011.2611	1.425333E+04	6.02	
152.0833	45811.0985	1.000000E+04	4.11	

166.0867	43220.6134	4.767333E+03	1.47
167.0951	43041.6844	2.177333E+03	0.67
175.0758	41662.4792	1.973000E+03	0.61
176.0747	41494.2937	2.724800E+04	8.41
177.0849	41325.1891	2.708533E+04	8.36
178.0921	41157.5273	5.961067E+04	18.40
179.0969	40991.2126	2.587733E+04	7.99
180.0985	40826.3661	1.029733E+04	3.18
181.0414	40672.0118	1.406500E+04	4.34
182.0854	40502.0505	1.667333E+03	0.51
187.0760	39702.8427	7.656667E+02	0.24
189.0812	39387.7195	4.552000E+03	1.41
193.0779	38769.4621	5.191333E+03	1.60
194.0796	38616.5155	2.620000E+03	0.81
195.0813	38464.3363	7.140000E+02	0.22
200.0646	37718.7918	2.357333E+03	0.73
201.0826	37568.7905	6.880000E+02	0.21
202.0876	37421.4652	7.258667E+03	2.24
203.0957	37274.4256	9.170000E+02	0.28
205.0778	36987.4720	6.017333E+03	1.86
209.0736	36417.4911	6.686000E+03	2.06
213.0920	35855.1927	2.879000E+03	0.89
215.0989	35578.2669	1.129600E+04	3.49
216.1033	35440.6394	1.042000E+03	0.32
224.0724	34370.0321	2.767667E+03	0.85
225.1025	34234.3756	2.182333E+03	0.67
226.0866	34105.3645	1.956433E+04	6.04
227.0918	33974.1581	6.651333E+03	2.05
228.1089	33842.0058	9.317334E+03	2.88
229.1126	33712.1779	1.295333E+03	0.40
237.0790	32701.9830	2.307667E+03	0.71
238.1141	32573.2588	1.843667E+03	0.57
239.0982	32451.3696	7.446667E+04	22.99
240.1077	32326.8594	3.880534E+04	11.98
241.1145	32203.1831	3.006400E+04	9.28
242.1197	32080.1943	3.784333E+03	1.17
250.0872	31122.5204	1.750667E+04	5.40
251.0838	31004.8763	1.026033E+04	3.17
252.1028	30885.0870	1.006457E+05	31.07
253.1065	30767.5967	9.617567E+04	29.69
254.1179	30649.6958	7.871800E+04	24.30
255.1266	30532.5996	2.847147E+05	87.89
256.1291	30416.7215	5.953600E+04	18.38
257.1313	30301.3544	4.777000E+03	1.47
263.0997	29623.7305	2.203000E+03	0.68
265.1214	29397.6577	5.665600E+04	17.49
266.1259	29285.9370	1.196933E+04	3.69
267.1154	29176.2842	5.982667E+03	1.85
268.1077	29066.6978	9.315334E+03	2.88
269.1139	28955.9578	1.247467E+04	3.85
270.1239	28845.1865	5.604267E+04	17.30
271.1222	28736.0659	9.140000E+03	2.82
280.1506	27766.6782	2.822667E+03	0.87
281.1094	27665.6100	1.464133E+05	45.20
282.1117	27560.3505	7.072967E+04	21.83
283.1216	27454.6873	4.283200E+04	13.22
284.1266	27349.9347	6.430667E+03	1.99
286.1180	27143.4975	1.407667E+03	0.43
287.1144	27040.7705	2.016667E+03	0.62
289.1112	26835.9924	1.223333E+03	0.38
313.1676	24472.1453	1.554000E+03	0.48
315.1287	24287.2943	1.342333E+03	0.41
326.1291	23272.0364	3.758000E+03	1.16
327.1339	23181.0676	2.494000E+03	0.77
328.1477	23089.5693	1.880333E+03	0.58
329.1637	22998.1561	8.523334E+02	0.26
331.1703	22818.4362	9.243334E+02	0.29
339.1472	22114.1491	4.833333E+03	1.49
340.1569	22026.0902	1.296333E+03	0.40
341.1631	21938.5635	2.675733E+04	8.26
342.1677	21851.3929	2.540533E+04	7.84
343.1668	21764.9275	8.652667E+03	2.67
344.1581	21679.3390	2.212333E+03	0.68
345.1480	21594.0969	5.172000E+03	1.60
346.1513	21507.9275	6.520000E+02	0.20
358.1675	20496.5099	1.443000E+03	0.45
359.1950	20414.8485	4.520000E+04	13.95
360.1692	20331.8909	3.239507E+05	100.00
362.1749	20249.5473	9.511467E+04	29.36
363.1755	20167.7577	1.044667E+04	3.22

File: 28SEP950 Ident: 151_161 Mer Def 0.25 Acq: 28-SEP-1995 13:24:09 +5:18 Cal: 28SEP95N_1
EI+ Magnet BpM: 55 BpI: 138600 TIC: 1401682 Flags: HALL
Text: HPLC Fraction#7, Major Diastereomer



```

MS_USER:SPE_DEFAULT.LIS 29-SEP-1995 08:11
Listing of raw data for -
data file 28SEP950
data ident 151_161 Mer Def 0.25
Axis display range X_MASS (45.00, 500.31)
Normalising intensity 1.38600E+05
Data threshold 0.17% of normalising intensity

```

MASS	TIME	ABS HEIGHT	REL HEIGHT(%)	FLAGS
50.0187	78653.2001	1.953455E+03	1.41	
51.0274	78062.8113	2.701546E+03	1.95	
52.0359	77484.1428	1.245546E+03	0.90	
53.0464	76915.4298	1.009346E+04	7.28	
54.0552	76358.3412	2.835418E+04	20.46	
55.0592	75814.1675	1.386000E+05	100.00	
56.0728	75274.7762	3.966055E+04	28.62	
57.0815	74747.5771	1.027189E+05	74.11	
58.0652	74242.3577	5.728091E+03	4.13	
59.0545	73742.7733	3.550000E+03	2.56	
60.0341	73256.3075	2.159709E+04	15.58	
61.0398	72765.0877	4.031364E+03	2.91	
63.0361	71813.5114	6.747273E+02	0.49	
65.0506	70883.3171	2.364182E+03	1.71	
66.0589	70428.4681	2.534727E+03	1.83	
67.0654	69981.3501	5.440146E+04	39.25	
68.0723	69540.6954	2.636218E+04	19.02	
69.0794	69106.4528	8.010473E+04	57.80	
70.0858	68678.7826	2.557891E+04	18.46	
71.0936	68256.6147	4.548655E+04	32.82	
72.0852	67847.0933	1.097273E+03	0.79	
73.0413	67457.5992	3.437746E+04	24.80	
74.0419	67055.3769	3.796909E+03	2.74	
75.0347	66661.7501	1.882909E+03	1.36	
77.0408	65882.1796	5.144545E+03	3.71	
78.0487	65498.2811	1.962546E+03	1.42	
79.0563	65119.4942	1.487746E+04	10.73	
80.0657	64744.9443	9.268000E+03	6.69	
81.0730	64375.9525	4.510046E+04	32.54	
82.0808	64011.4658	2.709755E+04	19.55	
83.0891	63651.3400	5.990255E+04	43.22	
84.0729	63304.2401	3.334327E+04	24.06	
85.1073	62943.6906	2.442618E+04	17.62	
86.0988	62602.2365	2.937273E+02	0.21	
87.0538	62277.0592	3.882546E+03	2.80	
91.0690	60947.8251	1.012600E+04	7.31	
92.0759	60623.6259	2.134091E+03	1.54	
93.0844	60302.3879	8.775637E+03	6.33	
94.0909	59985.2018	5.330909E+03	3.85	
95.1002	59670.4536	3.418546E+04	24.66	
96.0937	59363.8259	2.211318E+04	15.95	
97.1085	59053.8022	4.291027E+04	30.96	
98.0907	58756.7873	6.729891E+04	48.56	
99.1001	58454.5648	8.804728E+03	6.35	
100.0697	58167.1070	1.441091E+03	1.04	
101.0740	57872.2588	1.855636E+03	1.34	
105.0732	56726.2895	4.471455E+03	3.23	
106.0800	56444.7340	5.759091E+02	0.42	
107.0880	56165.5372	4.895000E+03	3.53	
108.0965	55888.9020	2.532727E+03	1.83	
109.1040	55615.1447	1.626291E+04	11.73	
110.1066	55345.3292	8.192000E+03	5.91	
111.1034	55079.5981	1.979127E+04	14.28	
112.0982	54816.8745	1.532946E+04	11.06	
113.0917	54556.9192	4.019273E+03	2.90	
114.0779	54301.2234	3.798182E+02	0.27	
115.0730	54045.5007	3.483091E+03	2.51	
116.0624	53793.4280	4.730909E+03	3.41	
117.0720	53538.4537	4.183637E+03	3.02	
118.0891	53283.7574	2.947273E+02	0.21	
119.0957	53033.7930	1.664909E+03	1.20	
120.1035	52785.5931	3.029091E+02	0.22	
121.1142	52538.6996	5.532909E+03	3.99	
122.1215	52294.6067	1.221364E+03	0.88	
123.1252	52053.3422	8.002728E+03	5.77	
124.1227	51814.0569	3.340727E+03	2.41	
125.1221	51577.2653	5.587637E+03	4.03	
126.1211	51341.6910	1.758182E+03	1.27	
127.1205	51110.3057	2.485273E+03	1.79	
128.1197	50659.6599	1.261127E+04	9.22	
129.1187	50429.4844	2.705455E+02	0.20	
130.1177	50200.3089	1.012600E+04	7.31	

137.1268	48876.4022	4.600000E+03	3.32
138.1347	48660.3866	1.977182E+03	1.43
139.1332	48447.9654	1.199727E+03	0.87
140.1450	48234.3105	2.694546E+02	0.19
141.1263	48028.5802	5.880000E+02	0.42
143.1104	47617.0496	5.768182E+02	0.42
145.1116	47207.8337	2.805455E+02	0.20
147.1000	46806.7787	2.454636E+03	1.77
149.1370	46401.2739	1.368636E+03	0.99
150.1457	46202.3796	4.099091E+02	0.30
151.1410	46007.3412	3.024182E+03	2.18
152.1424	45812.3126	1.442273E+03	1.04
153.1421	45618.8269	8.583636E+02	0.62
154.1437	45426.2000	2.499091E+02	0.18
155.1371	45236.3620	1.279000E+03	0.92
157.1267	44859.7530	7.075455E+02	0.51
158.0926	44678.6424	3.269091E+02	0.24
163.1431	43749.1843	3.193636E+02	0.23
165.1387	43389.8146	1.186000E+03	0.86
166.1797	43204.0742	5.029091E+02	0.36
167.1546	43031.1689	2.770909E+02	0.20
169.1192	42685.7565	6.910909E+02	0.50
171.1142	42339.0876	2.368364E+03	1.71
177.0399	41332.6909	8.247273E+02	0.60
185.1536	40008.1482	1.642364E+03	1.18
191.0233	39085.6947	1.306364E+03	0.94
193.1046	38765.3820	3.500909E+02	0.25
207.0589	36703.4853	4.583564E+04	33.07
208.0618	36560.7729	6.793091E+03	4.90
209.0616	36419.1800	3.867182E+03	2.79
213.1938	35841.0794	6.265455E+02	0.45
221.1378	34759.9080	4.444546E+02	0.32
227.1679	33964.2532	3.805455E+02	0.27
239.2637	32430.9251	9.047455E+03	6.53
240.2614	32307.9413	4.042727E+02	0.29
256.2534	30402.3850	1.297182E+03	0.94
262.2601	29718.1182	4.612182E+03	3.33
263.2604	29605.6913	1.373455E+03	0.99
264.2746	29492.1452	1.377891E+04	9.94
265.2817	29379.7938	8.816455E+03	6.36
266.2789	29268.9613	5.734546E+02	0.41
267.2622	29160.0522	9.206364E+02	0.66
281.0799	27668.7145	7.233273E+03	5.22
282.0880	27562.8256	6.401818E+02	0.46
283.1056	27456.3553	5.260909E+02	0.38
313.3126	24458.4346	1.085527E+04	7.83
314.3140	24363.9407	9.018182E+02	0.65
338.3203	22186.4387	2.082636E+03	1.50
339.3334	22097.8895	6.621637E+03	4.78
340.3320	22010.8444	4.500000E+02	0.32
341.2762	21928.7395	1.897091E+03	1.37
342.2884	21849.6041	5.920909E+02	0.43
344.1896	21676.6268	1.833818E+03	1.32
355.1115	20749.8809	5.230909E+02	0.38
367.3334	19749.8568	4.147273E+02	0.30

Minor Isomer (14b)

Elemental Composition

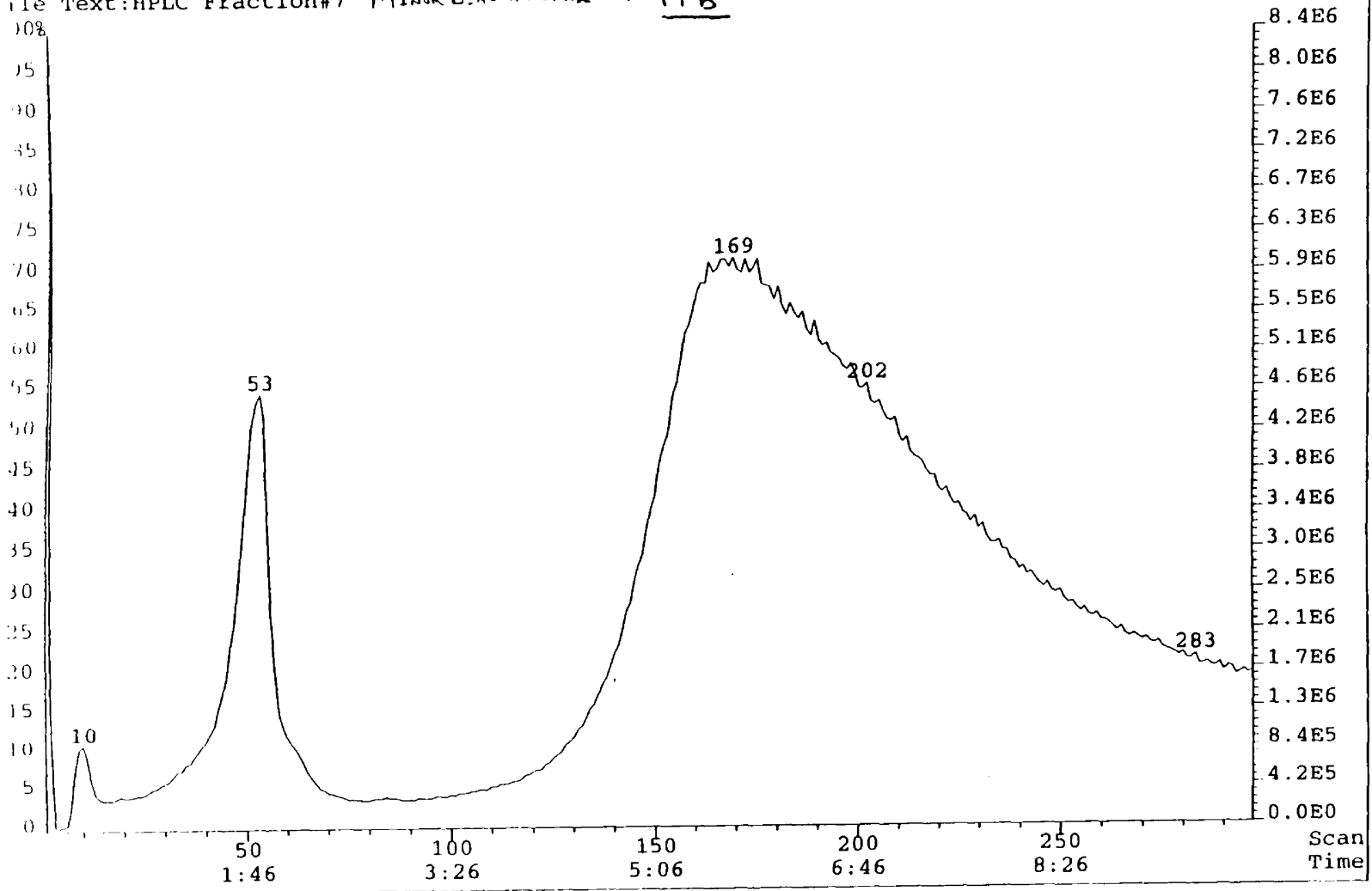
File:10OCT95B1 Ident:1 Acq:10-OCT-1995 07:36:57 +3:10 Cal:10OCT95B1
70S EI+ Voltage BpM:331 BpI:1017344 TIC:4198684 Flags:NORM
File Text:ew; minor diastereomer Created from 10OCT95B 42_52 SMO(1,7)
Heteroatom Max: 20 Ion: Both Even and Odd
Limits:

360.150482	10.0			-0.5	5	10	0
				20.0	30	50	3
Mass	mDa	PPM	Calc. Mass	DBE	C	H	O
360.150482	0.9	2.6	360.151415	18.0	27	20	1

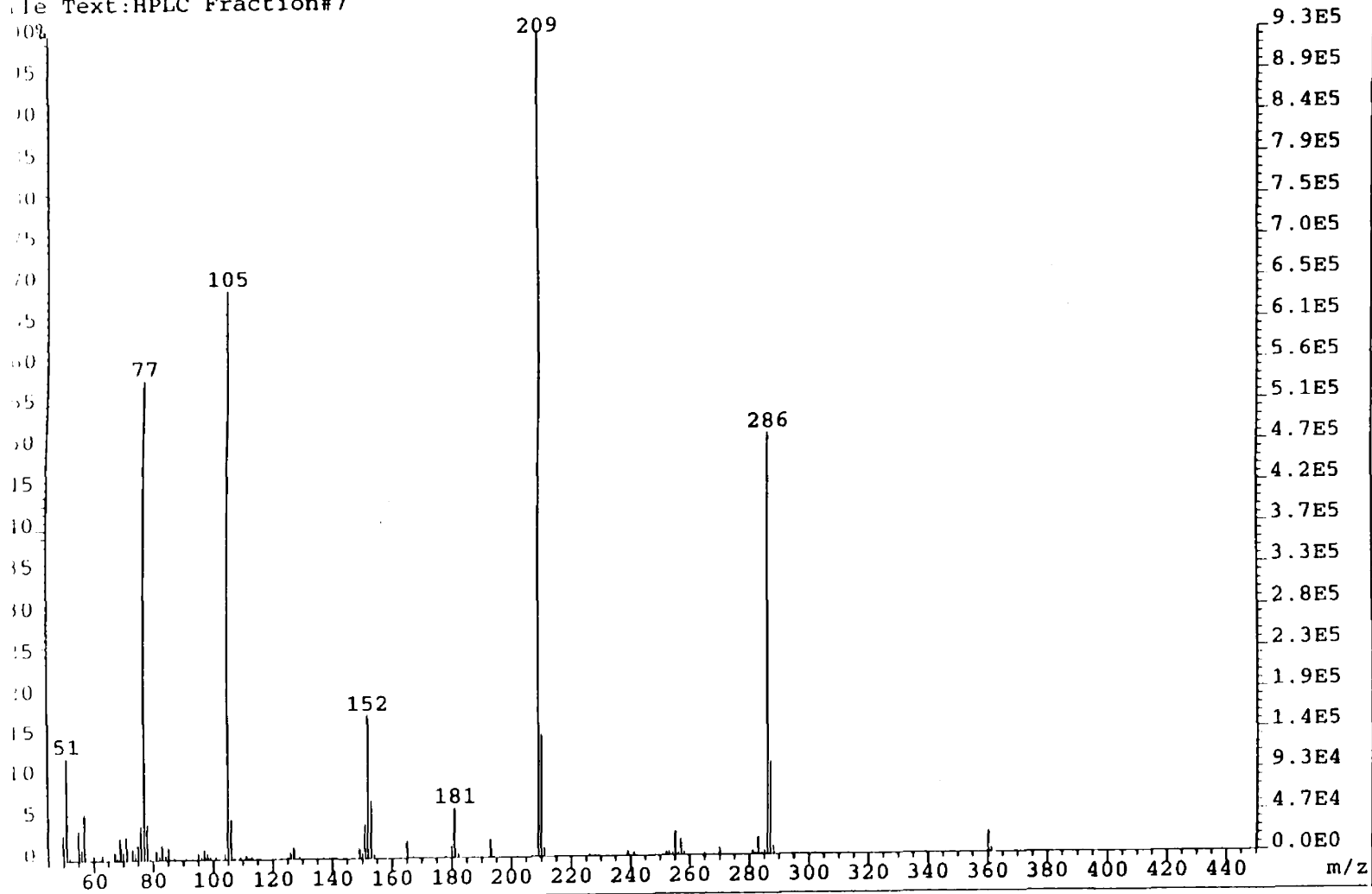
le:28SEP95N #1-297 Acq:28-SEP-1995 12:52:54 Septum EI+ Magnet 70S

IC (+RP) Exp:PROBE

File Text:HPLC Fraction#7 Minor Diastereomer - 14b



File: 28SEP95N Ident: 50_55 Mer Def 0.25 Acq: 28-SEP-1995 12:52:54 +1:51 Cal: 28SEP95N_1
MS EI+ Magnet BpM: 209 BpI: 933139 TIC: 4132302 Flags: HALL
File Text: HPLC Fraction#7

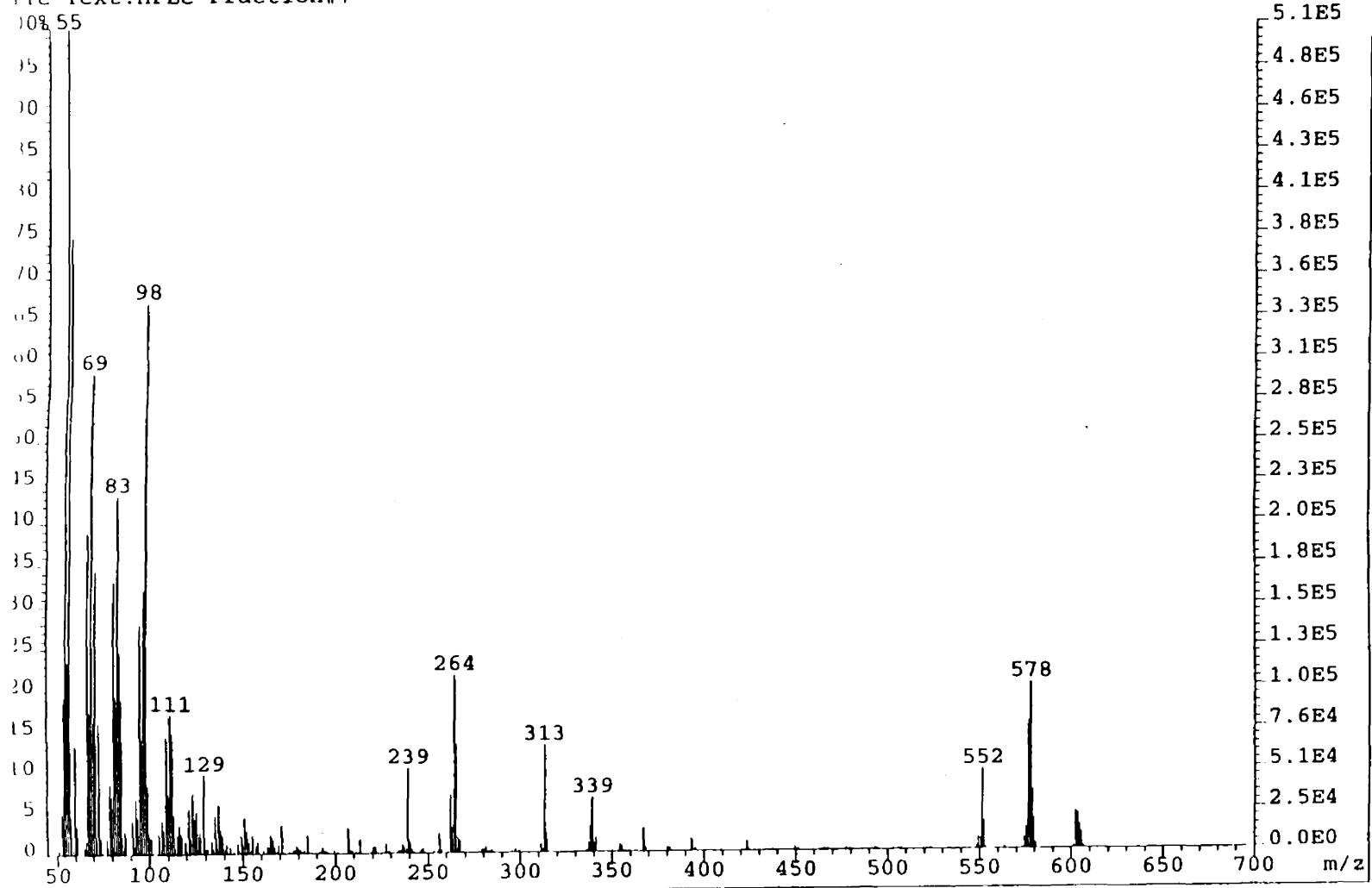


MS_USER:SPE_DEFAULT.LIS 28-SEP-1995 13:07
 Listing of raw data for -
 data file 28SEP95N
 data ident 50.55 Mer Def 0.25
 Axis display range X_MASS (45.00, 450.23)
 Normalising intensity 9.33139E+05
 Data threshold 0.17% of normalising intensity

MASS	TIME	ABS HEIGHT	REL HEIGHT (%)	FLAGS
50.0193	78652.8778	2.994800E+04	3.21	
51.0282	78062.3891	1.162453E+05	12.46	
52.0340	77485.1979	5.268833E+03	0.56	
54.0557	76358.0719	2.924333E+03	0.31	
55.0631	75812.0831	3.443584E+04	3.69	
56.0728	75274.7838	1.384133E+04	1.48	
57.0810	74747.8526	5.229017E+04	5.60	
60.0340	73256.3622	5.942667E+03	0.64	
63.0347	71814.1569	6.220000E+03	0.67	
67.0650	69981.5136	9.454667E+03	1.01	
68.0705	69541.4751	3.895167E+03	0.42	
69.0786	69106.7704	2.527733E+04	2.71	
70.0842	68679.4271	1.020600E+04	1.09	
71.0925	68257.0882	2.663733E+04	2.85	
73.0432	67456.8205	1.361533E+04	1.46	
74.0224	67063.1807	9.289334E+03	1.0	
75.0285	66664.2029	1.819733E+04	1.95	
76.0328	66271.2921	3.976800E+04	4.26	
77.0411	65882.0553	5.431240E+05	58.20	
78.0451	65499.6407	4.148667E+04	4.45	
79.0550	65119.9860	2.989333E+03	0.32	
81.0709	64376.7471	1.075933E+04	1.15	
82.0790	64012.1406	5.291000E+03	0.57	
83.0884	63651.6000	1.638400E+04	1.76	
84.0795	63301.9318	5.933667E+03	0.64	
85.1046	62944.6194	1.390533E+04	1.49	
87.0383	62282.2974	2.834167E+03	0.30	
91.0649	60949.1377	1.984000E+03	0.21	
95.0984	59670.9926	7.445833E+03	0.80	
96.1066	59359.8517	3.580833E+03	0.38	
97.1132	59052.3899	1.155217E+04	1.24	
98.0919	58756.4428	7.162833E+03	0.77	
99.1091	58451.8981	3.039500E+03	0.33	
101.0514	57878.8512	3.074167E+03	0.33	
104.0345	57019.6774	7.452667E+03	0.80	
105.0409	56735.3892	6.448055E+05	69.10	
106.0441	56454.7210	4.664534E+04	5.00	
107.0544	56174.8090	2.114667E+03	0.23	
109.1032	55615.3735	3.276333E+03	0.35	
111.1157	55076.3377	4.457667E+03	0.48	
112.1124	54813.1574	2.348667E+03	0.25	
113.0967	54555.6239	3.474333E+03	0.37	
123.1268	52052.9562	1.849333E+03	0.20	
125.1244	51578.4821	2.265000E+03	0.24	
126.0645	51357.7450	7.336667E+03	0.79	
127.0699	51123.4457	1.296000E+04	1.39	
129.0839	50659.6019	2.852500E+03	0.31	
149.0442	46419.6275	1.203600E+04	1.29	
150.0619	46218.8682	7.059667E+03	0.76	
151.0704	46021.1332	3.957900E+04	4.24	
152.0796	45824.5196	1.634250E+05	17.51	
153.0855	45629.7599	6.533067E+04	7.00	
154.0916	45436.1978	5.000167E+03	0.54	
165.0888	43398.7617	1.928867E+04	2.07	
167.0646	43047.0891	2.001833E+03	0.21	
178.0956	41156.9517	2.280667E+03	0.24	
180.0745	40830.2986	1.377467E+04	1.48	
181.0803	40665.6512	5.593067E+04	5.99	
182.0866	40501.8424	5.981500E+03	0.64	
193.0797	38769.1884	2.021333E+04	2.17	
209.0778	36416.8981	9.331390E+05	100.00	
210.0831	36275.2244	1.405173E+05	15.06	
211.0853	36134.6535	1.106283E+04	1.19	
226.0942	34104.3621	1.938333E+03	0.21	
228.1088	33842.0104	1.658833E+03	0.18	
239.1066	32450.2341	5.933333E+03	0.64	
241.1206	32202.4342	4.201000E+03	0.45	
252.0984	30885.6030	4.193667E+03	0.45	
253.1140	30766.7233	4.920167E+03	0.53	
254.1203	30649.2622	3.722333E+03	0.40	
255.1266	30532.3811	2.770467E+03	0.30	
256.1329	30415.5000	1.718600E+03	0.18	

281.1017	27666.4218	4.486667E+03	0.48
282.1239	27559.0636	1.892500E+03	0.20
283.1292	27453.8953	2.006233E+04	2.15
284.1263	27349.9697	2.833333E+03	0.30
285.1091	27247.8979	4.871667E+03	0.52
286.1162	27143.6928	4.783513E+05	51.26
287.1195	27040.2434	1.050830E+05	11.26
288.1232	26937.1278	9.678334E+03	1.04
360.1707	20331.7688	2.386667E+04	2.56
361.1835	20248.8438	5.155167E+03	0.55

File: 28SEP95N Ident: 166_174 Mer Def 0.25 Acq: 28-SEP-1995 12:52:54 +5:46 Cal: 28SEP95N_1
MS EI+ Magnet BpM: 55 BpI: 509938 TIC: 5965793 Flags: HALL
File Text: HPLC Fraction#7



MS_USER:SPE_DEFAULT.LIS 28-SEP-1995 13:08
 Listing of raw data for -
 data file 28SEP95N
 data ident 166_174 Mer Def 0.25
 Axis display range X_MASS (45.00, 700.00)
 Normalising intensity 5.09938E+05
 Data threshold 0.17% of normalising intensity

MASS	TIME	ABS HEIGHT	REL HEIGHT(%)	FLAGS
50.0178	78653.7269	1.286000E+03	0.25	
51.0268	78063.1548	3.246333E+03	0.64	
52.0347	77484.7821	1.744444E+03	0.34	
53.0456	76915.8568	2.665778E+04	5.23	
54.0546	76358.6836	9.846045E+04	19.31	
55.0548	75816.5420	5.099377E+05	100.00	
56.0679	75277.3875	1.197738E+05	23.49	
57.0788	74749.0062	3.819314E+05	74.90	
58.0693	74240.2718	2.405289E+04	4.72	
59.0551	73742.5003	1.237467E+04	2.43	
60.0323	73257.1889	5.795911E+04	13.33	
61.0393	72765.3281	1.748045E+04	3.43	
65.0483	70884.3498	5.407778E+03	1.06	
66.0549	70430.2594	9.260667E+03	1.82	
67.0634	69982.2209	1.986133E+05	38.95	
68.0704	69541.5448	8.896000E+04	17.45	
69.0775	69107.2571	2.976853E+05	58.38	
70.0790	68681.6442	8.397178E+04	16.47	
71.0911	68257.6528	1.756160E+05	34.44	
72.0830	67848.0234	9.906667E+03	1.94	
73.0344	67460.3757	8.235734E+04	16.15	
74.0389	67056.6016	1.870489E+04	2.10	
75.0398	66659.7205	2.302667E+03	0.45	
77.0401	65882.4552	1.027244E+04	2.01	
78.0471	65498.8619	4.758000E+03	0.93	
79.0546	65120.1078	4.385245E+04	8.60	
80.0615	64746.4845	3.627733E+04	7.11	
81.0706	64376.8483	1.688818E+05	33.12	
82.0777	64012.5844	9.784534E+04	19.19	
83.0865	63652.2739	2.210702E+05	43.35	
84.0648	63307.0677	1.263360E+05	24.77	
85.1039	62944.8663	9.678223E+04	18.98	
86.1035	62600.5953	5.907333E+03	0.98	
87.0513	62277.8880	1.485867E+04	2.91	
91.0651	60949.0687	2.092622E+04	4.10	
92.0710	60625.1907	5.661778E+03	1.11	
93.0811	60303.4339	3.453689E+04	6.77	
94.0890	59985.7936	2.333245E+04	4.58	
95.0978	59671.1769	1.425565E+05	27.96	
96.1034	59360.8399	7.365155E+04	14.44	
97.1053	59054.7767	1.637689E+05	32.12	
98.0859	58758.2423	3.414357E+05	66.96	
99.0955	58455.9584	4.296000E+04	8.42	
100.0669	58167.9441	1.343867E+04	2.64	
101.0716	57872.9585	1.063956E+04	2.09	
102.0576	57586.2545	2.841889E+03	0.40	
105.0738	56726.1247	1.245556E+04	2.44	
106.0799	56444.7521	3.625556E+03	0.71	
107.0866	56165.9278	2.079111E+04	4.08	
108.0920	55890.1274	1.536889E+04	3.01	
109.1010	55615.9540	7.324089E+04	14.36	
110.1040	55346.0396	3.788978E+04	7.43	
111.0972	55081.2652	8.722134E+04	17.10	
112.0923	54818.4322	7.549511E+04	14.80	
113.0853	54558.5969	2.519567E+04	4.94	
114.0756	54301.8050	4.180778E+03	0.81	
115.0760	54044.7270	1.222489E+04	2.40	
116.0592	53794.2554	1.809022E+04	3.55	
117.0674	53539.5928	1.264578E+04	2.48	
118.0802	53285.9784	9.174445E+02	0.18	
119.0941	53034.1942	8.016889E+03	1.57	
120.1002	52786.4010	3.062222E+03	0.60	
121.1127	52539.0707	2.836889E+04	5.56	
122.1180	52295.4547	9.644889E+03	1.89	
123.1226	52053.9770	3.769955E+04	7.39	
124.1279	51814.2383	2.157511E+04	4.23	
125.1344	51578.4747	2.646489E+04	5.19	
126.1421	51343.5632	1.355822E+04	2.66	
127.1511	51111.0625	1.186844E+04	2.72	
128.1610	50885.8188	1.212111E+03	0.24	
129.1720	50659.7614	4.322911E+04	9.56	
130.1841	50441.8112	3.127333E+03	0.61	

136.1227	49093.1941	7.322889E+03	1.37
137.1178	48878.3331	3.258756E+04	6.00
138.1289	48661.6357	1.538400E+04	3.02
139.1283	48449.0092	1.276311E+04	2.31
140.1341	48236.6024	3.272333E+03	0.64
141.1309	48027.6149	5.293778E+03	1.16
143.1049	47618.1751	4.185444E+03	0.82
145.1069	47208.8049	1.484111E+03	0.28
147.1209	46802.5870	6.370222E+03	1.25
148.1293	46601.2051	2.818444E+03	0.40
149.1424	46400.2099	1.147067E+04	2.25
150.1406	46203.3874	5.501778E+03	1.10
151.1369	46008.1440	2.240800E+04	4.39
152.1458	45811.6579	1.431067E+04	2.81
153.1432	45618.6262	7.496889E+03	1.51
154.1471	45425.5486	3.322889E+03	0.59
155.1359	45236.5873	1.136622E+04	2.23
157.1295	44859.2389	5.027000E+03	0.99
158.0766	44681.6294	7.731333E+03	1.52
159.1079	44489.4418	1.122556E+03	0.22
161.1388	44114.5691	2.279778E+03	0.45
163.1507	43747.8087	4.796444E+03	0.94
164.1486	43567.5741	4.503111E+03	0.88
165.1490	43387.9773	1.141867E+04	2.24
166.1732	43205.2218	4.453333E+03	1.66
167.1534	43031.3862	4.534556E+03	0.89
168.1639	42853.2101	1.556444E+03	0.31
169.1511	42680.1955	5.585667E+03	1.10
171.0996	42341.6159	1.773956E+04	3.48
172.1151	42166.6728	1.262000E+03	0.25
175.1540	41649.2769	1.076889E+03	0.21
177.1651	41311.7909	1.985889E+03	0.39
178.1567	41146.8081	2.447889E+03	0.40
179.1641	40980.1164	4.745333E+03	0.93
180.1821	40812.6427	3.276556E+03	0.64
181.1675	40651.4247	2.240000E+03	0.44
183.1545	40329.0008	1.967222E+03	0.39
185.1392	40010.4413	1.104844E+04	2.17
191.1595	39064.6148	8.991111E+02	0.18
192.1575	38910.7108	1.100667E+03	0.22
193.1610	38756.7468	3.654556E+03	0.72
194.1994	38598.2699	1.790333E+03	0.35
195.1842	38448.7489	1.392778E+03	0.27
199.1573	37853.1263	2.831556E+03	0.40
207.0650	36702.6122	1.577422E+04	3.09
208.1077	36554.2540	2.142889E+03	0.42
209.1430	36407.6867	1.718667E+03	0.34
211.2024	36118.2720	1.242444E+03	0.20
213.1888	35841.7757	4.661111E+03	1.70
220.2359	34880.7516	3.517111E+03	0.69
221.2136	34749.7726	4.491222E+03	0.88
222.2259	34614.7679	1.392889E+03	0.27
227.1622	33964.9880	5.592222E+03	1.10
229.1628	33705.6875	1.303333E+03	0.26
234.2350	33058.5899	1.852222E+03	0.36
235.2189	32934.7316	1.498000E+03	0.29
236.2325	32807.6765	5.527556E+03	1.08
237.2367	32682.3312	4.303333E+03	0.84
238.2443	32557.0962	3.316889E+03	0.65
239.2504	32432.5720	5.300622E+04	10.39
240.2505	32309.2853	7.711333E+03	1.51
241.1990	32192.8207	3.206000E+03	0.63
246.2405	31581.0865	2.284778E+03	0.40
247.2468	31460.4319	2.297000E+03	0.57
253.2093	30755.5932	1.063667E+03	0.21
255.1913	30525.1080	1.310778E+03	0.26
256.2454	30403.3076	1.198089E+04	2.35
257.2526	30287.4196	2.263778E+03	0.40
261.2352	29833.7313	1.247778E+03	0.24
262.2440	29719.9287	3.648355E+04	7.15
263.2511	29606.7153	1.639645E+04	3.22
264.2535	29493.3855	1.108836E+05	21.74
265.2697	29381.1298	6.228445E+04	13.29
266.2758	29269.3074	1.037911E+04	2.04
267.2807	29158.0006	8.388667E+03	1.65
269.2177	28944.5620	8.928889E+02	0.19
279.2444	27862.5355	2.259556E+03	0.44
280.2522	27755.9361	2.144556E+03	0.42
281.2505	27660.2843	3.688333E+03	0.70
284.2548	27334.1111	1.310000E+03	0.35
285.2581	27230.7611	1.225556E+03	0.33
287.2611	27120.4811	1.139333E+03	0.41

337.2976	22276.0745	6.204222E+03	1.22
338.3113	22187.2334	1.645067E+04	3.23
339.3150	22099.5016	3.380000E+04	6.63
340.3173	22012.1231	6.276667E+03	1.23
341.3293	21924.1292	9.080667E+03	1.78
354.2819	20819.1228	4.380556E+03	0.86
355.2831	20735.5861	3.184333E+03	0.62
367.3197	19750.9570	1.451956E+04	2.85
368.3272	19669.8515	2.319333E+03	0.45
380.3186	18719.1582	2.708000E+03	0.53
381.3170	18641.3657	2.321778E+03	0.46
393.3306	17721.8040	7.552000E+03	1.48
394.3335	17646.2727	1.036111E+03	0.20
395.3365	17570.9036	1.885222E+03	0.37
423.3839	15536.0134	5.956444E+03	1.17
449.3915	13762.4911	2.297778E+03	0.45
451.4089	13629.3961	1.357667E+03	0.27
465.4097	12717.3714	1.172889E+03	0.23
467.3947	12590.1397	1.230778E+03	0.24
477.4201	11957.0444	1.586889E+03	0.31
479.4116	11832.9409	9.572222E+02	0.19
493.4383	10971.7860	1.600667E+03	0.31
523.4960	9198.7273	1.208667E+03	0.24
548.5075	7793.0277	2.932333E+03	0.58
549.5201	7737.2136	7.782444E+03	1.53
550.5156	7682.4332	7.160000E+03	1.40
551.5279	7626.8388	4.971555E+04	9.75
552.5344	7571.6686	1.783867E+04	3.50
553.5344	7516.9644	1.622000E+03	0.32
563.5328	6976.1646	1.275667E+03	0.25
574.5748	6388.8676	7.413556E+03	1.45
575.5783	6335.9340	1.415844E+04	2.78
576.5891	6282.6962	8.072178E+04	15.83
577.6002	6229.5215	1.039329E+05	20.38
578.6069	6176.6541	3.753867E+04	7.36
579.6233	6123.3562	2.000356E+04	3.92
580.6177	6071.2952	3.973111E+03	0.78
600.5987	5037.2510	9.198889E+02	0.18
601.5392	4988.9893	2.038778E+03	0.40
602.6227	4933.4375	2.310667E+04	4.53
603.6210	4882.3006	2.195022E+04	4.30
604.6167	4831.3354	1.510978E+04	2.96
605.6209	4779.9855	1.090222E+04	2.14
606.6234	4728.7744	2.154000E+03	0.42

Bibliography

1. March, J. *Advanced Organic Chemistry: Reactions, Mechanisms, and Structures*; John Wiley: NY, 1992; p198.
2. Stang, P.J. Vinyl Triflate Chemistry: Unsaturated Cations and Carbenes. *Acct. Chem. Res.* **1978**, *11*, 107.
3. Huheey, J.E.; Keiter, E.A.; Keiter, R.L. *Inorganic Chemistry: Principles of Structure and Reactivity*; Harper-Collins: NY, 1993; p26.
4. Carey, F.A.; Sundberg, R.J. *Advanced Organic Chemistry: Reactions and Synthesis*; Plenum Press: NY, 1992; p522.
5. Rawson, R.J.; Harrison, I.T. A Convenient Procedure for the Methylenation of Olefins to Cyclopropanes. *J. Org. Chem.* **1970**, *35*, 2057.
6. Winstein, S.; Sonnenberg, J. Homoconjugation and Homoaromaticity. III. The 3-Bicyclo[3.1.0]hexyl System. *J. Am. Chem. Soc.* **1961**, *83*, 3235.
7. Grieco, P.A.; Oguri, T.; Wang, C.-L.; Williams, E. Stereochemistry and Total Synthesis of (+/-)-Ivanguilin. *J. Org. Chem.* **1977**, *42*, 4113.
8. Simmons, H.E.; Smith, R.D. *J. Am. Chem. Soc.* **1959**, *81*, 4256.
9. Anciaux, A.J.; Hubert, A.J.; Noels, A.F.; Petiniot, N.; Teyssie, P. Transition-Metal-Catalyzed Reactions of Diazo Compounds 1. Cyclopropanation of Double Bonds. *J. Org. Chem.* **1980**, *45*, 695.
10. Alonso, M.E.; Jano, P.; Hernandez, M.I. Catalytic Decomposition of Ethyl Diazopyruvate in the Presence of Electron-Deficient and Hydrocarbon Alkenes. Cyclopropanation vs. Carbon Hydrogen Insertion. *J. Org. Chem.* **1980**, *45*, 5299.
11. Paquette, L.A.; Wilson, S.E.; Henzel, R.P.; Allen, G.P., Jr. The Effect of Methyl Substitution on the Competitive Rearrangements of Tricyclo[4.1.0.0]heptanes by Silver(I) Ion. *J. Am. Chem. Soc.* **1972**, *94*, 7761.
12. Closs, G.L.; Moss, R.A. Carbenoid Formation of Arylcyclopropanes from Olefins, Benzal Bromides, and Organolithium Compounds and from Photolysis of Aryldiazomethanes. *J. Am. Chem. Soc.* **1964**, *86*, 4042.
13. Gripp, H.N.; Kiefer, E.F. *Org. Syn.* **1962**, *42*, 12.

14. Bottini, A.T.; Frost, K.A.; Anderson, B.R.; Dev, V. The Addition of 1-Halocycloheptanes with Potassium *t*-Butoxide and with Sodium Pyrrolidide. *Tetrahedron* **1973**, *29*, 1975.
15. Harnos, S.; Tivakompannarai, S.; Waali, E.E. The Addition of 1,2-Cyclohexadiene to Substituted Styrenes. *Tetrahedron Lett.* **1986**, *27*, 3701.
16. Gardner, P.D.; Narayana, T. A Convenient Synthesis of *cis*-Cyclononene. *J. Org. Chem.* **1961**, *26*, 3518.
17. Marchand, A.P.; Lehr, R.E. *Pericyclic Reaction; Vol. 2*; Academic Press: NY, 1977; p126.
18. Jones, W.M.; Ennis, C.L. Cycloheptatrienyliidene. *J. Am. Chem. Soc.* **1969**, *91*, 6391.
19. Jones, W.M.; Ennis, C.L. Formation of Spiroonatriene and Heptafulvalene from an Attempt to Generate Cycloheptatrienyliidene. *J. Am. Chem. Soc.* **1967**, *89*, 3069.
20. Gleiter, R.; Hoffmann, R. On Stabilizing a Singlet Methylene. *J. Am. Chem. Soc.* **1968**, *90*, 5457.
21. Mukai, T.; Nakazawa, T.; Isobe, K. Thermal Decomposition of Troponetosylhydrazone. *Tetrahedron Lett.* **1968**, *No. 5*, 565.
22. Christensen, L.W.; Waali, E.E.; Jones, W.M. Reactivity of Cycloheptatrienyliidene with Substituted Styrenes. *J. Am. Chem. Soc.* **1972**, *94*, 2118.
23. Jones, W.M.; Duell, B.L. Nucleophilicity of Cycloheptatrienyliidene Generated from a Nitrogen-Free Precursor. Evidence for a Free Carbene in the Decomposition of Troponetosylhydrazone Sodium Salt. *J. Org. Chem.* **1978**, *43*, 4901.
24. Untch, K. International Symposium on the Chemistry of Non-Benzenoid Aromatic Compounds, Sendai, Japan; August, 1970.
25. Jones, W.M.; Mayor, C. On the Origin of Cycloheptatrienyliidene from the Dehydrohalogenation of Chlorocycloheptatriene; Evidence for the Initial Formation of Cycloheptatetraene. *Tetrahedron Lett.* **1977**, *No. 44*, 3855.
26. Tyner, R.L.; Jones, W.M.; Ohrn, Y.; Sabin, J.R. Semiempirical Calculations on Phenylcarbene, Cycloheptatrienyliidene, and Cycloheptatetraene and Their Benzo-Annulated Derivatives. *J. Am. Chem. Soc.* **1974**, *96*, 3765.
27. Waali, E.E. The Cycloheptatrienyliidene-Cycloheptatetraene Problem. A MNDO Investigation. *J. Am. Chem. Soc.* **1981**, *103*, 3604.
28. Janssen, C.L.; Schaefer, H.-D. Cycloheptatrienyliidene. Singlet-Triplet Energetics: Theory Responds. *J. Am. Chem. Soc.* **1987**, *109*, 5030.

29. McMahon, R.J.; Chapman, O.L. Triplet Ground-State Cycloheptatriene. *J. Am. Chem. Soc.* **1986**, *108*, 1713.
30. Kuzaj, M.; Holger, L.; Wentrup, C. ESR Observation of Thermally Produced Triplet Nitrenes and Photochemically Produced Triplet Cycloheptatrienylienes. *Angew. Chem., Int. Ed. Engl.* **1986**, *No. 5*, 480.
31. Harris, J.W.; Jones, W.M. Definitive Evidence for Cycloheptatetraene from Dehydrobromination of Bromocycloheptatrienes. *J. Am. Chem. Soc.* **1982**, *104*, 7329.
32. Kirmse, W.; Loosen, K.; Sluma, H.-D. Carbenes and the O-H Bond: Cycloheptatrienyliene and Cycloheptatetraene. *J. Am. Chem. Soc.* **1981**, *103*, 5935.
33. Tivakornpannarai, S.; Waali, E.E. Facile Net Loss of a Carbon Atom from a Constrained Intermediate. *J. Am. Chem. Soc.* **1986**, *108*, 6058.
34. Zepp, J., University of Montana, unpublished results; Waali, E.E., personal communication.
35. Doering, W.v.E.; Knox, L.H. Reactions of the Cycloheptatrienylium (Tropylium) Ion. *J. Am. Chem. Soc.* **1957**, *79*, 352.
36. SYBYL and Alchemy III, 3D Molecular Modeling Software; TRIPOS Associates, Inc., 1699 South Hanley Road, Suite 303, St. Louis, Missouri 63144.
37. HRMS performed by Joe Sears, Montana State University.
38. Radlick, P. Synthesis of Tropone. *J. Org. Chem.* **1964**, *29*, 960.
39. Saito, K.; Omura, Y.; Mukai, T. Reactions of Tropone Tosylhydrazone Sodium Salt with Anthracene, 1,3-Diphenylisobenzofuran, and Phenylacetylene: [2+2] and [4+2] Type Cycloaddition Reactions of Cycloheptatrienyliene or 1,2,4,6-Cycloheptatetraene. *Bull. Chem. Soc. Jpn.* **1985**, *58*, 1663.
40. Amounts of reagent varied. The amounts listed here are typical amounts used.

